Università degli Studi di Napoli "PARTHENOPE"

DIPARTIMENTO DI INGEGNERIA

TESI DI DOTTORATO

IN

ENERGY SCIENCE AND ENGINEERING

XXXVIII CYCLE

Design, Modeling and Experimental Validation of an Integrated Bifacial PV–Hydrogen–Fuel Cell System

TUTOR
Ch.mo Prof. Alessandro Mauro

DOTTORANDO
Ing. Davide Capuano

COORDINATORE
Ch.ma Prof.ssa Laura Vanoli

Napoli, 2025

Author: Eng. Davide CAPUANO

Graded S.p.A

Via Generale Girolamo Calà Ulloa, 38

80141 NAPOLI

ITALY

e-mail: davide.capuano@graded.it

Naples 14/11/2025

CONTENTS

ACKNOWLEDGMENTS

This doctoral work marks the conclusion of a very important journey for me—professionally, academically, and personally. For this reason, these acknowledgements are many and truly heartfelt.

I would like to thank Prof. Alessandro Mauro for his constant support and availability throughout my doctoral years. His trust in my work has been fundamental, allowing me to approach this entire path with serenity and determination. I also owe him sincere thanks for the experience I gained during the previous years as a research fellow, a period in which I had the opportunity to grow professionally.

An equally sincere thank you goes to Prof.ssa Laura Vanoli for her continuous support, availability, and attention. Her professionalism, clarity, and human warmth have played an important role throughout my journey. I am also deeply grateful to her for the experience I gained in the previous years as a research fellow, during which she was a very important guide for me.

I would also like to thank Graded S.p.A. for giving me the opportunity to grow professionally and enrich my background through this PhD. My deepest gratitude goes to Ing. Claudio Miranda, the company's R&D manager, who has been—and still is—a very important figure for me, both inside and outside the company.

My thanks also go to the University of Sharjah for the opportunity to carry out this research project.

My heartfelt gratitude goes to my entire family, to those who are here and to those who are no longer with us, because everything I am today, I owe solely to them and to the trust they have always placed in me.

I would also like to thank all my friends, who have been an important source of support in my life—something I will never forget.

A special thought goes to my little Diana, who even supported me while I was preparing my doctoral presentation. I don't know how much she understood, but it doesn't matter; doing it together was wonderful, and I will remember it forever.

Finally, I want to thank someone who — though she does not know it — has been instrumental in this doctoral work. Or, even more so, in this journey. More than she could ever imagine.

To all of you, thank you from the bottom of my heart.

LIST OF FIGURES

LIST OF TABLES

NOMENCLATURE

Latin symbols

A – Area of PV module [m²]

Albedo – Surface reflectance factor [–]

C – Capacity [F, Ah]

cp – Specific heat [J/kgK]

E – Energy [J, Wh]

E_{cell} – Cell potential [V]

E° – Standard potential [V]

F – Faraday constant [96 485 C/mol]

G – Solar irradiance [W/m²]

H – Height [m]

I_d – Diode current [A]

I – Electric current [A]

I_0 – Reverse saturation current [A]

I_{ph} – Photogenerated current [A]

j – Current density [A/cm²]

k – Boltzmann constant [1.38×10^{-23} J/K]

L – Length [m]

m – Mass [kg]

$\dot{m}$ – Mass flow rate [kg/s]

$\dot{m}_{H_2}$ – Hydrogen flow rate [kg/s or Nl/min]

n – Number of cells / moles / nodes [–]

N_{cell} – Number of cells in series [–]

P – Power [W]

P_{in} – Input power [W]

P_{out} – Output power [W]

P_{max} – Maximum power of PV [W]

P_{H_2} – Hydrogen partial pressure [bar]

P_{O_2} – Oxygen partial pressure [bar]

P_{eq} – Equilibrium pressure [bar]

Q – Charge [C]

R – Resistance [Ω]

R_s – Series resistance [Ω]

R_{sh} – Shunt resistance [Ω]

t – Time [s, min]

T – Temperature [K, °C]

U – Voltage [V]

U_{stack} – Stack voltage [V]

V_{oc} – Open-circuit voltage [V]

V – Volume [m³]

V_{cell} – Fuel cell voltage [V]

V_{rev} – Reversible voltage [V]

η – Efficiency [–]

Greek symbols

α – Temperature coefficient [1/°C]

Δ – Variation of a variable [–]

ΔH – Enthalpy of reaction [kJ/mol]

ΔS – Entropy of reaction [J/mol·K]

λ – Thermal conductivity [W/mK]

ρ – Density [kg/m³]

σ – Electrical conductivity [S/m]

τ – Time constant [s]

θ – Temperature [°C]

μ – Dynamic viscosity [kg/ms]

ν – Kinematic viscosity [m²/s]

Constants

F – Faraday constant [96 485 C/mol]

R – Universal gas constant [8.314 J/mol·K]

q – Elementary charge [1.602×10^{-19} C]

k – Boltzmann constant [1.38×10^{-23} J/K]

Acronyms

BOS – Balance of System

CAES – Compressed Air Energy Storage

CSP – Concentrated Solar Power

DAQ – Data Acquisition

DOE – Department of Energy

FC – Fuel Cell

GHG – Greenhouse Gas

HHV – Higher Heating Value

H_2 – Hydrogen

IEA – International Energy Agency

IRENA – International Renewable Energy Agency

LCA – Life Cycle Assessment

LCOE – Levelized Cost of Energy

LCOH – Levelized Cost of Hydrogen

LOHC – Liquid Organic Hydrogen Carriers

LHV – Lower Heating Value

MENA – Middle East and North Africa

OPEX – Operational Expenditure

PEM – Proton Exchange Membrane

PPA – Power Purchase Agreement

PV – Photovoltaic

SCADA – Supervisory Control and Data Acquisition

SOC – State of Charge

TRL – Technology Readiness Level

OUTLINE OF THE THESIS

This doctoral thesis work was born in the context of the collaboration between Graded S.p.A. and the University of Sharjah (UAE), with the aim of studying, implementing and testing an integrated system for the production and use of green hydrogen powered by a bifacial photovoltaic system. The energy produced is used to power an electrolyzer and then a fuel cell, configuring a complete cycle of hydrogen generation and use in a real context.

The research activity combines experimental investigation and numerical modeling, paying particular attention to the characterization of the performance of the plant in real operating conditions and to the evaluation of the benefits deriving from the use of bifacial photovoltaic technology in an area with high solar radiation and high albedo conditions.

The thesis is divided into several phases:

- Analysis of the context and state of the art of the technologies used.
- Design of the innovative experimental system.
- Experimental campaign and data analysis.
- System modeling and simulation.
- Discussion of results and development prospects.

The goal is to demonstrate the technical-operational feasibility of a system for the production and use of green hydrogen integrated with bifacial photovoltaics and to provide guidelines for the design and optimization of similar solutions in future scenarios, contributing to the progress of the energy transition towards zero-emission carriers.

1 INTRODUCTION

1.1 The energy transition and the role of green hydrogen

1.1.1 Global energy scenario

The world energy system has entered a phase of epochal change. For more than a century, economic growth and technological development have been based on fossil fuels – coal, oil and natural gas – which have provided abundant energy at low cost. However, this model is unsustainable today: on the one hand because of the environmental impact, on the other hand because of the geopolitical vulnerability linked to the concentration of fossil resources in a few countries.

According to the International Energy Agency (IEA), in 2021, 80% of global primary energy demand was still met by fossil fuels, contributing to 73% of global greenhouse gas emissions [1]. At the atmospheric level, the CO_2 concentration exceeded 420 ppm, an increase of more than 50% compared to pre-industrial values. The direct consequence is climate change, the effects of which are increasingly evident: extreme heat waves, intense weather events, desertification and loss of biodiversity.

Added to this is geopolitical instability: the energy crisis of 2021–2022, linked to tensions between Russia and Europe, has highlighted the vulnerability of globalized energy systems. Over-reliance on foreign fossil fuel suppliers is not only risky in economic terms but also undermines national security.

1.1.2 The need for an energy transition

In this context, the energy transition takes on a central role: it is not just a technological evolution, but a structural transformation of economic and social systems. It involves the shift from a fossil fuel-based economy to a sustainable, resilient and decarbonised model.

The main pillars of the transition are:

- **Decarbonization**: drastically reduce CO_2 emissions through the replacement of fossil fuels with renewables and the use of clean technologies.
- **Electrification of final consumption**: Converting the transport, heating and industrial sectors towards the direct use of electricity produced from renewable sources.
- **Energy efficiency**: improve the performance of production, distribution and consumption systems, reducing waste and unnecessary consumption.
- **Diversification and energy security**: reducing dependence on a few sources or suppliers, ensuring resilience against external shocks.

The IEA, in its Net Zero by 2050 (2021) report, outlined the most ambitious scenario: to limit global warming to 1.5 °C, the share of energy produced from renewables must exceed 70% by 2050, while the consumption of fossil fuels will have to be reduced by 80% [2].

1.1.3 Hydrogen as a strategic energy carrier

Hydrogen is not a primary source, but an energy carrier: it must be produced from other sources. Its versatility – it can be stored, transported and used in different sectors – makes it a key candidate to complete the energy transition.

Different types of hydrogen are distinguished:

- **Grey hydrogen**: produced by steam reforming of methane or gasification of coal, without capturing emissions. It is the most widespread (over 90% of world production), but also the most polluting.
- **Blue hydrogen**: obtained from the same processes as grey, but with CO_2 capture and storage (CCS). It reduces emissions by 60–90%, but it doesn't eliminate them completely and is still expensive.
- **Green hydrogen**: produced by electrolysis of water powered by renewable energy. It is the only one capable of guaranteeing zero emissions and, in perspective, competitive costs thanks to the drop in the price of renewables.

Typology	Source of production	CO_2 emissions	Approximate cost (€/kg)	Technology Baccalaureate
Grey	Methane reforming, coal gasification	High	1–1,5	High
Blue	Fossils + CCS	Low	1,5–2,5	Average
Green	Electrolysis + RES	Void	2–6 (present) → <2 (2030)	Growing

Table 1.1 – Types of hydrogen and main characteristics

This classification is useful not only from a technical point of view, but also for political strategies: several countries are defining official "hydrogen certification" standards based on carbon intensity.

1.1.4 Applications of green hydrogen

Green hydrogen is used in several strategic sectors:

- **Transportation**: Fuel cell vehicles (FCVs) are already marketed in Japan, South Korea and California. Hydrogen is particularly suitable for heavy-duty transport (trucks, buses, trains, ships), where electric batteries are less competitive in terms of range and charging times.
- **Industry**: Steel production is one of the most promising sectors. Pilot projects such as **HYBRIT (Sweden)** use green hydrogen instead of coke to reduce iron ore. Ammonia and fertilizer production can also be decarbonized by replacing the gray hydrogen currently used in Haber-Bosch processes.
- **Energy**: Hydrogen can be used to generate electricity via fuel cells or modified gas turbines. It can also power high-efficiency cogeneration systems.
- **Seasonal storage**: hydrogen allows excess renewable electricity produced in the summer months to be stored and used in winter, overcoming the limitations of electrochemical batteries, which have limited storage capacity.

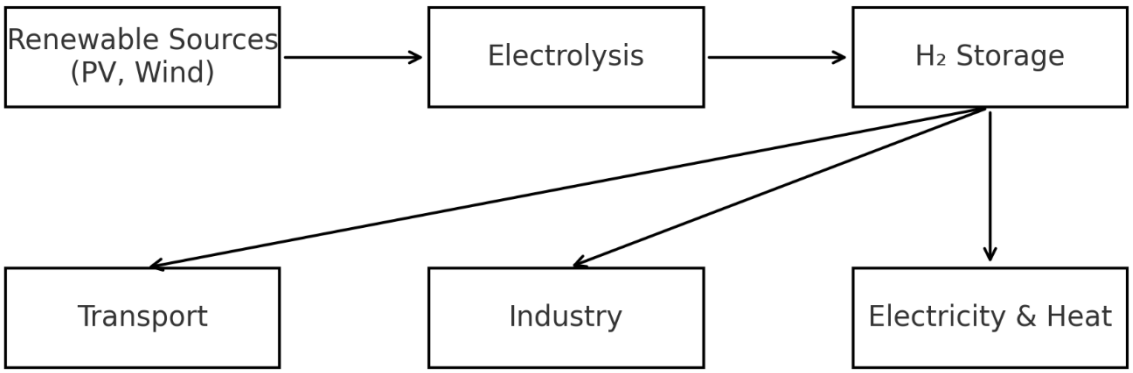

Figure 1.1 – Outline of the energy transition and the role of green hydrogen

The figure represents the role of hydrogen as a link between intermittent renewable production and end-uses in different sectors. It shows the main flows: solar and wind energy → electrolysis → hydrogen → storage → transport, industry, electricity and heat. This scheme summarizes the concept of hydrogen as a transversal vector, capable of enabling a resilient and decarbonized energy system.

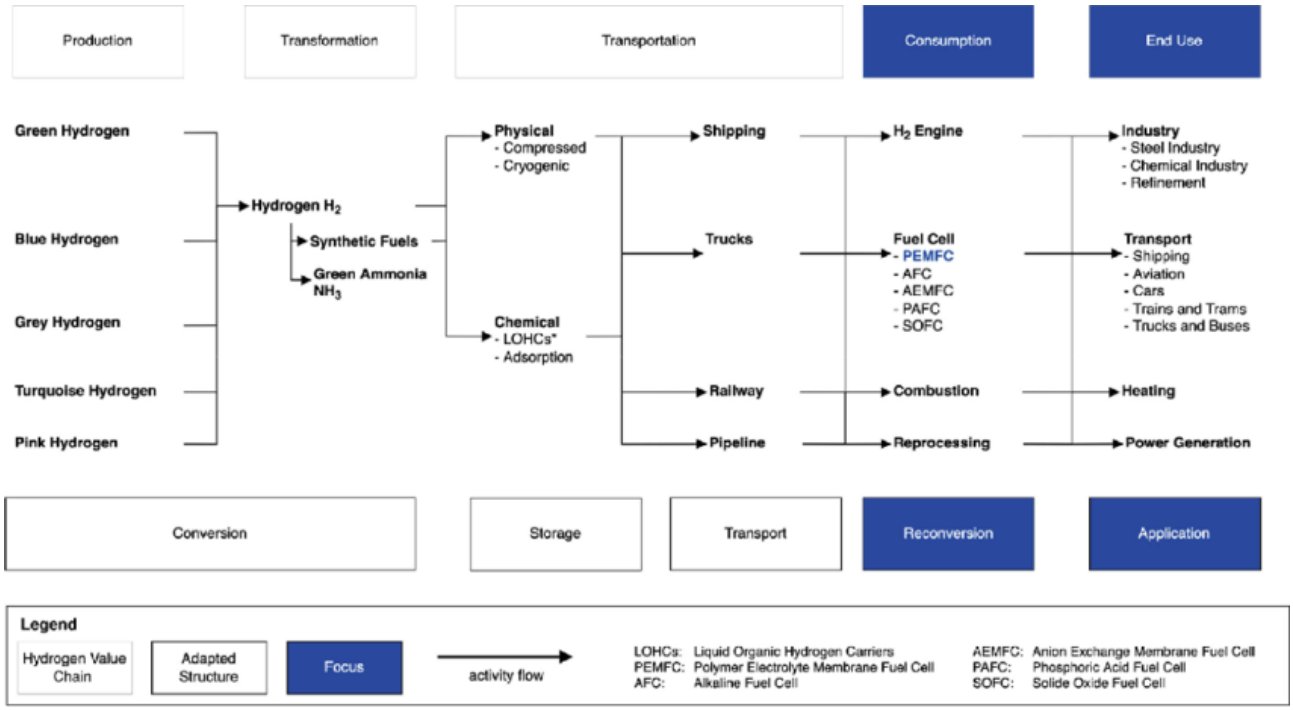

Figure 1.2 – Simplified diagram of the hydrogen value chain, from production by electrolysis to transport, storage and end uses in industry, transport and energy. Source: IRENA, 2020.

1.1.5 Challenges and prospects

Green hydrogen presents significant challenges:

- High cost: it currently ranges between € 2 and € 6/kg, compared to € 1–1.5/kg for grey hydrogen. However, according to IRENA, costs will fall below € 2/kg by 2030 thanks to the reduction in the price of renewables and advances in electrolysers [3].
- **Poor infrastructure**: there is a lack of distribution networks, refuelling stations and large-scale storage capacity.
- **Limited efficiency**: The complete PV → H_2 chain → electricity is 30–35% efficient, lower than that of batteries.
- **Regulations and standards**: we need internationally shared rules to certify the sustainability of hydrogen.

Despite these obstacles, the prospects are very promising. The European Union, with the REPowerEU (2022) plan, has set the goal of producing 10 Mt/year of renewable hydrogen by 2030. At the same time, projects in the Middle East and Australia are planning mega-plants for export to Asia and Europe.

1.1.6 Geopolitical and economic impacts

Green hydrogen can redraw global geopolitical maps. Countries with abundant solar and wind resources (UAE, Saudi Arabia, Australia, Chile) aim to become production and export hubs. Europe, poor in fossil resources, is the main importer, with bilateral agreements already underway with North Africa and the Middle East.

From an economic point of view, the green hydrogen sector can generate millions of new jobs by 2050, both in the production chain and in the transport and end-use sectors. The Hydrogen Roadmap Europe (2019) estimates that the sector can generate an economic value of over 800 billion euros by mid-century [4].

1.1.7 Support Policies

The role of public policies is decisive.

- **European Union**: approved the European Hydrogen Strategy (2020) and the IPCEI-Hydrogen programme, with investments of billions of euros.
- **United States**: The Inflation Reduction Act (2022) provides tax credits of up to $3/kg for the production of green hydrogen.
- **Japan**: adopted the first national hydrogen strategy in 2017, with the aim of becoming a world technology leader.
- **The UAE and Saudi Arabia** aim to become net exporters, taking advantage of the abundance of solar and wind resources and strategic geographical location.

1.2 Bifacial photovoltaic technology

1.2.1 Evolution and context

Photovoltaics (PV) is now the fastest-growing renewable technology: in 2022, global installed capacity exceeded 1,000 GW and according to the IEA it will reach over 3,000 GW by 2030 [9]. In this scenario, bifacial technology has taken on a role of growing interest, representing one of the most effective solutions to increase energy production without increasing surface consumption.

The concept of bifacial cells is not new: as early as the 1960s, some laboratories experimented with configurations capable of exploiting light incident on both sides. However, it is only with the evolution of production processes and the lowering of silicon costs that this technology has found

large-scale industrial application since 2015. Today, bifacial modules make up more than 15% of the global market and are expected to reach 30–40% by 2030 101010.

1.2.2 Working principle and definitions

A bifacial module converts into electricity both the radiation incident on the front face and that which reaches the rear face, reflected by the ground or scattered by the atmosphere.

Bifacial gain *(BG)* is calculated as:

$$BG = \frac{(E_{bif} - E_{mono})}{E_{mono}} \, x \, 100$$

Where:

E_{bif} is the annual energy produced by the bifacial module and that produced by the corresponding monofacial module.E_{mono}

Typical gain values are between 5% and 20%, but under optimal conditions (high ground reflectance and adequate plant configuration) they can reach 30% [1].

1.2.3 Construction configurations and materials

Bifacial modules are distinguished from traditional single-sided modules by:

- **Glass-to-glass structure**: both sides are protected by tempered glass, which gives greater mechanical resistance and protection from humidity and atmospheric agents.
- **Transparent glass-polymer structure**: lighter and less expensive, but with lower durability.
- **Cell technologies**: monocrystalline silicon PERC, TOPCon and HJT are the most widespread. The bifacial factor varies between 0.6 and 0.95 depending on the technology.

Another important parameter is the bifaciality ratio, which represents the performance of the posterior cell compared to the anterior cell. High values (>85%) allow you to make the most of the reflected radiation.

1.2.4 Influence of albedo and plant parameters

The albedo of the ground – i.e. the fraction of reflected radiation – is the most determining factor. Some typical values:

- New snow: 0.75–0.90
- Light sand: 0.40–0.60
- Concrete: 0.30–0.40
- Grass: 0.20–0.25
- Dark asphalt: 0.10–0.15 121212

In addition to albedo, performance depends on:

- **Ground clearance**: Higher height reduces shading and increases radiation captured at the rear.
- **Row spacing (pitch):** if too small, it increases mutual shading; if too large, it reduces the power density per area.
- **Tilt**: Must be optimized to maximize both frontal and reflected radiation.

Factor	Influenza	Typical range	Considerations
Albedo	Direct	0,1–0,9	The higher → higher the gain
Height	Direct	0.5–1.5 m	Reduces back shading
Pitch	Indirect	3–8 m	Too low penalizes energy
Tilt	Direct	20–40°	Optimize Retro Radiation

Table 1.2 – Factors Affecting the Performance of Bifacial Modules

This table shows how the design of a bifacial system requires an integrated approach: it is not enough to choose modules with high bifaciality, but it is necessary to carefully evaluate the site, the type of soil and the geometric layout.

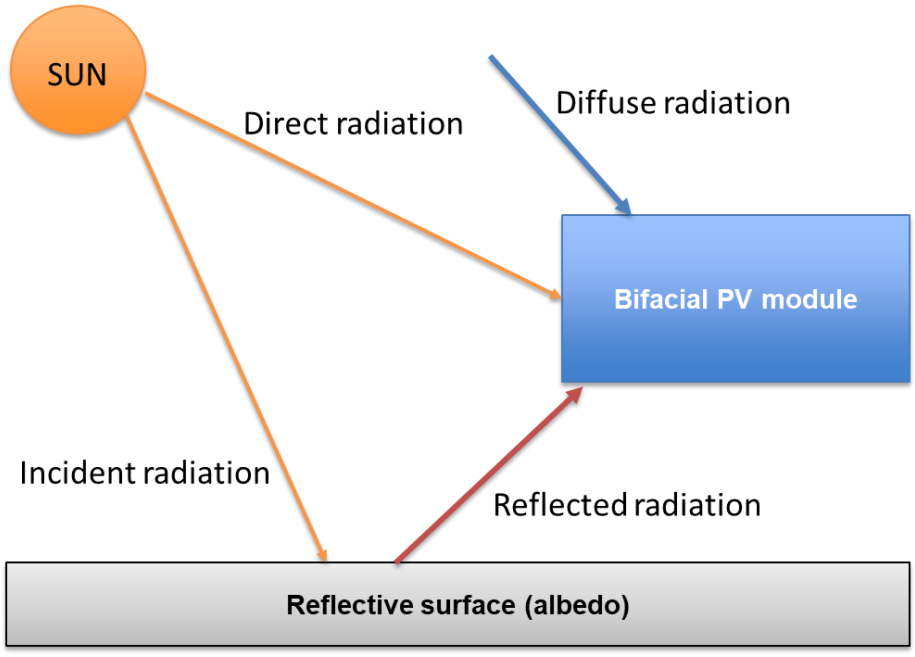

Figure 1.3– Schematic of a bifacial PV module

The figure shows the paths of direct, diffuse and reflected solar radiation that contribute to production. It highlights the role of albedo and geometric parameters (height, tilt, pitch) in optimizing performance.

1.2.5 Advantages and limitations of technology

Key benefits:

- Greater production for the same surface area.
- Reduced LCOE (Levelized Cost of Electricity) by 5–10% compared to single-sided modules.
- Greater durability (in glass-to-glass modules).
- Excellent performance in arid and desert climates.

Main limitations:

- Higher upfront cost (5–10%).
- Performance is highly dependent on local conditions.
- Need for advanced simulation models to correctly estimate the back gain.
- Measurement standards still evolving: there are still no universally shared methodologies to certify bifacial gain 131313.

1.2.6 State of research and real-world applications

Numerous studies confirm the effectiveness of bifacial modules:

- **Yang et al. (2019)** observed an average increase of 12% in experimental plants in the Gobi Desert.
- **Marion et al. (2020)** validated predictive models on several sites in the United States, with gains between 7% and 15%.
- **Pilot projects in the Middle East** have reported increases of up to 20% in high-reflectance sandy sites 141414.

From an industrial point of view, bifacial modules are increasingly used in large photovoltaic parks (*utility scale*). In 2021, China installed over 10 GW of new bifacial capacity, while in Europe several experimental projects have demonstrated technical feasibility even in temperate climates.

1.2.7 Concluding remarks

Bifacial photovoltaic technology represents an innovation that can significantly increase the energy production of solar systems. Even with slightly higher initial costs, the increased production and durability of the modules improve their economic and environmental metrics.

1.3 Hydrogen production by electrolysis

1.3.1 Introduction to the Electrolysis Process

Water electrolysis is the process by which electrical energy is used to split water molecules (H_2O) into their building blocks, oxygen and hydrogen. This is a technology that has been known for over a century, but which has only taken on strategic importance in the context of the energy transition in recent decades.

The basic principle is based on the electrochemical reaction:

$$2\ H2O\ (l) \rightarrow 2\ H2\ (g) + O2\ (g)$$

During the process, two electrodes – an anode and a cathode – are immersed in an electrolyte. By applying a potential difference, the water molecules are split: hydrogen collects at the cathode and oxygen at the anode.

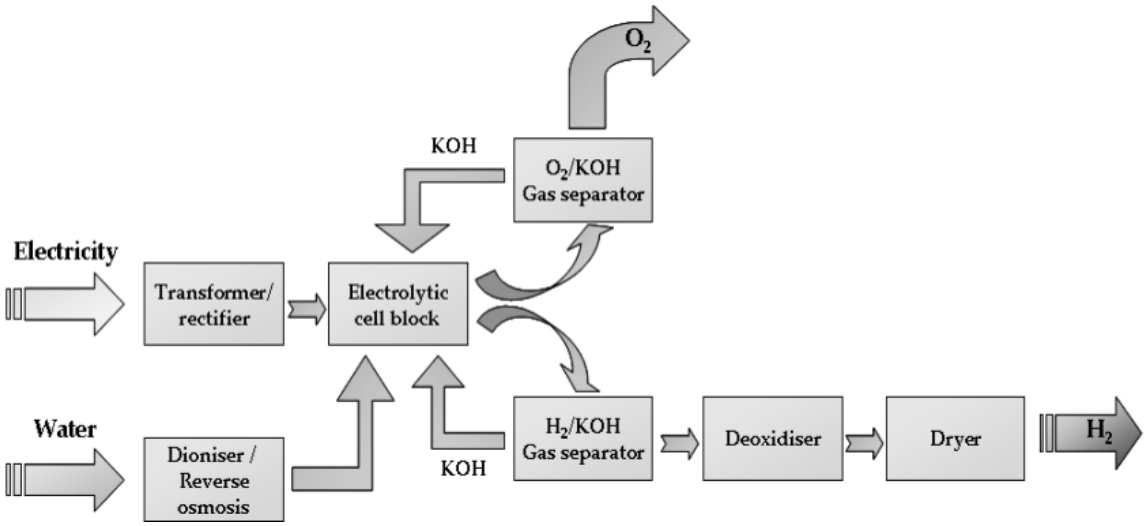

Figure 1.4 – Process diagram of alkaline electrolysis for hydrogen production: shows the main steps from water treatment to electrolysis and gas separation.

Source: IEA-ETSAP, P12 Hydrogen Production & Distribution, Technology Brief, February 2014

1.3.2 Types of electrolysers

There are three main technology configurations, each with advantages and limitations.

1. Alkaline Electrolyzers (AELs)

- Consolidated and widespread technology.
- It uses an alkaline solution (KOH or NaOH) as an electrolyte.
- Typical efficiency: 60–70%.
- Slow response times, less suitable for intermittent sources.

- Low cost, long operating life.

2. Proton exchange membrane electrolyzers (PEMs)

- They use polymer membranes as an electrolyte.
- High power density and 65–80% efficiencies.
- Quick start-up and good flexibility, therefore optimal for integration with photovoltaic and wind power.
- Higher cost due to the use of noble catalysts (platinum, iridium).

3. Solid Oxide Electrolyzers (SOEC)

- They operate at high temperatures (650–850 °C).
- Potential efficiency > 80–90%.
- Still in the development phase and with problems of durability of the materials.

Type	Efficiency	Operating Temp.	Response time	Relative cost	Technology Baccalaureate
AEL	60–70%	60–90 °C	Slow	Low	High
PEM	65–80%	50–80 °C	Fast	Medium-High	Average
SOEC	80–90%	650–850 °C	Medium	High	Low

Table 1.3 – Comparison of the main types of electrolysers

The table clearly shows that there is no "best" technology ever: the choice depends on the application context. AELs are ideal for centralized plants with a stable load profile, PEMs are preferable for applications with variable renewables, while SOECs remain confined to research.

1.3.3 Energy efficiency and yield

The efficiency of an electrolysis process is calculated as the ratio between the energy contained in the hydrogen produced (Higher Heating Value, HHV, or Lower Heating Value, LHV) and the electrical energy consumed.

- **AEL:** 60–70% (HHV)
- **PEM**: 65–80%
- **SOECs**: > 80%

The main losses derive from ohmic resistance, reaction kinetics and operating conditions (temperature, pressure). In particular, electrolyzers operating at high pressures reduce the need for subsequent hydrogen compression, improving the overall efficiency of the system.

1.3.4 Costs and prospects for reduction

The current cost of green hydrogen varies between € 4 and € 6/kg, but forecasts are for a drop below € 2/kg by 2030 in areas with a strong penetration of renewables. Economies of scale, reducing the cost of renewable electricity, and innovation in materials are the key factors.

According to the IEA Hydrogen Outlook 2022, the cost of PEM electrolysers has fallen by 60% over the past decade and could be reduced by a further 40% by 2030. AELs, being already mature, will have more limited reductions, while SOECs could only become competitive after 2035.

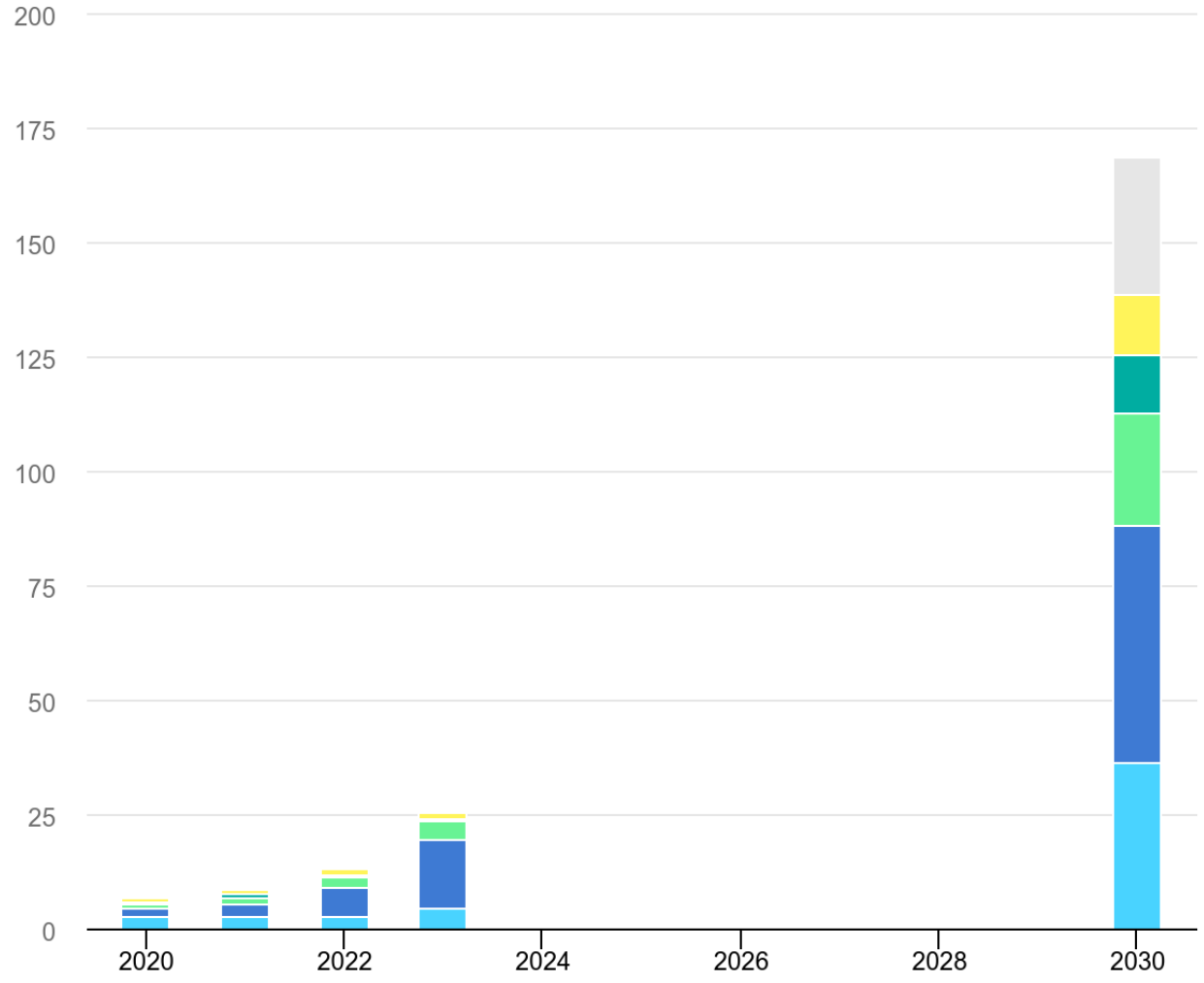

Figure 1.5 – Cumulative installed capacity of electrolysers globally through 2023 and growth scenarios through 2030. The data highlights the expected rapid acceleration, from 1.4 GW in 2023 to over 500 GW by 2030. Source: IEA, 2023

1.3.5 Applications of large-scale electrolysis

Electrolysers can be used in different configurations:

- **Centralized plants**: large electrolysers coupled with renewable power plants for large-scale production and distribution.
- **Distributed plants**: small electrolysers integrated into microgrids or industrial sites.
- **Power-to-gas**: conversion of renewable electricity into hydrogen, which is then fed into natural gas networks.
- **Power-to-liquid**: synthesis of liquid fuels (e.g. methanol, ammonia) from green hydrogen.

1.4 Fuel cells

1.4.1 General Introduction

Fuel cells (*FCs)* are electrochemical devices that directly convert the chemical energy of a fuel into electrical energy and heat, without going through a conventional combustion process. The most used fuel is hydrogen, which reacts with oxygen to produce electricity, water and heat as its only by-product.

The idea of fuel cells dates back to the nineteenth century, but it was only in the second half of the twentieth century that technology began to find practical applications, initially in space (NASA missions). Today, thanks to advances in materials and the growing need for low-emission solutions, fuel cells are considered a key technology for the energy transition.

1.4.2 Working principle

The basic principle of a fuel cell is like that of a battery: both are electrochemical devices that produce electricity. However, while a battery stores chemical energy within it, the fuel cell produces it continuously, if fuel and oxidizer are supplied.

The operation is based on three main components:

- **Anode** – fuel inlet (H_2). Here hydrogen separates into protons (H^+) and electrons (e^-).
- **Electrolyte**: membrane that allows the passage of protons but not electrons.
- **Cathode**: Oxidant (O_2) inlet Here protons and electrons recombine with oxygen to produce water and heat.

The overall reaction is:

$$2\ H_2 + O_2 \rightarrow 2\ H_2O + \text{energy (electricity + heat)}$$

1.4.3 Types of fuel cells

The main fuel cell technologies are distinguished by the type of electrolyte and the operating conditions.

- **PEMFC (Proton Exchange Membrane Fuel Cell)**
  - Electrolyte: polymer membrane.
  - Operating temperature: 60–80 °C
  - Quick start-up, high power density.
  - Sensitive to fuel purity.
  - Ideal for transportation and residential applications.
- **SOFC (Solid Oxide Fuel Cell)**
  - Electrolyte: Solid ceramic.
  - Temperature: 600–1000 °C.
  - High efficiency (up to 60% electric, >85% in cogeneration).
  - Slow start-up, but suitable for stationary industrial applications.
- **MCFC (Molten Carbonate Fuel Cell)**
  - Electrolyte: Molten carbonates.
  - Temperature: 600–700 °C.
  - Can be used with various fuels, including methane and biogas.
  - Durability limited by corrosion problems.
- **AFC (Alkaline Fuel Cell)**
  - Electrolyte: alkaline solution.
  - Temperature: 60–90 °C.
  - Historical technology, used in the Apollo space missions.
  - High efficiency, but very sensitive to impurities.

Type	Electrical efficiency	Operating Temperature	Main applications	Technology Baccalaureate
PEMFC	40–60%	60–80 °C	Transportation, residential	High
SOFC	45–60% (up to 85% in CHP)	600–1000 °C	Industrial, cogeneration	Average
MCFC	45–55%	600–700 °C	Industrial, pilot plants	Average
AFC	50–60%	60–90 °C	Special applications	Low

Table 1.4 – Comparison of the main types of fuel cells

The table shows how each type has strengths and weaknesses. PEMFCs dominate mobile applications, while SOFCs are preferred in the industrial sector. MCFCs are promising but still limited by durability issues, while AFCs now have a niche role.

1.4.4 Advantages and Criticalities of Fuel Cells

Advantages:

- Direct conversion of chemical → electrical energy, with higher efficiency than traditional combustion engines.
- Zero local emissions: the by-product is pure water.
- Possibility of cogeneration: use of the heat produced for residential and industrial applications.
- Modularity: adaptable to powers ranging from a few kW to several MW.

Criticality:

- High cost of materials, especially platinum-based catalysts.
- Limited durability: degradation of the membrane and electrodes.
- Sensitivity to fuel purity: The presence of CO or impurities can damage the cell.
- Infrastructures not yet widespread for the distribution of hydrogen.

1.4.5 State of research and future developments

The research focuses on several fronts:

- **Reduction of platinum content** in PEMFC catalysts.
- **New ceramic materials** to improve the durability of SOFCs.
- **Hybrid systems** that combine fuel cells with batteries to optimize performance in vehicles.
- **Demonstration projects**: fuel cell buses in several European cities (e.g. London, Hamburg) and SOFC power plants in Japan and South Korea.

The cost of fuel cells is expected to halve by 2030, making them competitive with internal combustion engines and gas turbines.

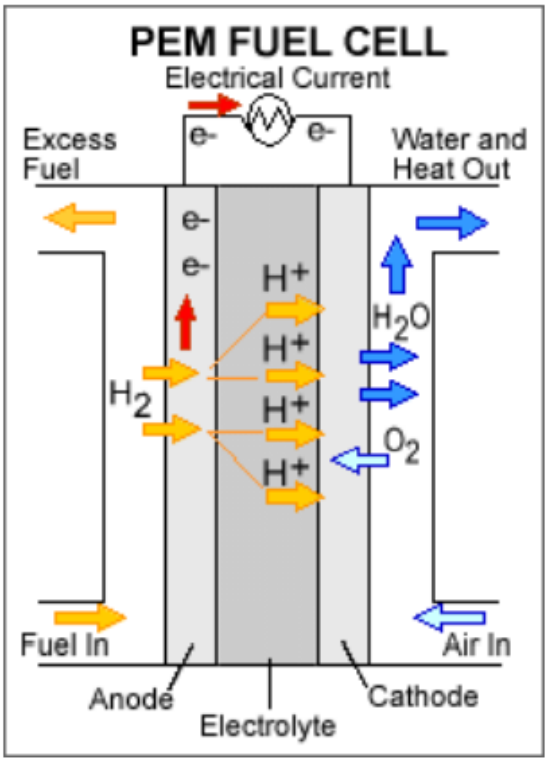

Figure 1.6 – Diagram of operation of a PEMFC (proton exchange membrane) fuel cell. Source: U.S. DOE, Fuel Cell Technologies Office (2016).

The figure illustrates the structure and operating principle of PEMFC: hydrogen feeds the anode, where it dissociates into protons and electrons thanks to the catalyst; protons cross the polymer membrane (electrolyte), while electrons travel through the external circuit producing electricity. At the cathode, protons and electrons recombine with oxygen to generate water and heat. The diagram highlights the reasons for the spread of PEMFCs (quick start, high power density) and their sensitivity to fuel purity.

1.5 Regulatory framework and international strategies

1.5.1 Introduction

The rapid development of green hydrogen and associated technologies (bifacial photovoltaics, electrolysers and fuel cells) requires not only technological innovation, but also a robust regulatory and strategic framework to guide their deployment. Norms, standards and public policies play a fundamental role in ensuring security, reliability, interoperability and attracting private investment. Without a clear and coherent regulatory framework, hydrogen projects would risk remaining confined to pilot demonstrations, without making the leap to large-scale applications.

1.5.2 International Technical Standards

On a technical level, several bodies have developed standards for hydrogen:

- **ISO 14687**: defines the purity requirements for hydrogen intended for fuel cells. It sets very strict limits for contaminants such as CO, SO_2, NH_3, which can damage catalysts.
- **ISO 19880**: Specifies safety requirements for hydrogen refueling stations, with a focus on high pressures (350–700 bar).
- **IEC 62282**: Series of standards covering design, safety, performance, and test methods of fuel cells.
- **EN 17127 (Europe):** regulates the safety and quality requirements for refuelling infrastructures in Europe.

Standard	Main object	Scope
ISO 14687	Hydrogen purity	Fuel cells
ISO 19880	Filling station safety	H_2 Mobility
IEC 62282	Performance and Fuel Cell Testing.	Energy sector
EN 17127	H_2 safety and quality	Europe

Table 1.5 – Main technical standards for hydrogen

This table shows that standardization is already very advanced, especially in relation to safety and performance, but the issue of a global hydrogen sustainability certification scheme remains open .

1.5.3 European strategies

The European Union is one of the world's leading promoters of a hydrogen economy. Key documents include:

- **EU Hydrogen Strategy (2020):** target installation of 40 GW of electrolysers by 2030 and production of **10 Mt/year of green hydrogen**.
- **REPowerEU (2022):** in response to the energy crisis, increased the target to 20 Mt/year by **2030** (10 Mt domestically produced and 10 Mt imported).
- **IPCEI – Important Projects of Common European Interest**: mechanism to finance transnational strategic projects, including electrolysis plants and H_2 transport infrastructure.

Countries such as Germany, France, Italy and Spain have published their own national strategies, with coherent objectives but calibrated on local resources. Germany, for example, aims to become a net

importer, while Spain aims to take advantage of the high availability of solar resources to produce low-cost green hydrogen.

1.5.4 Strategies outside Europe

- **Japan**: first country in the world to adopt a national hydrogen strategy (2017). It aims to power a large part of public transport with fuel cells by 2030.
- **South Korea**: launched the Hydrogen Economy Roadmap (2019), which envisages the mass production of hydrogen vehicles and the expansion of refuelling stations.
- **United States**: The Department of Energy (DOE) launched the Hydrogen Energy Earthshot (2021) with the goal of reducing the costs of green hydrogen to $ 1/kg by 2030. The Inflation Reduction Act (2022) introduced tax incentives of up to $3/kg for the production of renewable H_2.
- **China**: has integrated hydrogen into the 2021–2025 five-year plan, with investments in production and mobility infrastructure.
- **UAE and Saudi Arabia**: thanks to the abundance of solar and wind resources, they aim to become global exporters. Projects such as NEOM (Saudi Arabia) and the Hydrogen Leadership Roadmap (UAE) are concrete examples of this.

Figure 1.7 – State of national hydrogen strategies at global level (recent update). Source: IRENA (2024)

The map summarises the spread of national hydrogen strategies, highlighting the breadth of political

commitment in different countries and geographical areas. Europe and Asia are the most advanced poles, with mature strategies and quantitative targets for 2030; North America shows a strong acceleration driven by federal incentives; The Middle East and Australia are aiming to be exporters thanks to the high availability of renewable resources. The comparison allows the regulatory framework of chapter 1.5 to be placed in a coherent international perspective.

1.5.5 Role of certification and guarantee of origin schemes

A key aspect for international hydrogen trade will be the certification of its sustainability. To date, several countries are developing Guarantee of Origin (GoO) schemes to certify that the hydrogen produced is truly renewable. The EU is working on a unified certification system that will become crucial for international trade.

1.5.6 Concluding remarks

The international regulatory and strategic framework shows a strong convergence towards hydrogen as a pillar of decarbonisation. However, differences in approaches persist: while Europe pushes domestic production and imports, the United States and Asia focus on technological competitiveness. Countries in the Middle East and Australia, on the other hand, aim to carve out the role of exporters.

1.6 Research trends and perspectives

1.6.1 Introduction

Scientific and technological research on green hydrogen and related technologies (bifacial photovoltaics, electrolysers, fuel cells) is evolving very rapidly. Publications, patents and investments in demonstration projects have grown exponentially over the past decade. This dynamic reflects the awareness that hydrogen is no longer just a future prospect, but a key element in achieving climate neutrality by 2050.

1.6.2 Photovoltaic–hydrogen–fuel cell integration

One of the most promising lines of research concerns the integration of PV–H_2–FC systems, in which solar energy powers an electrolyzer that produces hydrogen, which is then stored and converted back into electricity by means of fuel cells. This scheme, also known as power-to-power, allows renewable energy to be stored on a seasonal scale.

The challenge is to improve the overall efficiency of the system: currently, all conversions result in a net return of 25–35%. Studies focus on:

- development of algorithms for the optimal management of energy flows;
- use of high-reflectance surfaces to maximize bifacial production;
- reduction of losses in hydrogen compression and storage processes.

1.6.3 Innovation in materials

Another crucial area of research is represented by advanced materials:

- **Electrolyzers**: Development of non-noble catalysts to reduce dependence on platinum and iridium. New membranes with higher proton conductivity and mechanical strength.
- **Fuel cells**: study of alternative catalysts to platinum, ceramic electrolytes for more stable and resistant SOFCs, more durable membranes for PEMFCs.
- **Bifacial photovoltaics**: optimization of transparent materials and improvement of the mechanical resistance of glass-glass configurations.

These advancements can reduce costs and increase the useful life of systems, improving overall economic competitiveness.

1.6.4 Cost reduction and scalability

The economic factor remains decisive. International agencies estimate that:

- The cost of green hydrogen (LCOH) will fall from €4–6/kg (2020) to less than €2/kg by 2030 in areas with a strong renewable resource 161616.
- Electrolyser costs could be reduced by 70% by 2040 thanks to economies of scale and manufacturing innovations.
- Fuel cells, which are expensive today, will be able to halve the price by 2030, making the use of hydrogen in heavy mobility competitive.

Scalability is a priority objective: modular electrolysers of hundreds of MW and bifacial PV plants of over 1 GW are being developed to be integrated into hubs for the production and export of hydrogen.

1.6.5 Pilot and demonstration projects

In recent years, a number of pilot projects have been launched that demonstrate the technical and commercial feasibility of hydrogen solutions:

- **REFHYNE (Germany):** 10 MW PEM electrolyser powered by renewable energy, integrated into a refinery.

- **NEOM (Saudi Arabia):** one of the largest projects in the world, with photovoltaic and wind power plants integrated with 2 GW electrolysers to produce green ammonia for export.
- **HyDeploy (UK):** project to blend hydrogen with natural gas in existing networks, up to 20% by volume.
- **Hydrogen Park South Australia**: pilot plant for the production of green hydrogen and feeding local microgrids.

These projects demonstrate how research is not confined to laboratories, but is translating into concrete applications on a large scale.

1.6.6 Future prospects

Looking to the future, the main lines of research and development are:

- **Hydrogen microgrids**: integrated local systems that leverage photovoltaics, electrolysers, H_2 storage and fuel cells to provide stable and resilient energy to communities or industrial sites.
- **Power-to-X**: production of hydrogen derivatives (ammonia, methanol, synthetic fuels) as energy carriers for long-distance transport.
- **Circular economy and sustainability**: LCA (Life Cycle Assessment) analysis to assess the overall environmental impact of H_2 technologies.
- **Digitalization and AI:** use of artificial intelligence algorithms to optimize the real-time management of energy flows and improve the predictive reliability of plants.

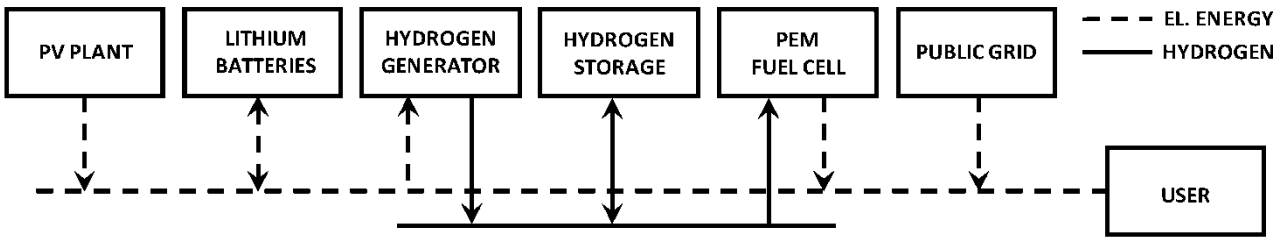

Figure 1.8 – Conceptual scheme of a hydrogen microgrid: integration between renewables, electrolyzer, H_2 tanks and fuel cells to support loads. Source: Serra et al., Energies (2020).

The scheme represents the typical architecture of an H_2-based microgrid: electricity from photovoltaic/wind power feeds the electrolyzer, the hydrogen produced is stored and subsequently converted back into electricity via fuel cells, with the possible co-existence of batteries for short-term regulation. The solution enables seasonal storage, increases the renewable share and improves the resilience of the local system with respect to the intermittency of sources.

1.6.7 Conclusions

Research and innovation in the green hydrogen sector are moving at an unprecedented pace. Public and private investments, combined with the consolidating regulatory framework, indicate that hydrogen will be one of the pillars of the global energy transition. The medium-long term prospects are positive: by 2050, green hydrogen could cover more than 20% of the world's energy demand, becoming an essential element for achieving climate neutrality.

2 DESIGN OF THE INNOVATIVE EXPERIMENTAL SYSTEM

2.1 General description of the system

The experimental system created integrates three key technologies of the energy transition into a single platform:

- **bifacial photovoltaic system**, intended for the generation of electricity from solar sources;
- **electrolyser**, for the production of green hydrogen from renewable electricity;
- **fuel cell**, for the conversion of stored hydrogen into electricity and heat.

The plant was conceived as a demonstration microgrid, capable of operating in stand-alone mode, simulating a complete *power-to-gas-to-power (P2G2P)* chain. The chosen installation site, on the campus of the University of Sharjah, has climatic conditions particularly suitable for this type of test: high global solar radiation, clear skies for most of the year, ambient temperatures often above 35 °C. These conditions allow to experimentally validate the performance of bifacial modules and electrolysers operating in a desert context, with significant implications for future large-scale projects in the United Arab Emirates and other areas with strong insolation. [21]

2.1.1 System block structure

The system can be described through the following functional blocks:

1. **Renewable generation (bifacial PV)**
    - Bifacial photovoltaic modules mounted on fixed structures with optimized tilt angle. [22]
    - Connected to a DC/AC inverter responsible for power conditioning and grid interfacing.
2. **Conversion and storage (Electrolyzer + H_2 storage)**
    - PEM electrolyzer, powered directly by the energy produced by the PV.
    - Production of hydrogen stored in high-pressure tanks.
3. **Reconversion (Fuel Cell)**
    - PEMFC fuel cell connected to tanks.
    - Electricity and heat generation for local applications or for feeding into microgrids.
4. **Auxiliary and monitoring systems**
    - Sensors for temperature, irradiance, voltage, current, pressure and flow rate.
    - Data acquisition system (DAQ) and remote monitoring software platform.
    - Integrated security and control logics.

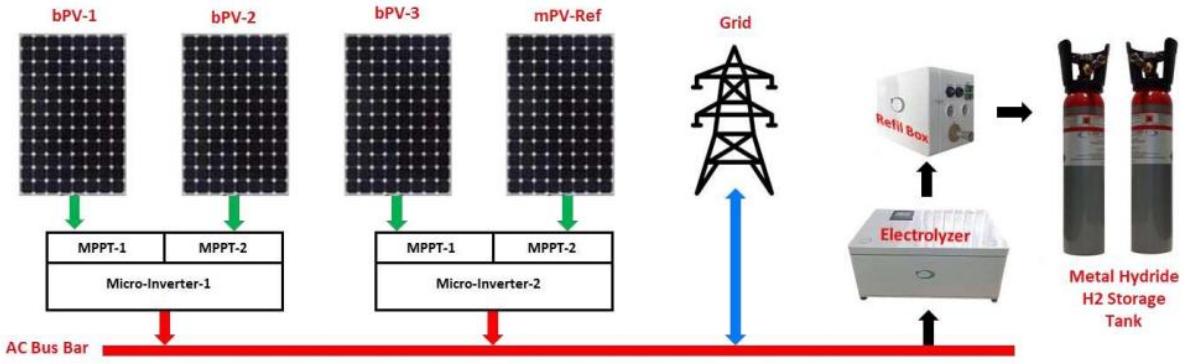

Figure 2.1 – Schematic of Solar PV system for Hydrogen Production System. The grid connection highlights the potential bidirectional operation of the system: photovoltaic energy can be supplied both to the hydrogen production system and to the grid, while the electrolyzer can also be directly powered by the grid when photovoltaic generation is insufficient

The inverter-based architecture enables flexible energy management, allowing bidirectional power exchange with the grid depending on photovoltaic availability and system operating conditions.

2.1.2 Functional objectives of the system

The plant has been designed with a dual purpose:

- **scientific research**: validation of the experimental performance of the individual components and of the integrated PV-Electrolysis-FC chain, with high-resolution data acquisition;
- **technological demonstration**: creation of a functioning and replicable platform, capable of showing industrial and institutional bodies the feasibility of an integrated system based on green hydrogen.

The system has been designed with modular logic, so as to allow future expansions (e.g. increase in PV power, addition of batteries as rapid storage, expansion of H_2 storage capacity).

2.2 Bifacial photovoltaic field: architecture, surfaces and performance

The bifacial photovoltaic system is the heart of the experimental system, as it provides the primary electrical energy necessary to power the electrolyzer and, indirectly, to the entire *power-to-gas-to-power* chain. The choice to use bifacial modules, rather than conventional monofacial modules, responds to the need to maximize energy production in a context characterized by high solar radiation

and strong ground reflection, typical of the environmental conditions of the United Arab Emirates. [23].

2.2.1 Architecture of the experimental photovoltaic system

The photovoltaic field installed on the roof of the W12 building of the University of Sharjah was designed to test in real conditions the integration of bifacial modules in an experimental system for hydrogen production. The system consists of:

- **3 bifacial modules** of 365 Wp (Jollywood brand, bifacial PERC technology);
- **1 single-sided module** of 365 Wp (Jinko brand, used as a reference);
- **Hoymiles HM-1500 micro-inverters**, for independent monitoring and MPPT for each module.

All modules are mounted with a fixed inclination of 25°, oriented to the south and placed 76 cm from the roof level. This configuration is optimized for the local climatic context, characterized by high direct radiation, clear skies and low presence of dust at high altitude in the winter months. [24]

Figure 2.2 – Positioning of photovoltaic panels in the field

The figure shows the real-field positioning of the photovoltaic panels, which are installed on the roof of the W12 building of the University of Sharjah.

2.2.2 Reflective surfaces and albedo

In order to evaluate the effect of albedo on electricity production, the bifacial modules were installed on three different surfaces:

- Surface 1 – Green (PVC similar to artificial turf)
- Surface 2 – Grey (standard flooring)

- Surface 3 – White (high reflectance sheet metal, cool roof effect)

The choice of these materials allows you to simulate real-world scenarios with increasing levels of reflectance. In particular, the white surface was selected to maximize the reflection of light towards the back of the bifacial modules. [25]

Surface	Description	Estimated albedo [-]
Green	Synthetic turf	0.18 – 0.25
Grey	Neutral flooring	0.25 – 0.35
White	Cool roof with high reflectance	0.65 – 0.85

Table 2.1 – Type of surfaces and expected albedo

Table 2.1 reports expected albedo ranges for different ground surface typologies, as commonly adopted in literature. Experimental insight into ground optical behavior is provided by the spectral reflectance measurements reported in Fig. 4.5. Highly reflective surfaces exhibit consistently higher reflected radiance across the visible and near-infrared spectrum, in qualitative agreement with the albedo ranges reported in Table 2.1.

2.2.3 Electrical Configuration and Monitoring

Each PV module is connected to a Hoymiles HM-1500 micro-inverter, which allows you to independently monitor:

- instantaneous power (W),
- daily energy (Wh),
- DC voltage and current on the module side,
- overall inverter-module efficiency.

The data were acquired in continuous mode via a dedicated gateway with a sampling rate per minute, and saved in CSV format for experimental analysis.

2.2.4 Experimental tests on reflective surfaces

The tests were conducted on 17 February and 3 March 2023, both with ideal weather conditions (clear skies, low relative humidity, ambient temperature between 25 °C and 29 °C).

In each test, the three bifacial modules were placed on top of the three different surfaces, keeping the inclination and orientation constant. The reference single-sided module was kept on a gray surface.

The aim was to assess the difference in performance attributable solely to the albedo of the underlying surface.

2.2.5 Analysis of the results: comparison between surfaces

Analysis of the instantaneous power curves highlights a clear performance improvement for the high-reflectance (white) surface compared to the other investigated configurations. In particular, during the central hours of the day, the white surface exhibits a peak power increase exceeding 25% with respect to the monofacial reference, due to the enhanced rear-side irradiance contribution.

The effect of surface reflectance is further confirmed when considering daily energy production, as reported in Table 2.2.

Configuration	Daily energy [kWh]	Increase vs. monofacial [%]
Monofacial PV (reference)	1.94	–
Bifacial PV – Green surface	2.27	+17.26
Bifacial PV – Grey surface	2.32	+19.72
Bifacial PV – White surface	2.49	+28.47

Table 2.2 – Daily energy production for different ground surface configurations (day: 17/02/2023)

Table 2.2 compares the daily energy production of bifacial configurations against a common monofacial reference (mPV-Ref), allowing a consistent evaluation of bifacial gain for the investigated ground treatments.

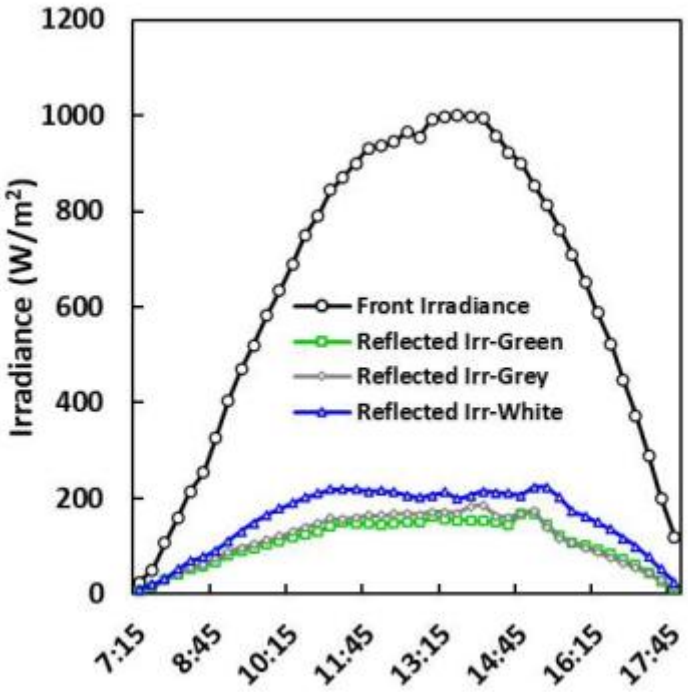

Figure 2.3 – Measured front-side irradiance and reflected irradiance profiles for the three investigated ground surface configurations (green, grey, white) during February 17.).

Figure 2.3 shows the measured irradiance profiles during the experimental day, highlighting the contribution of reflected irradiance for different ground surface treatments. The higher reflected irradiance associated with the white surface explains the increased rear-side contribution observed in bifacial photovoltaic performance.

2.2.6 Technical considerations and perspectives

The experimental results obtained confirm the theoretical expectations about the impact of albedo on the performance of bifacial modules. Especially:

- The increase in production is more marked during the hours of greatest sunshine;
- The white surface proves to be particularly effective in environments with little shading;
- The albedo effect is amplified by the height from the ground and the tilt of the module.

These findings confirm the validity of the double-sided approach with a reflective surface in desert or high-insolation contexts, and lay the foundations for a more accurate design of PV systems integrated with electrolysers.

Sharjah's bifacial photovoltaic plant is an example of design aimed at enhancing local environmental conditions. The combination of high radiation, medium-high albedo and optimized orientation allows you to make the most of the potential of bifacial technology. At the same time, the presence of high

temperatures and soiling phenomena introduces operational challenges that enrich the experimental analysis, making the plant a test bed of particular scientific and technological interest.

2.3 Electrolysis System

The electrolysis system forms the heart of the green hydrogen production process, transforming the electrical energy produced by the bifacial photovoltaic modules into stored chemical energy in the form of H_2. The selection of technology, operating parameters and ancillary subsystems was driven by the need to achieve a trade-off between efficiency, operational flexibility and cost, with a focus on direct integration with variable PV generation.

2.3.1 Technology Adopted

A PEM (Proton Exchange Membrane) electrolyser was chosen for the Sharjah experimental plant. This technology has several advantages over traditional alkaline electrolysers and solid oxide electrolysers (SOEC):

- **Fast response**: PEM electrolysers are able to quickly adapt to the power fluctuations typical of intermittent renewable sources, with reduced start-up and stop times (in the order of seconds) [26].
- **High efficiency**: the electrical efficiency is between 65 and 80% on an HHV basis, in line with the values reported in the literature for systems of comparable size [27].
- **Compactness and modularity**: The small footprint allows for easier integration into demonstration plants.
- **High-pressure production**: The ability to achieve H_2 already at pressures above 20–30 bar reduces the need for external compressors, with energy and safety benefits.

Compared to alkaline electrolyzers, PEMs guarantee higher current density and higher purity of the gas produced; compared to SOECs, they offer much faster response times, but with moderate operating temperatures and currently higher costs [28].

2.3.2 Operating Parameters

The electrolyzer installed at the experimental plant is a Hy-PEM-XP Home supplied by H2 Planet. It is a compact system, designed for demonstration applications and for integration into small hydrogen plants.

Its main nominal characteristics are:

- power consumption equal to 1300 W,

- hydrogen production capacity of approximately 2000 cm^3/min, equivalent to 120 L/h (≈ 0.12 Nm^3/h),
- Adjustable operating pressure between 1 and 16 bar, compatible with low-pressure tanks such as metal hydride tanks.

Parameter	Face value	Unit	Notes
Electrical power consumption	1300	W	Nominal consumption
Production capacity H_2	0,12	Nm^3/h	≈ 2000 cm^3/min = 120 L/h
Adjustable pressure	1–16	bar	Suitable for low-pressure storage
Purity H_2	> 99.99	%	Declared by the manufacturer
Electrical efficiency	65–75	% LHV	In line with values in the literature [29]
Operating Temperature	50–80	°C	Liquid-cooled
Electrolyte	Proton conduction polymer membrane	–	PEM

Table 2.3 – Hy-PEM-XP Home (H2 Planet) electrolyzer nominal parameters

Although Table 2.3 reports the nominal operating parameters of the electrolyzer, its actual behavior under photovoltaic-driven operation is influenced by additional operational constraints. The system requires demineralized water to ensure stable membrane performance and prevent long-term degradation associated with ionic contamination.

During operation, the electrolyzer adapts its operating voltage according to the supplied current, following the characteristic polarization behavior of PEM technology. Hydrogen production is effectively inhibited below a minimum power threshold, due to auxiliary system requirements and electrochemical activation limits. As a result, under low-power operating conditions, the relationship between electrical input power and hydrogen production deviates from ideal linearity.

The electrolyzer operates within the adjustable pressure range reported in Table 2.3 and does not include an integrated hydrogen compression stage. Auxiliary components, including control

electronics and cooling systems, contribute to the overall electrical consumption and have a non-negligible impact on system efficiency, particularly under partial-load operation. These effects are further analyzed in the experimental results presented in Chapter 5.

2.3.3 Auxiliary systems

In addition to the electrolytic stack, the plant includes subsystems that are critical to operation:

- **Water treatment**: deionization and degassing to ensure conductivity < 0.1 μS/cm, essential to avoid membrane degradation.
- **Cooling**: liquid circuit with heat exchangers, necessary to dissipate the heat generated by internal electrical losses.
- **Pressure regulation**: Redundant valves and sensors to keep the operating pressure within safe limits.
- **Monitoring**: voltage, current, gas flow and purity sensors for real-time control.

2.3.4 Integration with the photovoltaic field

The power generated by the bifacial photovoltaic modules is processed through an inverter-based power conditioning stage, enabling stable and flexible electrical coupling between the PV generator and the PEM electrolyzer.

This configuration allows to:

- analyze performance under real-world conditions of solar variability,
- test logic to maximize overall PV–H_2 efficiency,
- avoid excessive on/off cycles that would accelerate membrane degradation.

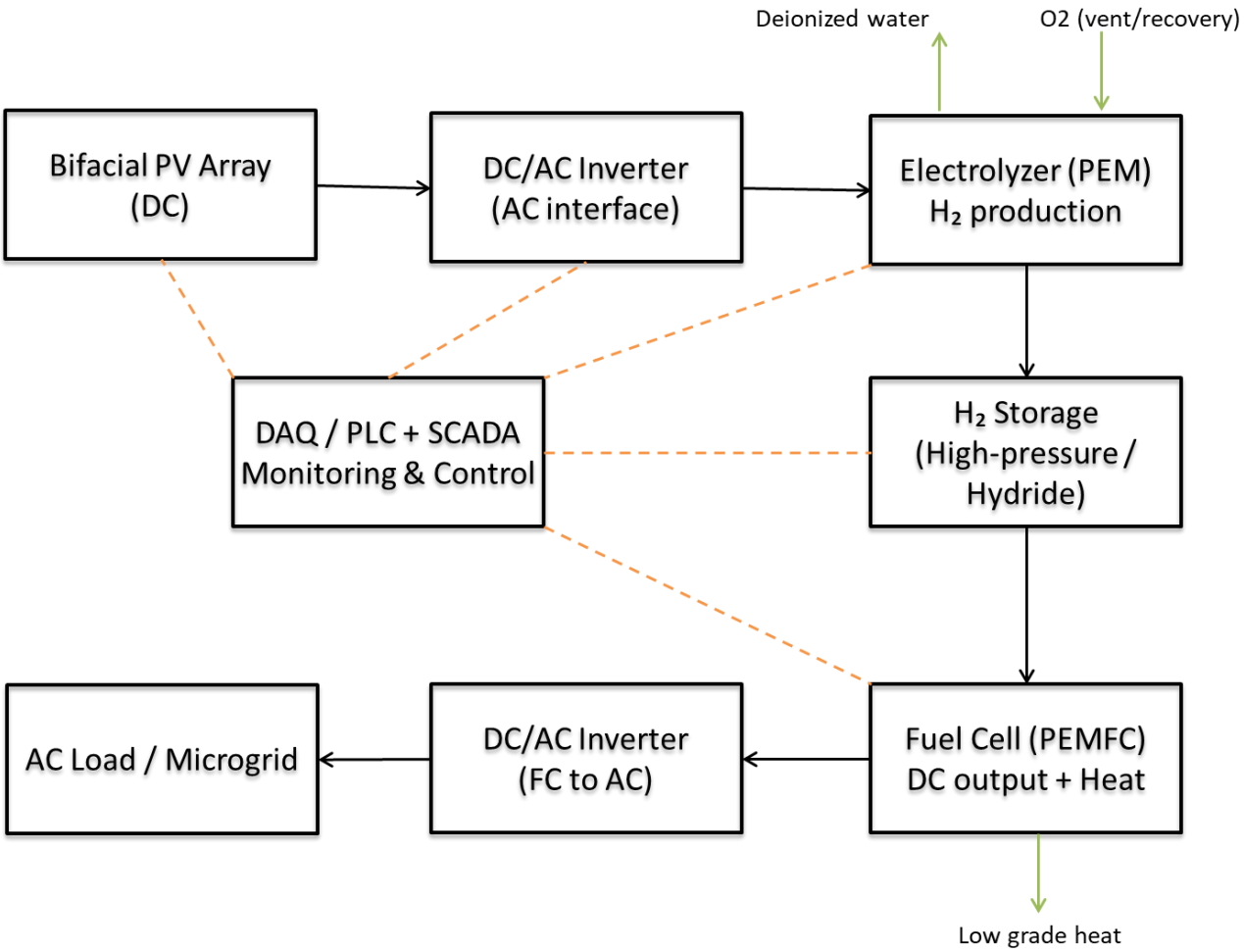

Figure 2.4 – Block diagram of the integration between bifacial photovoltaic field and PEM electrolyzer

2.3.5 Dynamic performance and critical aspects

Under full irradiance conditions, the electrolyzer can reach the nominal output. However, the variability of the solar source is reflected in power fluctuations, resulting in a reduction in average efficiency.

The electrolysis process can be described by Faraday's law:

$$n_{H2} = \frac{I * t}{2F}$$

where:

- n_{H2} is the amount of moles of hydrogen produced,
- I the current applied,
- t the operating time,

- F is Faraday's constant (96.485 C/mol).

This relationship shows how the production of hydrogen is directly proportional to the current absorbed, and therefore to the power available from the PV field.
The main critical issues identified are:

- dependence on the continuity of the solar source, in the absence of electricity storage systems,
- degradation of the polymer membrane, accelerated by rapid start/stop cycles,
- the need for high water purity, otherwise the efficiency and duration of the system will be reduced [30].

2.3.6 Operational safety

Hydrogen plants require strict safety protocols. The electrolyzer is therefore equipped with:

- H_2 sensors at the threshold < 1% vol. to detect leaks,
- overpressure valves to avoid critical conditions in the tanks,
- forced ventilation of the technical area,
- automatic shutdown logics in case of failures,
- Electrical interlock systems to prevent unauthorized ignition.

These measures guarantee compliance with international standards (e.g. IEC 62282-4-101 for PEM electrolysers) [31].

2.3.7 Concluding remarks

The integration of a PEM electrolyzer with a bifacial photovoltaic system in desert conditions constitutes a technologically advanced solution to produce green hydrogen. The analyses carried out in this section provide the basis for subsequent experimental evaluation (Chapter 3) and for the modeling of the system (Chapter 4).

2.4 Hydrogen Storage System

Hydrogen storage is a fundamental element of the *power-to-gas-to-power* chain, as it makes it possible to decouple the production phase (linked to solar variability) from the use phase (electric conversion through fuel cells or industrial use). [32] In the Sharjah experimental system, storage is entrusted to an innovative metal hydride tank, chosen to ensure safety, compactness and ease of integration in a university demonstration context.

2.4.1 Type of tanks adopted

A My H_2 2000 tank based on metal hydride technology was used for the plant. The main features are:

- **Storage capacity**: 2 Nm^3 H_2.
- **Interior volume**: 3 L.
- **Total weight**: 14 kg.

Unlike high-pressure tanks or liquid hydrogen, metal hydride systems allow hydrogen to be stored in safer conditions, thanks to its absorption in solid form within the metal matrix [33].

2.4.2 Technical Parameters

Parameter	Typical value	Unit
Storage capacity	2	Nm^3 H_2
Internal volume	3	L
Weight	14	Kg
Technology	Metal hydride	–

Table 2.4 – Technical parameters of the My H_2 2000 tank.

2.4.3 Security systems

The metal hydride tank guarantees a higher level of safety than compressed gas systems:

- in the event of a rupture there is no immediate release of hydrogen in large quantities;
- the working pressure is relatively low;
- the release of H_2 occurs by controlled thermal desorption.

However, there are pressure and H_2 concentration sensors, as well as safety valves and forced ventilation in the technical area [34].

2.4.4 Integration into the PV–H_2–FC system

The connection between the electrolyzer and the tank is made by means of certified stainless steel pipes, with non-return valves and pressure monitoring systems. The hydrogen stored in My H_2 2000 is then sent to the fuel cell through a dedicated circuit, which regulates its pressure and flow rate. The stored hydrogen can be fed back into the system through a direct supply line to the fuel cell.

Figure 2.5 – Hydrogen storage system: High-pressure composite steel tank used in the Sharjah experimental plant.

2.4.5 Operational considerations

The adoption of a metal hydride tank allows you to:

- improve operational safety,
- simplify management in the university environment,
- experiment under realistic conditions without the risks associated with high-pressure systems.

The sizing (2 Nm^3 capacity) guarantees a few hours of fuel cell operating autonomy, allowing to validate off-grid microgrid scenarios in real conditions [35].

2.5 Fuel cells

Fuel cells (FC) are the device for converting the chemical energy contained in hydrogen into electricity and heat. Within the PV–H_2–FC experimental system in Sharjah, the fuel cell constitutes the final link in the *power-to-gas-to-power* chain, allowing to test the continuity of electricity supply even in the absence of solar radiation [36].

2.5.1 Technology Adopted

A PEMFC (Proton Exchange Membrane Fuel Cell) was selected for the experimental plant, specifically the GreenHub2 PRO 1000 (H2 Planet) model, chosen in line with the type of electrolyzer adopted.

The main reasons are:

- **Compatibility**: PEMFC uses high-purity hydrogen, in line with the output of the PEM electrolyzer.
- **Low operating temperature**: 60–80 °C, which allows for fast start-ups and fewer thermal management issues [37].
- **Modularity**: possibility of creating stacks with scalable powers from a few kW up to hundreds of kW.
- **Demonstration applicability**: Suitable for experimental systems, residential and mobility applications.

2.5.2 Technical Parameters

The installed fuel cell has a maximum power of 1000 W and a nominal power between 800 and 900 W, depending on the operating mode (AC/DC). The stack voltage is in the range of 12.2–13.8 VDC, with an electrical efficiency of 45–55% [38].

Parameter	Value	Unit
Maximum power	1000	W (5 s peak)
Rated power	800–900	W
Electrical efficiency	45–55	%
Output voltage	12,2–13,8	VDC / AC Schuko
Power pressure H_2	6–25 (max 27)	bar
Required purity H_2	99,995 (grade 4.5, 5.0 recommended)	%
Operating Temperature	60–80	°C
Dimensions	600 × 400 × 250	Mm
Weight	24–28	Kg

Table 2.5 – Technical parameters of the PEMFC GreenHub2 PRO 1000 fuel cell

2.5.3 Balance of Plant (BoP) system

In addition to the stack, the fuel cell requires several auxiliary subsystems:

- **Hydrogen fuel system**: Pressure regulators, valves, and sensors to ensure stable flow.
- **Air/cathode system**: compressor or fan to supply the oxidizer (oxygen from the air).
- **Cooling system**: liquid heat exchanger to maintain the operating temperature.
- **Control system**: electronic logics for monitoring voltages, currents and operating parameters.
- **Safety**: H_2 sensors, emergency valves, automatic shutdown procedures [38].

2.5.4 Integration with the PV–H_2–Electrolysis system

The fuel cell is connected to the high-pressure hydrogen tanks described in §2.4. The H_2 is adjusted to operating pressure (1–3 bar) via a dedicated supply line and sent to the stack.

#	Description	#	Description
1	Key switch	7	I/O ports
2	Display LCD Touch 3.2"	8	USB port
3	Power led	9	AC output main socket
4	Ground connection	10	DC output socket (banana-plug)
5	H2 gas inlet connector	11	4 A fuse for banana-plug
6	H2O Outlet		

Figure 2.6 – GreenHub2 PRO 1000 PEMFC fuel cell used in the PV–H_2–FC experimental plant at the University of Sharjah with legend of connection and use points.

The figure shows the installed fuel cell with the various connection or use points of the system described in the legend

2.5.5 Performance and criticality

During operation, the fuel cell achieves:

- **Electrical production**: equal to about 0.7–0.8 V/cell, with an efficiency of 45–55% [38].
- **Cogeneration**: possibility of exploiting low-temperature heat for thermal uses (e.g. space heating or domestic hot water).

The main critical issues to consider are:

- **Limited durability**: degradation of the membrane and catalysts over time [39].
- **Fuel purity**: The presence of CO or other impurities can poison the platinum catalyst [37].
- **Costs are still high**: especially related to catalyst materials.

Within the overall PV–H_2–FC system, durability and cost considerations are not limited to the fuel cell but also apply to the electrolyzer, which plays a key role in determining the long-term performance and scalability of the hydrogen conversion chain.

Proton Exchange Membrane electrolyzers are characterized by high efficiency and fast dynamic response, making them particularly suitable for integration with variable renewable energy sources. However, durability and capital cost remain key factors influencing large-scale deployment. Typical PEM electrolyzer lifetimes reported in the literature range between 50.000 and 80.000 operating hours, with degradation rates strongly affected by operating conditions such as current density, start–stop cycles, and water purity.

Current capital costs for PEM electrolyzers are commonly reported in the range of 900–1.500 €/kW, although significant cost reductions are expected in the coming years due to technological improvements and economies of scale. These aspects directly impact the economic feasibility and scalability of photovoltaic-driven hydrogen production systems and should be carefully considered when evaluating long-term system performance.

2.5.6 Considerations

The adoption of a PEM fuel cell in the experimental system makes it possible to demonstrate the feasibility of the energy conversion of locally produced hydrogen. Despite limitations in terms of durability and cost, the technology is already among the most promising for decentralized, residential and hydrogen mobility applications [36].

2.6 Instrumentation and monitoring

Accurate monitoring of operating parameters is an essential element for the experimental validation of the PV–H_2–FC system. Without a reliable measurement system, the data collected would be incomplete or unrepresentative, making it difficult to assess actual performance. The plant was therefore equipped with an integrated set of sensors, transducers and data acquisition (DAQ) systems, with the aim of monitoring both energy flows and environmental and operational variables in real time.

2.6.1 Measured quantities

The main quantities monitored are:

- **Global and diffuse solar irradiance** (W/m²), by means of dedicated pyranometers and bifacial sensors.
- **Ambient and PV module temperature** (°C), via thermocouples and PT100 sensors.
- **Electrical quantities of the PV field**: string voltage (V), current (A), instantaneous power (kW).
- **Operating parameters of the electrolyzer**: cell voltage and current, water flow rate, outlet pressure, operating temperature.
- **Pressure and flow rate of hydrogen in tanks**.
- **Fuel cell performance**: stack voltage, current output, electrical power, operating temperature.
- **Flow rate and pressure of incoming** and outgoing gases.

2.6.2 Equipment used

Measured quantity	Sensor/Instrument	Measuring range	Typical accuracy
Sunlight	Pyranometer Class A	0–2000 W/m²	±2%
Module/room temperature	Thermocouples, PT100	−20 ÷ 100 °C	±0.5 °C
PV voltage	Voltage Transducer	0–1000 V	±0.5%
PV Current	Current transducer	0–100 A	±0.5%
Voltage/current electrol.	Built-in DC/DC sensors	0–5 V, 0–100 A	±0.2%
H_2 Pressure	Piezoelectric transducer	0–350 bar	±0.25%
Flow rate H_2	Thermoflow meter	0–100 Nl/min	±1%

Fuel cell parameters	Sensors integrated into the stack	0–60 V, 0–200 A	±0.5%

Table 2.6 – Main measuring instruments installed in the experimental plant.

2.6.3 Data Acquisition System (DAQ)

All signals from the sensors are collected by a centralized DAQ system, based on:

- **analog-to-digital acquisition modules** (with 16-bit resolution and sampling rate up to 1 Hz),
- **SCADA** (Supervisory Control and Data Acquisition) supervision software, for real-time visualization and storage on databases,
- **Web interface** for remote access by researchers.

The system allows continuous data recording, with the possibility of exporting it in CSV/Excel format for subsequent analysis. Data validation algorithms have also been implemented to discard any outliers or out-of-range values.

2.6.4 Innovative monitoring system

Compared to other experimental plants described in the literature, the Sharjah system stands out for some innovative aspects:

- **multi-level integration**: all electrical, thermal and chemical quantities are acquired from a single centralized system;
- **time synchronization**: all data are recorded with the same time reference, facilitating the analysis of energy flows;
- **high sampling rate**: it allows you to capture rapid dynamics, such as sudden changes in solar radiation or transient responses of the fuel cell;
- **User-friendly interface**: Graphical dashboards allow intuitive control of the plant, which is also useful in demonstration contexts.

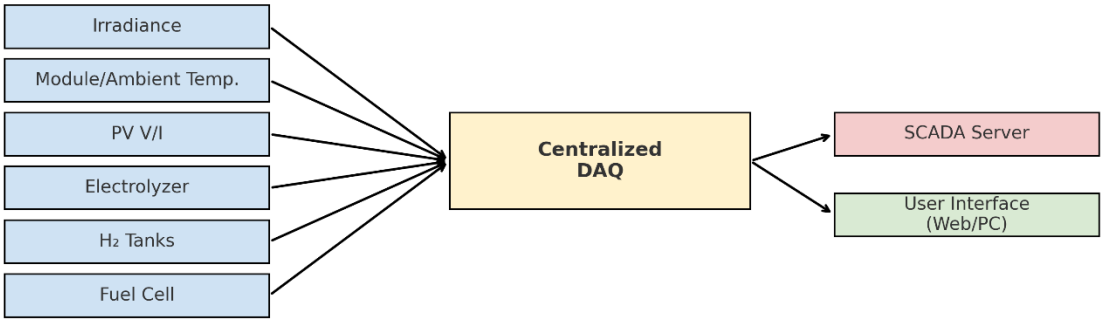

Figure 2.7 – Data Acquisition System (DAQ) architecture

Block diagram showing the installed sensors (irradiance, temperature, PV parameters, electrolyzer, H_2 tanks and fuel cell) and their connection to the centralized DAQ system, connected to the SCADA server and the remote user interface.

2.6.5 Considerations

The instrumentation adopted guarantees the possibility of conducting a detailed analysis of the performance of the system in all its components. This will allow accurate energy balances to be drawn up, experimental data to be compared with the mathematical models developed in subsequent chapters and to identify any room for improvement.

2.7 Control logic and operational strategies

The control logic is the element that allows the PV–H_2–FC system to operate safely, efficiently and in a coordinated manner. In the absence of a centralized management system, the individual subsystems (photovoltaic, electrolyzer, storage, fuel cell) would function as isolated entities, with the risk of inefficiencies and malfunctions. The implementation of integrated control algorithms is therefore crucial to ensure the stability of the system and to maximize the use of the renewable energy produced.

2.7.1 Objectives of the control system

The main objectives of the control system are:

- **maximize local self-consumption** of photovoltaic energy;
- **ensure the safe operation of the** devices, respecting the operating limits of voltage, current, pressure and temperature;
- **optimize hydrogen production**, adapting it to the variable conditions of solar radiation;
- **ensure continuity of supply** through conversion to electricity with the fuel cell during periods of low or no solar production;
- **manage energy priorities** according to loads, available hydrogen reserves and operating conditions.

2.7.2 Control architecture

The control architecture is based on a PLC (Programmable Logic Controller) integrated with the data acquisition system described in §2.6.

The main functional levels are:

1. **Local control of subsystems**
    - MPPT (Maximum Power Point Tracking) for the photovoltaic field.
    - Voltage/current regulation for the electrolyzer.
    - Pressure and flow monitoring for tanks.
    - Control of voltage and current supplied by the fuel cell.
2. **Central supervision**
    - Management of energy flows between the different subsystems.
    - Definition of operational priorities (e.g. first power electrolyzer, then load tanks, finally power fuel cell).
    - Safety logics and shutdown in case of anomalies.
3. **User interface**
    - Dashboard to view the main parameters.
    - Possibility of operating in automatic or manual mode.

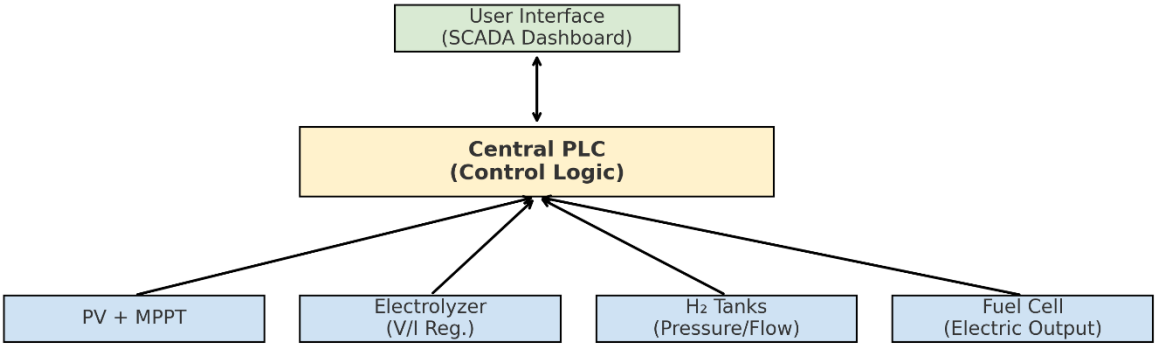

Figure 2.8 – PV–H₂–FC system control logic architecture

Block diagram illustrating the integration of the local subsystems (PV, electrolyzer, tanks and fuel cell) with the central PLC, responsible for the control logic and connected to the user interface for monitoring and operational management.

2.7.3 Strategy operational

The operational strategies adopted have been designed to maximize overall efficiency and adapt to the different conditions of solar radiation and hydrogen availability.

1. **High PV Production Condition**
    - The photovoltaic energy in excess of the immediate requirement is entirely conveyed to the electrolyser.
    - The hydrogen produced is stored in high-pressure tanks.
2. **Low PV Production Condition**
    - If the production is not sufficient to cover the demand, the system reduces the power to the electrolyzer.
    - The fuel cell can be activated to ensure continuity of power supply.
3. **Absence of PV production (night or adverse conditions)**
    - The fuel cell provides electricity using stored hydrogen.
    - The PLC constantly monitors the pressure of the tanks to prevent deep discharges.
4. **Emergency management**
    - In the event of abnormal values of pressure, temperature or concentration of hydrogen in the environment, the system automatically **shuts down** the subsystems.
    - Ventilation and alarm systems are activated.

2.7.4 Optimization algorithms

Optimization algorithms have been developed to improve the efficiency of the system, including:

- **predictive logic based on weather forecast**: the expected output of the PV is used to adjust the power of the electrolyzer in advance;
- **load management algorithm**: priority to the supply of critical loads, with possible deferral of non-essential loads;
- **Multi-objective optimization**: maximization of hydrogen production and simultaneous reduction of fuel cell start/stop cycles [37].

2.7.5 Considerations

The implemented control logic is a distinctive element of the experimental system, as it allows to simulate the behavior of a real hydrogen microgrid. The integration of local controls and central supervision ensures flexibility and security, while the adoption of predictive strategies represents a step towards smart energy systems.

2.8 Innovativeness of the experimental system

The experimental PV–H_2–FC system developed at the University of Sharjah stands out for a series of innovative features that make it unique compared to other demonstration plants described in the literature. The main objective of the project is not only to validate individual technologies, but to integrate a complete power-to-gas-to-power cycle into a single platform, with particular attention to the extreme environmental conditions typical of the Middle East region.

2.8.1 Multi-technology integration

One of the main innovations lies in the integration, in a single plant, of:

- **bifacial photovoltaic modules**, capable of increasing energy production compared to monofacial modules thanks to the exploitation of reflected radiation;
- **PEM electrolyzer**, able to operate flexibly following the intermittent course of the solar source;
- **metal hydride storage system**, which allows hydrogen to be stored in significant quantities for prolonged periods;

- **PEMFC fuel cell**, used for the conversion of hydrogen into electricity and heat, closing the P2G2P cycle.

This configuration provides a complete experimental platform, capable of simulating concrete application scenarios for off-grid microgrids, energy communities or industrial applications.

2.8.2 Climate contextualization

Another innovative aspect is the choice of the installation site: the Sharjah campus, in a desert context characterized by:

- **very high solar radiation**, which allows PV electricity production to be maximized;
- **high ambient temperatures**, which pose a challenge for the efficiency of the modules and the durability of the electrolyte membranes;
- **soiling phenomena** (dust and sand), which negatively affect performance but allow maintenance and cleaning strategies to be tested.

These extreme conditions make the system a real test bed for the development of future plants in the MENA (Middle East and North Africa) regions.

Although a dedicated soiling monitoring system was not implemented during the experimental campaign, qualitative indications of dust and haze effects can be inferred from variations in measured irradiance and spectral characteristics observed during the test days. A systematic assessment of soiling losses and cleaning strategies represents an important direction for future experimental investigations in similar desert environments.

2.8.3 Advanced monitoring system

Compared to other experimental facilities, the Sharjah monitoring system stands out for:

- **high data sampling rate** (up to 1 Hz), which allows you to capture fast transients;
- **time synchronization** of all quantities (electrical, thermal, chemical);
- **SCADA interface with remote access**, which allows real-time supervision by researchers, even remotely.

These characteristics are typical of industrial plants, but rarely implemented in university experimental platforms.

2.8.4 Demonstrative value and replicability

The plant was conceived not only as a research laboratory, but also as a technology demonstrator. Its modular and compact architecture allows it to be presented as a model that can be replicated in different contexts:

- **isolated energy communities**, which require seasonal storage;
- **industrial areas**, which can exploit hydrogen for energy and chemical applications;
- **mobility sector**, as a basis for hydrogen refuelling stations.

Replicability is favored by the use of commercial components already available on the market, integrated with a control logic developed ad hoc.

2.8.5 Comparison with the state of the art

In the literature there are numerous studies on experimental PV–Electrolysis or Electrolysis–FC systems, but rarely has a PV–Electrolysis–Storage–FC integration been carried out in real conditions and with such extensive monitoring. Most of the previous projects focus on:

- laboratory tests, with controlled conditions;
- validation of individual components;
- numerical simulations not supported by complete experimental data.

The Sharjah plant fills this gap, positioning itself as a reference platform for integrated experimentation.

2.8.6 Considerations

The innovativeness of the experimental system lies not only in the individual technologies adopted, but in their synergistic integration. The project demonstrates how a P2G2P cycle can be implemented and monitored under real-world conditions, providing useful results not only from a scientific point of view, but also for possible future commercial applications.

3 PV–H_2–FC SYSTEM MODELING

3.1 Introduction to Modeling

Mathematical modeling is an essential tool for understanding and predicting the behavior of complex energy systems. In the case of the integrated photovoltaic–electrolyzer–storage–fuel cell (PV–H_2–FC) chain, modeling allows to describe the physical and electrochemical processes that regulate each subsystem and to estimate the overall efficiency of the energy cycle.

A reliable model allows not only to interpret experimental data, but also to extend the analysis to conditions not directly observed in the laboratory. This is crucial when dealing with innovative systems, such as the one implemented in Sharjah, in which technologies are directly coupled and subject to extreme environmental variability.

The approach followed is based on two levels:

- **modeling of the subsystems**: bifacial photovoltaic field, PEM electrolyzer, metal hydride tank and fuel cell are described by means of characteristic equations that capture their electrical, chemical and thermodynamic behavior;
- **Integrated modeling**: the individual models are coupled into an overall energy and mass balance, useful for evaluating the performance of the chain and quantifying the losses in the intermediate steps.

To make the model manageable and consistent with the available data, some simplifying assumptions have been introduced:

- almost stationary operating conditions on the acquisition time step (1 min),
- nominal parameters calibrated on the datasheets and subsequently experimentally verified,
- negligibility of minor losses (wiring, marginal auxiliary dissipations),
- uniformity of environmental conditions on each subsystem.

These assumptions do not reduce the validity of the model, but increase its application robustness, allowing a quantitative picture of the entire supply chain to be obtained. In Chapter 4 the models developed in this section will be compared with the experimental data, in order to evaluate their degree of accuracy and predictive capacity.

3.2 Bifacial PV Field Model

The modeling of the photovoltaic field is the first step in the mathematical representation of the PV–H_2–FC chain. In particular, bifacial modules require a more articulated approach than traditional single-sided modules, since the power generated depends both on the radiation incident on the front face and on the reflected and diffuse contribution captured by the rear side.

3.2.1 Electrical Model Equations

The electrical behavior of a photovoltaic module can be described by means of the single diode model, widely used for the simulation of PV systems thanks to the good compromise between accuracy and computational complexity [38].

The characteristic equation is as follows:

$$I = I_{ph} - I_0 \left[exp\left(\frac{q(V + IR_s)}{nkT} \right) - 1 \right] - \frac{V + IR_s}{R_{sh}}$$

where:

- I is the current supplied by module [A],
- V is the voltage at the terminals of the module [V],
- I_{ph} is the photogenerated current [A], proportional to the radiation,
- $I_0$is the diode saturation current [A],
- q is the elementary charge ($1{,}602 \times 10^{-19}$ C),
- n is the ideality factor of the diode,
- k is Boltzmann's constant ($1{,}381 \times 10^{-23}$ J/K),
- T is the absolute temperature of the cell [K],
- R_s is the resistance series [Ω],
- R_{sh} is the shunt resistance [Ω].

This relationship allows us to describe the entire current-voltage curve (I–V) of the module, from the short-circuit condition (V=0, $I=I_{sc}$) to the open-circuit condition (I=0, $V=V_{oc}$), up to the point of maximum power (MPP), where P=V·I is maximum.

3.2.2 Effects of temperature and radiation

The model must take into account the dependence of PV performance on environmental conditions. The photogenerated current is proportional to the incident radiation:

$$I_{ph}(G) = I_{sc,STC} * \frac{G}{G_{STC}}$$

where G is the irradiance on the modulus plane [W/m²] and GSTC = 1000 W/m² is the reference condition.

The open circuit voltage, on the other hand, varies significantly with the cell temperature:

$$V_{oc}(T) = V_{oc,STC} + \beta_{Voc}(T_{cell} - 25)$$

where β_{Voc} is the temperature coefficient [V/°C].

Similarly, the short-circuit current changes according to the coefficient α_{Isc}

The instantaneous efficiency of the module can therefore be calculated as:

$$\eta_{pv} = \frac{P_{out}}{G * A}$$

where A is the active area of the module [m²].

3.2.3 Bifacial gain modeling

In bifacial modules, the contribution of posterior radiation G_{rear} must be introduced, which depends on the albedo of the underlying surface and the installation geometry. The total irradiation that feeds the module is therefore:

$$G_{tot} = G_{front} + \gamma * G_{rear}$$

where γ is the bifaciality coefficient (ratio between the efficiency of the posterior and anterior cell).

Bifacial gain (BG) is defined as:

$$BG = \frac{E_{bif} - E_{mono}}{E_{mono}} * 100$$

where E_{bif} is the energy produced by the bifacial module and E_{mono} that produced by the corresponding monofacial module of equal power.

Typical BG values are between 10% and 30% depending on the albedo and installation conditions [39].

3.2.4 Parameters of modules installed in Sharjah

In the Sharjah experimental system, bifacial JW-D72N-365 Jollywood modules and a Jinko JKM365M-72 single-sided module were used as a reference. Table 3.1 shows the main nominal parameters under STC conditions (1000 W/m², 25 °C, AM 1.5).

PARAMETER	JOLLYWOOD JW-D72N-365 (DOUBLE-SIDED)	JINKO JKM365M-72 (SINGLE-SIDED)
RATED POWER (P_{MAX})	365 Wp	365 Wp
V_{OC}	44,8 V	48,2 V
I_{SC}	10,14 A	9,57 A
V_{MP}	38,2 V	40,6 V
I_{MP}	9,56 A	9,00 A
STC EFFICIENCY	18,6 %	18,8 %
BIFACCIALITY	~85 %	–

Table 3.1 – Nominal electrical parameters of photovoltaic modules installed in Sharjah

The modules were installed with a fixed inclination of 25°, South orientation, and a height from the ground of 0,76 m.

3.2.5 Simulation of the power produced

The instantaneous electrical power produced by bifacial modules can be calculated as:

$$P(t) = V(t) * I(t) \sim \eta_{pv}(T, G) * G_{tot}(t) * A$$

where $G_{tot}(t)$ is the overall irradiation (front + rear).

To simulate the yield on surfaces with different albedos, typical average values are used:

Surface	Albedo [-]
Turf	0,18–0,25
Grey concrete	0,25–0,35
White sheet metal	0,65–0,85
Cool roof paint	0,30–0,40

Table 3.2 – Typical surface albedo values

The simulation makes it possible to estimate the difference in energy produced based on the underlying reflective surface, thus evaluating the effectiveness of engineering strategies aimed at optimizing bifacial gain.

3.2.6 Methodological discussion

The single-diode model, integrated with temperature and bifaciality corrections, provides an accurate representation of the performance of the modules used in Sharjah. Although some secondary losses (mismatch, fouling, degradation effects) are overlooked, the model is robust enough to calculate the power available to the electrolyzer and thus the entire PV–H_2–FC chain.

The developed model therefore provides a robust tool to describe the expected performance of the bifacial photovoltaic array, to be subsequently integrated into the hydrogen production and use chain.

3.3 PEM Electrolyzer Model

The electrolyzer represents the heart of the process of converting electrical energy into hydrogen. Proton **Exchange Membrane (PEM)** polymer technology was chosen in the experimental system for its compactness, ability to operate at moderate pressures, and rapid response to changes in electrical power [42].

3.3.1 Principles of operation and thermodynamics

The global reaction of water electrolysis can be written as:

$$H_2O\ (l) = H_2\ (g) + 1/2\ O_2\ (g)$$

The minimum theoretical potential required for water splitting is described by the Nernst equation:

$$E_{rev} = E^0 + \frac{RT}{2F}\ln\left(\frac{a_{H_2} * {a_{O_2}}^{1/2}}{a_{H_2O}}\right)$$

where:

- E^0 =1.229 V (at 25 °C and 1 bar) is the standard potential,
- R is the universal constant of gases (8.314 J·mol^{-1}· K^{-1}),
- T is the temperature [K],
- F is Faraday's constant (96485 C·mol^{-1}),
- $a_i$are the chemical activities of the species.

Under standard conditions, the value of E_{rev} is close to 1,23 V. However, due to the real losses, the operational potential is higher.

3.3.2 Overvoltages and bias curve

The real electrolyzer requires a higher voltage than the thermodynamic potential, due to the overvoltages that occur in electrochemical processes [43]:

- **Activation overvoltage (η_{act})** related to the slow kinetics of electron exchange reactions at the electrodes.
- **Ohmic overvoltage (η_{ohm})**: due to the ionic resistance of the membrane and the electrical resistances of the contacts.
- **Concentration overvoltage (η_{conc}):** related to reagent diffusion limitations.

The operating voltage of the cell is therefore:

$$V_{cell} = E_{rev} + \eta_{act} + \eta_{ohm} + \eta_{conc}$$

The sum of these contributions gives rise to the polarization curve of the electrolyzer, typically characterized by:

- a region with low currents dominated by η_{act}
- a quasi-linear intermediate region dominated by η_{ohm}
- a region with high currents in which η_{conc} prevails.

3.3.3 Faraday's Law and Hydrogen Production

The production of hydrogen is directly proportional to the current flowing through the cell, according to Faraday's law:

$$\dot{n}_{H_2} = \frac{I}{2F}$$

where $\dot{n}_{H_2}$ is the molar flow rate of hydrogen [mol/s] and the factor 2 in the denominator reflects the number of electrons needed to produce a molecule of H_2.

The corresponding volume flow is:

$$V_{H_2} = \frac{I * R * T}{2F * p}$$

with p operating pressure and T reference temperature.

From this relationship the typical electrolyzer yield is obtained: about 138,4 L of H_2 per kWh of electricity consumed, as observed in the experimental tests in Sharjah (see Chapter 4).

3.3.4 Electrolyzer Efficiency

Electrical conversion efficiency can be defined as:

$$\eta_{el} = \frac{\dot{n}_{H_2} * \Delta H}{P_{in}}$$

where:

- ΔH is the enthalpy of hydrogen formation (LHV = 241.8 kJ/mol or HHV = 285.8 kJ/mol is commonly used),
- $P_{in} = V_{cell} * I$ is the electrical power absorbed.

Typical values for small PEM electrolysers are between 45% and 60% (LHV based), depending on the operating conditions [44].

3.3.5 Parameters of the electrolyzer used

A Hy-PEM XP Home electrolyzer manufactured by H_2 Planet was used in the Sharjah experimental system. The main nominal characteristics are shown in Table 3.3.

Parameter	**Value**
Nominal power consumption	1300 W
Production capacity H_2	~2000 cc/min (120 L/h)

Adjustable operating pressure	1–16 bar
Cell voltage	1,8–2,0 V typical
Electrical Efficiency (LHV)	45–55 %

Table 3.3 – Technical specifications of the PEM electrolyzer used

3.3.6 Methodological discussion

The developed model allows to calculate the relationship between the electrical power provided by the photovoltaic field and the flow of hydrogen produced. The combination of Nernst's equation, polarization curves and Faraday's law ensures a consistent description of the electrolyzer's behavior. Although the model has some simplifications (neglecting rapid transient phenomena and complex thermal dynamics), it provides a robust tool for the integration of the electrolyzer subsystem into the PV–H_2–FC chain.

3.4 Metal hydride storage system model

Hydrogen storage is a crucial step in the PV–H_2–FC chain. A metal hydride tank (*My H_2 2000*) was used in the Sharjah experimental system, capable of storing up to 2 Nm^3 of hydrogen with an internal volume of 3 L and a total weight of 14 kg. This technology is based on the ability of some metal alloys to reversibly absorb large amounts of hydrogen, forming stable solid compounds.

3.4.1 Working principle

The absorption of hydrogen takes place according to the general reaction:

$$M + x/2\ H_2 \rightleftharpoons MH_x$$

where *M* represents the metal alloy and MH_x the hydride compound.

The process is exothermic: molecular hydrogen is dissociated into atoms on the metal surface and subsequently diffuses into the crystalline structure of the material.

3.4.2 Thermodynamic equilibrium: Van't Hoff equation

The equilibrium pressure between the gaseous phase and the solid phase is described by the Van't Hoff equation:

$$\ln(p_{eq}) = (\Delta H / (R*T)) - (\Delta S / R)$$

where:

- p_{eq} is the equilibrium pressure [bar],
- ΔH is the enthalpy of reaction [J/mol H_2],
- ΔS is the reaction entropy [J/mol· K],
- R is the gas constant (8.314 J/mol· K),
- T is the temperature [K].

This relationship shows that the equilibrium pressure increases exponentially with temperature: heating the material favors the release of hydrogen, while cooling favors its absorption.

3.4.3 Absorption and desorption kinetics

The reaction rate depends not only on the thermodynamic equilibrium, but also on the kinetics of atomic diffusion within the alloy. A common formulation is based on Arrhenius' law:

$$k = k_0 * \exp(-E_a / (R*T))$$

where:

- k is the kinetic constant of the process,
- k_0 is the pre-exponential factor,
- E_a is the activation energy [J/mol].
-

The rate of absorption/desorption is proportional to the difference between the partial pressure of hydrogen pH_2 and the equilibrium pressure p_{eq}:

$$r = k * (pH_2 - p_{eq})$$

when $pH_2 > p_{eq}$ absorption prevails, while when $pH_2 < p_{eq}$ hydrogen release occurs.

3.4.4 Tank mass balance

The hydrogen content in the tank, expressed as the filling fraction θ (0 to 1), can be described by the balance sheet:

$$d\theta/dt = (r / C\_H_2)$$

where C_H_2 is the specific capacity of the alloy (mol H_2/kg of active material).

The *My H_2 2000* tank has a total capacity of 2 Nm^3, equivalent to approx. 0.18 kg of H_2, and uses an AB_2 alloy.

3.4.5 Storage system efficiency

Storage efficiency can be defined as:

$$\eta_{st} = (m_{H_2,desorbed} / m_{H_2,absorbed}) * 100$$

Under correct operating conditions, the efficiency is close to 100%, but there are losses due to hysteresis phenomena between the charge and discharge cycles, as well as the need to provide thermal energy for the release of hydrogen.

3.4.6 Technical parameters of the My H_2 2000 tank

Parameter	**Value**
Model	My H_2 2000
Technology	Metal hydrides AB_2
Storage capacity	2 Nm^3 H_2
Internal volume	3 L
Maximum Operating Pressure	30 bar
Operating Temperature	10–65 °C
Total weight	14 kg

Table 3.4 – Specifications of the metal hydride tank used

3.4.7 Methodological discussion

The proposed model, based on the Van't Hoff equilibrium and the Arrhenius kinetics, allows to quantitatively describe the behavior of the metal hydride reservoir. This approach is particularly useful for estimating charging and discharging times, as well as the pressure available to power the fuel cell.

The main limitation consists in the need to know the specific thermodynamic parameters of the alloy used (ΔH, ΔS, Ea), often provided by manufacturers only in partial form. However, even with average data from the literature, the model offers a realistic representation of how the storage is operating.

3.5 PEMFC fuel cell model

The proton exchange membrane fuel cell (PEMFC) is the device in charge of converting hydrogen into electrical energy. This technology was chosen for the experimental system due to its high power density, the ability to operate at low temperatures (60–80 °C) and its rapid response to load changes [48].

3.5.1 Working principle

The overall reaction that takes place in PEMFC is as follows:

$$H_2 + 1/2\ O_2 \rightarrow H_2O + \text{energy (electrical + thermal)}$$

The individual interfaces are equipped with:

- **Anode**

$$H_2 \rightarrow 2H+ + 2e-$$

- **Cathode**:

$$1/2\ O_2 + 2H+ + 2e- \rightarrow H_2O$$

3.5.2 Thermodynamic potential

The reversible potential is described by the Nernst equation:

$$E_{rev} = E^0 + \frac{RT}{2F} \ln\left(\frac{a_{H_2} * {a_{O_2}}^{1/2}}{a_{H_2O}}\right)$$

where $E^0 = 1{,}229\ V$ (25 °C, 1 bar), a_{H_2} , a_{O_2} , a_{H_2O} are the partial pressures of the species, R is the gas constant, T the absolute temperature and F the Faraday constant.

3.5.3 Overvoltages and bias curve

Similarly to the electrolyzer, the real voltage of the cell is lower than the theoretical voltage due to losses:

$$V_{cell} = E_{rev} - (\eta_{act} + \eta_{ohm} + \eta_{conc})$$

where:

- η_{act} = activation overvoltage (slow kinetics of reduction of oxygen at the cathode),
- η_{ohm} = voltage drop due to ionic resistance of the membrane and electrical contacts,

- η_{conc} = concentration losses, evident at high loads when the inflow of reactants is limited.

The resulting curve (polarization) is characterized by:

- Initial region dominated by η_{act},
- regione intermedia quasi lineare (η_{ohm}),
- abrupt final fall due to η_{conc}.

3.5.4 Power and efficiency

The electrical power delivered by a cell is given by:

$$P = V_{cell} * I$$

Electrical efficiency η_{fc} can be defined as the ratio of electricity produced to the energy content of hydrogen consumed (expressed in LHV = 241,8 kJ/mol or HHV = 285,8 kJ/mol):

$$\eta_{fc} = (\dot{n_{H_2}} * 2F * V_{cell}) / (\dot{n_{H_2}} * \Delta H)$$

Simplifying:

$$\eta_{fc} = (2F * V\_cell) / \Delta H$$

where ΔH represents the molar enthalpy of hydrogen.

Typical values for a PEMFC are between 40% and 60% under standard operating conditions [49].

3.5.5 Fuel cell parameters of the experimental system

In the Sharjah demonstration, a laboratory PEMFC with a nominal power of the order of a few hundred watts was adopted, powered directly by the hydrogen accumulated in the metal hydride tank. Table 3.5 shows the main reference parameters.

Parameter	Indicative value
Technology	PEMFC
Rated power	~300 W
Voltage rating	24 V
Current rating	12–13 A
Operating Temperature	60–70 °C
Electrical Efficiency (LHV)	40–55 %

Table 3.5 – Specifications of the PEMFC fuel cell used

3.5.6 Methodological discussion

The proposed model for PEMFC, based on the Nernst equation and polarization curves, allows to estimate the cell voltage and therefore the power that can be delivered as a function of the hydrogen flow and the operating conditions. The approach is suitable for system-scale modeling, where it is of interest to evaluate the net available power and overall efficiency, rather than the microphysics of transport phenomena.

3.6 Integrated PV–H_2–FC chain modeling

After describing the individual subsystems, it is necessary to develop a model that integrates them into a single energy chain. The aim is to quantitatively represent the flow of energy from the sun to the electricity produced by the fuel cell, including conversion losses and partial efficiencies.

3.6.1 Hydrogen production and flow

The electrical power generated by the bifacial photovoltaic field $P_{PV}(t)$ is:

$$P_{PV}(t) = \eta_{PV}(T, G) * G_{tot}(t) * A$$

where $\eta_{PV}(T, G)$is the efficiency of the module, $G_{tot}(t)$ the total irradiance (front + rear) and A the active area.

The molar flow rate of hydrogen produced by the electrolyzer is derived from Faraday's law:

$$\dot{n}_{H_2} = \frac{I}{2F}$$

with

$$\mathrm{I} = P_{PV}(t)/\ \mathrm{V_{cell}}$$

where V_{cell} is the average operating voltage of the electrolyzer.

The cumulative amount of hydrogen stored in a time interval Δt is:

$$N_{H_2} = \int \dot{n}_{H_2} \text{ (t) dt}$$

which, expressed in volume at standard conditions, becomes:

$$V_{H_2} = (N_{H_2} * R * T) / p$$

3.6.2 Overall efficiency

The partial efficiencies of the subsystems are defined:

- **PV Efficiency**

$$\eta_{PV} = P_{PV} / (G_{tot} * A)$$

- **Electrolyzer efficiency**

$$\eta_{el} = (\dot{n}_{H_2} * \Delta H) / P_{PV}$$

- **Storage efficiency**

$$\eta_{st} = (m_{H_2,desorbed} / m_{H_2,absorbed}) * 100$$

- **Fuel cell efficiency**

$$\eta_{fc} = (2 * F * V_{cell}) / \Delta H$$

The overall efficiency of the system from solar radiation to converted electricity is therefore:

$$\eta_{TOT} = \eta_{PV} * \eta_{el} * \eta_{st} * \eta_{fc}$$

3.6.3 Considerations and comparison with literature

The integrated model provides a useful tool for estimating round-trip efficiency (RTE), i.e. the ratio between the electricity supplied by the fuel cell and the solar radiation incident on the photovoltaic generator.

$$RTE = E_{FC\_out} / (G_{tot} * A * \Delta t)$$

Typical values reported in the literature for hydrogen solar micro-chains are between 5% and 12% [51], depending on the quality of the components and the operating conditions. The developed model is placed within this range, providing a useful reference for validation and future simulation scenarios.

3.7 Final Thoughts

The modeling developed in the previous paragraphs has made it possible to mathematically represent the main subsystems that make up the PV–H_2–FC chain: the bifacial photovoltaic field, the PEM electrolyzer, the metal hydride tank and the PEMFC fuel cell.

The approach adopted was twofold: on the one hand, the use of consolidated models (single diode for photovoltaics, Nernst equation and bias curve for electrolyzer and fuel cell, Van't Hoff and Arrhenius for hydride storage), and on the other hand, systemic integration that allows the overall efficiency of the supply chain to be calculated.

The main conclusions that emerge are:

- **subsystem modeling** allows you to highlight the critical points of each device and estimate its intrinsic efficiency;
- the **integrated approach** makes it possible to quantify the cumulative losses along the chain and to estimate the round-trip efficiency, a key parameter for the technical-economic evaluation of the system;
- although based on simplifying assumptions (uniformity of operating conditions, negligibility of secondary losses), the models are adequate for a plant-scale representation, useful to support the experimentation;
- Modeling is the fundamental tool for the analysis of future scenarios, allowing to predict the behavior of the system in conditions not directly tested and to evaluate the impact of any technological improvements.

Chapter 3 therefore provides the theoretical and methodological basis necessary to understand the experimental results that will be presented in the following chapters, laying the foundations for a critical and comparative analysis of the entire solar-hydrogen energy chain.

4 EXPERIMENTAL ANALYSIS OF THE SYSTEM

4.1 Introduction to the measurement campaign

The experimental activity represents the heart of the present research, as it allows to validate in real conditions the performance of an integrated photovoltaic-electrolyzer-metal hydride-fuel cell (PV–H_2–FC storage) system. The demonstration plant was built at the University of Sharjah (United Arab Emirates), in a particularly challenging climatic context characterized by:

- high annual solar radiation intensity (over 2000 kWh/m²·year),
- summer ambient temperatures often above 40 °C,
- presence of dust and aerosols that affect the performance of photovoltaic modules,
- day-night temperature fluctuations that affect the operating conditions of electrochemical components.

4.1.1 Objectives of the experimental campaign

The measurement campaign has been planned to pursue the following main objectives:

1. **To characterize the behavior of the bifacial photovoltaic field** in real operating conditions and to compare its performance compared to conventional monofacial modules reported in the literature.
2. **Evaluate the efficiency and operational flexibility of the PEM electrolyzer**, which is subject to power fluctuations due to solar intermittency.
3. **Analyze the storage capacity of the metal hydride tank**, with particular reference to the charge/discharge times, the thermal balance and the operational stability.
4. **Determine the performance of the PEM fuel cell** powered by stored hydrogen, with analysis of polarization curves, electrical efficiency, and dynamic response.
5. **To study the integrated interaction of the entire PV–H_2–FC chain**, evaluating parameters of round-trip efficiency, reliability and replicability of the system in real scenarios.

4.1.2 Methodology

The measurements were carried out by means of an advanced monitoring system (described in Chapter 2), based on:

- global and reflex irradiance sensors for bifacial characterization,
- acquisition of current, voltage and power of the PV field,
- continuous recording of pressure, flow rate and temperature of the gas produced,
- logging of the charge/discharge parameters of the metal hydride tank,

- acquisition of the electric curves of the fuel cell.

The data collected was stored in log files on an hourly and daily basis, allowing both instant analysis and integrations over medium-term periods.

Trial day	Main weather conditions	Monitored quantities	Experimental notes
17 February	Sunny day, T ≈ 26 °C	Irradiance, PV power, H_2 produced	First instrument calibration session
3 March	Light haze, T ≈ 30 °C	Full data PV–Electrolysis–Storage–FC	Integrated system validation session
March–April	Variable trend, peaks >35 °C	Spot fuel cell measurements and storage	Stress test under dynamic load conditions

Table 4.1– Summary of the experimental campaign

4.1.3 Innovativeness of the campaign

The distinctive feature of the experimental campaign is that, unlike most of the experiences documented in the literature, it was conducted on a complete and integrated demonstration system, including all the phases of the conversion chain: renewable generation, electrolysis, storage and reconversion. This feature allows not only to validate theoretical models, but also to identify operational criticalities and optimization opportunities in view of real applications, such as residential microgrids or energy communities [38][39][40].

4.2 Experimental data of the bifacial photovoltaic field

4.2.1 Field Configuration

The photovoltaic field installed at the experimental site consists of monocrystalline silicon bifacial modules, characterized by a nominal power of 365 Wp per module. The overall configuration includes a 1,46 kWp array, mounted on a fixed structure with inclination optimized for the latitude of the site (≈ 25°). The orientation was chosen to maximize production in the central hours of the day, in line with the needs of the electrolyzer.

The peculiarity of bifacial modules is the ability to generate energy not only from the radiation incident on the front side, but also from the reflected and diffused radiation on the back. This aspect allows to increase energy production compared to monofacial modules of equal power, with estimated increases between 5% and 20% depending on the albedo conditions [41].

4.2.2 Data acquisition methodology

The monitoring system has been configured to capture:

- **Horizontal global irradiation (GHI)** by pyranometer,
- **Rear irradiance via** a dedicated sensor on the back of the modules,
- **Ambient temperature** and **cell temperature**,
- **Output current and voltage from the array**, logging in 1 min step,
- **Daily energy produced** (via inverter and meter).

The data below refer to the test days of 17 February and 3 March, characterized respectively by clear skies and the presence of light haze.

4.2.3 Main results

The experimental tests conducted on 17 February and 3 March allowed to analyze in detail the effect of surface albedo on the performance of bifacial modules.

In the first case (17 February), the frontal radiation reached values close to 1000 W/m² in the central hours, while the reflected radiation showed a trend strongly dependent on the type of surface: the white finish guaranteed the greatest contribution (up to ~200 W/m²), followed by the gray and green ones. This was also reflected in the power curve: bifacial modules on a white surface reached a peak of over 380 W, compared to about 310 W for modules on a green surface and lower values for reference monosides.

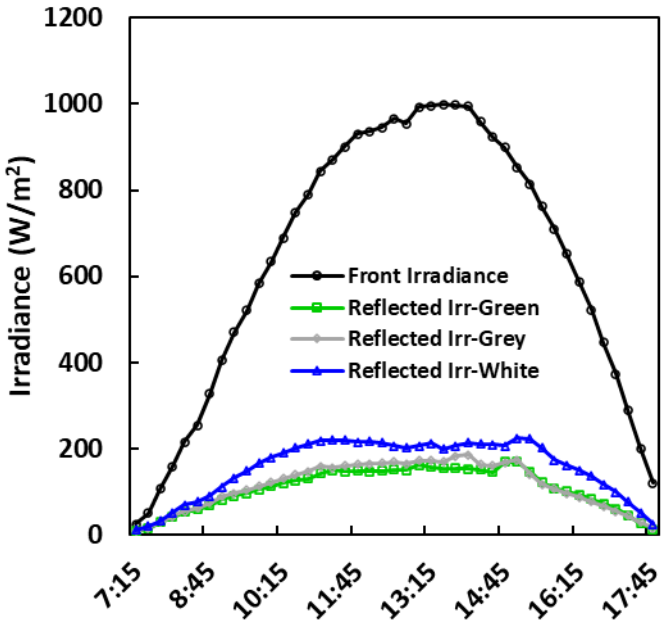

Figure 4.1 - Front and rear irradiance measured on 17 February with different surface conditions under the bifacial PV modules (green, grey, white).

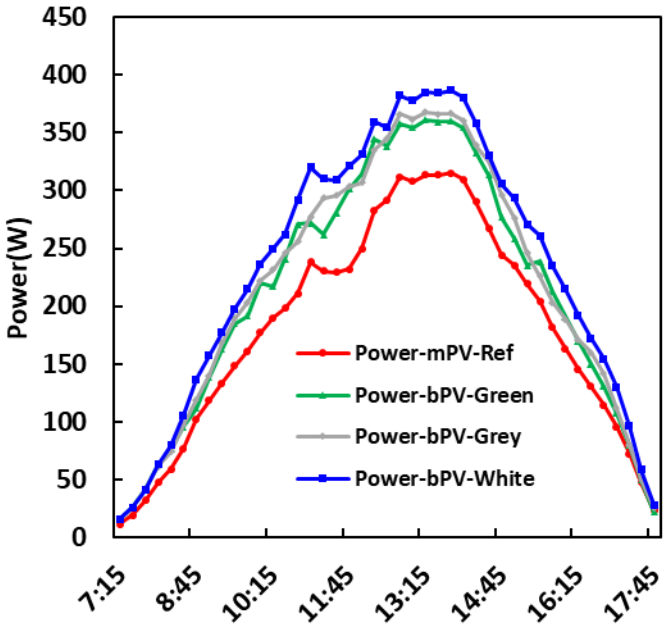

Figure 4.2 - Output power of monofacial and bifacial PV modules on 17 February, with bifacial modules operating on different surfaces (green, grey, white).

In the second case (3 March), characterized by light haze conditions, the maximum frontal radiation was lower (~950 W/m²), but the rear contribution was particularly significant with the treated surfaces (cool roof paint, wall paper, white board), remaining stable in the range of 150–250 W/m². Again, the power curves confirmed a clear advantage of the bifacial modules, which exceeded 380–400 W peak compared to about 300 W for the monofacial module.

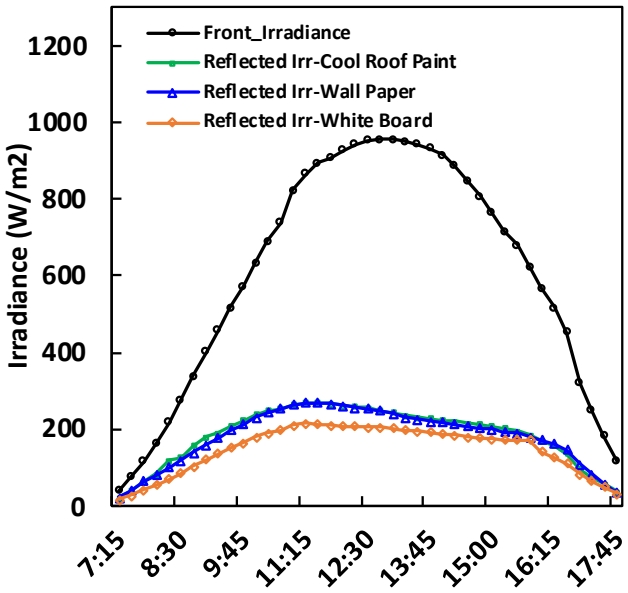

Figure 4.3 - Front and rear irradiance measured on 3 March with different surface conditions under the bifacial PV modules (cool roof paint, wall paper, white board).

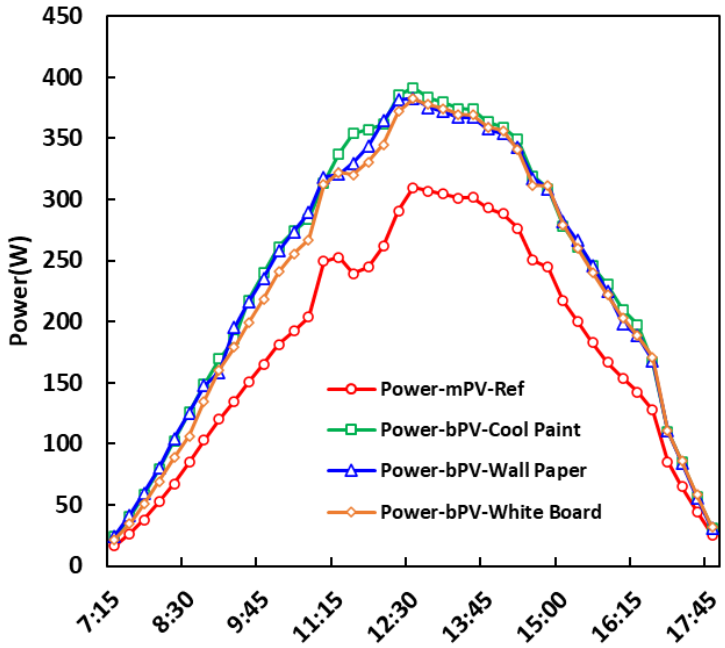

Figure 4.4 - Output power of monofacial and bifacial PV modules on 3 March, with bifacial modules operating on different surfaces (cool roof paint, wall paper, white board).

A localized power reduction is observed during late morning hours (approximately between 11:00 and 12:00), particularly in the monofacial reference profile, despite a smooth trend in the corresponding irradiance measurements. This behavior can be attributed to temperature-related effects on photovoltaic module performance and to short-term MPPT or control transients occurring under near-peak irradiance conditions. Such transient phenomena are captured in the electrical output but are not necessarily reflected in irradiance measurements alone and do not affect the overall comparative assessment between the investigated configurations.

The comparison between the two days clearly highlights how the adoption of high reflectance surfaces represents an effective strategy to maximize the yield of bifacial modules. This aspect is configured as an element of innovation of the Sharjah experimental plant, as it allows to increase the energy that can be produced without direct interventions on the modules, but simply through low-cost and replicable engineering solutions.

A further element of interest of the experimental campaign concerns the comparison between the different colors of the surfaces underlying the bifacial modules. The analysis shows that albedo is not a static parameter but can be modified in a targeted way through construction and aesthetic choices: light or treated surfaces (such as reflective paints, white boards or cool roof paints) significantly

increase the amount of radiation collected by the back of the module, while dark or vegetal surfaces reduce its contribution.

This experimental evidence represents an aspect of innovation of the Sharjah system, as it introduces the possibility of optimizing the performance of the modules not only through their intrinsic design, but also through relatively simple and low-cost interventions on the surrounding environment. Looking ahead, this approach paves the way for integrated architectural and energy design strategies, in which the choice of surface covering materials can be exploited as a lever to maximize the overall efficiency of the PV–H_2–FC chain.

To further investigate the albedo effect, spectral reflectance measurements were conducted on the different surfaces tested, the results of which are shown in Figure 4.5.

The spectral reflectance measurements reported in Fig. 4.5 were obtained through a spectroradiometric measurement approach based on the acquisition of spectral radiance. For each surface, the reflected spectral radiance was measured and normalized with respect to a reference spectral radiance, allowing the calculation of wavelength-dependent reflectance over the relevant solar spectrum.

The measurements were carried out on real surface materials under outdoor field conditions at the Sharjah experimental site, ensuring that the obtained spectral reflectance data are representative of actual operating environments.

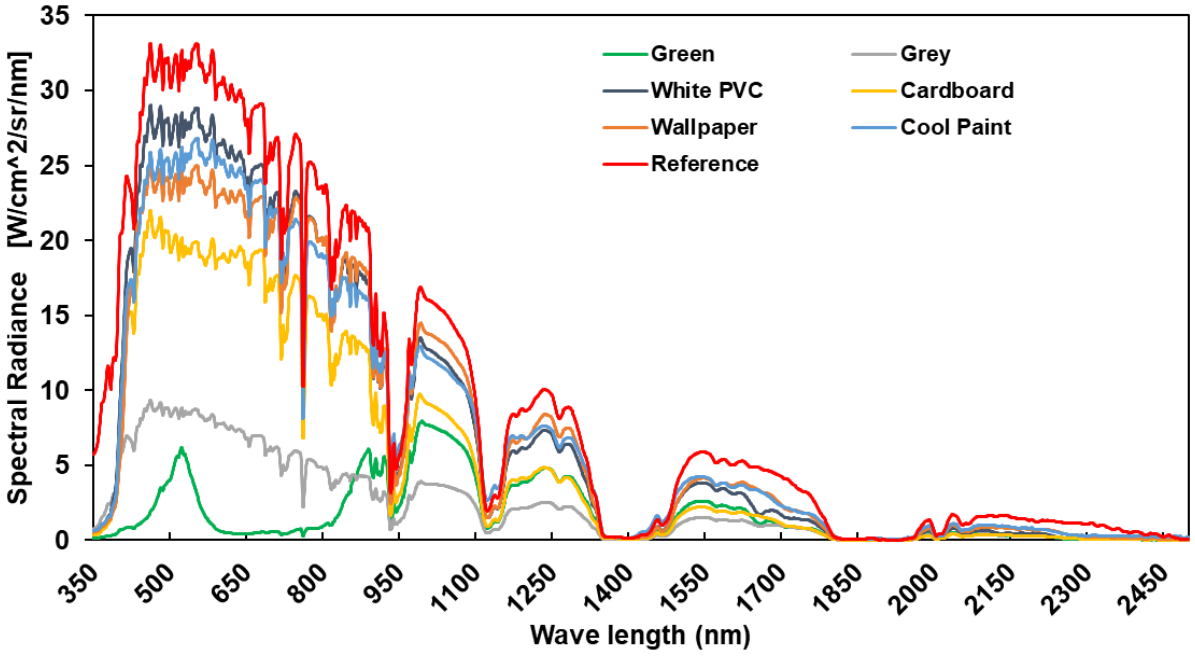

Figure 4.5 - Spectral reflectance of different surfaces tested under the bifacial PV modules (green, grey, white PVC, cardboard, wallpaper, cool paint). Surfaces with higher reflectance in the visible spectrum (e.g., white PVC, cool paint) provide a stronger contribution to rear irradiance, while darker surfaces (green, grey) show limited reflectance.

The spectral reflectance graph quantitatively confirms the experimentally observed differences in irradiance and power measurements. White or treated surfaces (white PVC, cool paint, wallpaper) show high reflectance values in the visible spectrum (400–800 nm), i.e. in the highest sensitivity band of PV modules. Conversely, dark surfaces (green, grey) reflect much less and therefore result in a reduced contribution to the back of the modules. This result reinforces the interpretation of experimental data and underlines the importance of the choice of coating materials as an innovative design lever to maximize the efficiency of bifacial systems.

Table 4.2 summarizes the average and maximum values of irradiance and power measured for the two test days, distinguishing the contributions of the different surfaces.

Day	Type	Series	Surface	Mean	Max	Rear/Front [%]	Albedo level / Note
17 Feb	Irradiance	Front irradiance	Front	638	1004	–	Incident irradiation reference
17 Feb	Irradiance	Rear irradiance	Grey	109	189	17	Low albedo – neutral surface (cement/grigio)
17 Feb	Irradiance	Rear irradiance	Green	119	205	19	Low-medium – simulates lawn/vegetation

17 Feb	Irradiance	Rear irradiance	White PVC	161	257	25	High albedo – clear reference surface
17 Feb	Power	Monofacial power	Ref	241	318	–	Single-sided control module
17 Feb	Power	Bifacial power	Grey	305	377	–	Limited gain from poorly reflective surface
17 Feb	Power	Bifacial power	Green	302	378	–	Intermediate performance
17 Feb	Power	Bifacial power	White PVC	321	394	–	Better performance thanks to high reflectance
3 Mar	Irradiance	Front irradiance	Front	608	964	–	Incident irradiation reference
3 Mar	Irradiance	Rear irradiance	Cool Paint	186	258	31	High albedo – reflective paint for roofs
3 Mar	Irradiance	Rear irradiance	Wall Paper	169	242	28	Medium-high – treated coating
3 Mar	Irradiance	Rear irradiance	White Board	171	246	28	High albedo – reflective panel
3 Mar	Power	Monofacial power	Ref	225	305	–	Single-sided control module
3 Mar	Power	Bifacial power	Cool Paint	309	390	–	Superior performance, targeted albedo effect

3 Mar	Power	Bifacial power	Wall Paper	305	387	–	Significant gain compared to single-sided
3 Mar	Power	Bifacial power	White Board	302	383	–	Good yield, confirms the effectiveness of light surfaces

Table 4.2 - Average and maximum values of irradiance (front and rear) and PV power (single-sided and bifacial) for the different surfaces tested.

The table highlights two key findings. On the one hand, in the February 17 test, the plain surfaces (gray and green) provided modest rear/front increases (17–19%), while the white PVC surface showed significantly higher values (~25%), resulting in a bifacial power peak of almost 400 W compared to 318 W for the single-sided module. On the other hand, in the test on 3 March, the treated surfaces (cool paint, wallpaper, white board) made it possible to achieve rear/front ratios of up to 31% and peak powers of more than 380–390 W, confirming the effectiveness of engineering strategies aimed at increasing reflectance.

These results demonstrate how the performance of bifacial modules does not depend only on weather conditions but can be optimized in a targeted way through the design of the underlying surfaces, introducing an additional, innovative and low-cost design variable.

4.2.4 Critical analysis

The experimental results clearly show that the performance of bifacial modules does not depend solely on atmospheric conditions, but is closely linked to the albedo of the underlying surface. In the test on 17 February, neutral surfaces (grey and green) produced relatively modest rear/front increases (17–19%), while white PVC surfaces achieved values of 25%. Even more significant were the results of 3 March, where treated surfaces (cool paint, wall paper, white board) guaranteed rear/front ratios between 28% and 31%.

When compared with the typical values reported in the literature — in which the average bifacial gain is usually in the range of 5–15% [41][42] — the data collected in Sharjah are much higher, confirming

the decisive role of light and reflective surfaces. In electrical terms, this results in an increase in peak power from ~300 W (single-sided) to over 380–390 W (double-sided with high-reflectance surfaces).

From a critical point of view, however, some limitations should be emphasized:

- the high sensitivity to the cell temperature, which reduces the overall efficiency in the hottest hours;
- the variability of bifacial gain as a function of atmospheric conditions (clear sky vs haze), which introduces uncertainty in production;
- the durability of the treated surfaces, which could be reduced over time due to aging, fouling or degradation of the materials, with a consequent decrease in effective reflectance.

4.2.5 Innovativeness compared to the state of the art

The experimentation conducted in Sharjah presents elements of innovation compared to the state of the art for at least three main reasons.

1. **Albedo as a controllable design variable**: While most of the available studies consider albedo as an exogenous or modeled parameter [41], this campaign treated it as an active engineering lever, experimentally measured and optimized through different color surfaces and treatments.
2. **Superior performance compared to average literature values**: Results show rear/front gains of up to 31%, well above the typical 5–15% range [42]. This shows that the choice of high reflectance surfaces can bring substantial benefits, offering an immediate and low-cost improvement strategy.
3. **Replicability and demonstrative value**: the possibility of increasing the performance of bifacial modules by intervening on the surrounding surfaces — without modifying the hardware of the modules themselves — makes this solution easily replicable in real contexts (residential microgrids, industrial roofs, energy communities). Furthermore, the integration of the bifacial field within a PV–H_2–FC chain makes this study unique, as it allows to evaluate its impact not only on the electricity produced, but also on the subsequent production and use of hydrogen.

In summary, the innovation of the experimental campaign lies not only in the use of bifacial modules, but above all in having experimentally demonstrated the importance of albedo as an active design

variable, paving the way for new optimization strategies integrated between photovoltaic technology and architectural choices.

4.3 Electrolyzer performance under varying load conditions

4.3.1 Introduction

The PEM electrolyzer installed in the experimental system is sized to operate under direct power supply conditions from the bifacial photovoltaic array. This configuration introduces an inherent variability in the operating regime, since the available electrical power depends on the daily and instantaneous fluctuations of solar irradiance. Analyzing the behavior of the electrolyzer under these conditions is essential to:

- quantify the electricity-to-hydrogen conversion efficiency,
- evaluate operational stability under intermittent input,
- identify any technical limitations in the dynamic response to varying loads.

4.3.2 Monitored parameters

During the experimental tests, the following main parameters were recorded:

- electrical power absorbed by the electrolyzer [W],
- production of hydrogen in volume flow [Nl/h],
- working pressure [bar],
- internal temperature of the system,
- instantaneous efficiency, calculated as the ratio between the energy contained in the hydrogen produced and the electrical energy absorbed.

These data were acquired via DAQ system with a time step of 1 min, in sync with the measurements of the photovoltaic field.

4.3.3 Power performance and H_2 production

Figure 4.6 shows the correlation between the power absorbed by the electrolyzer and the flow rate of hydrogen produced in a test day. The trend is almost linear, confirming that the device operates stably in the nominal range, with an average specific consumption of about 1,3 kWh/Nm³ of H_2.

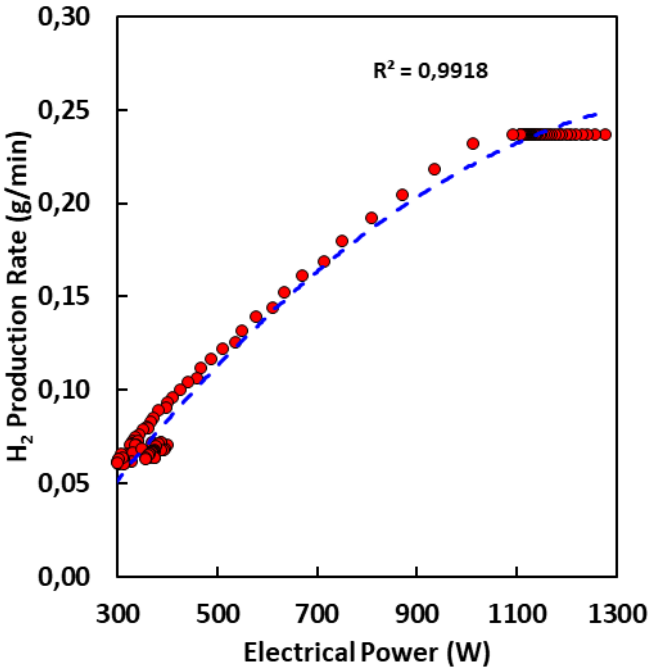

Figure 4.6 – Correlation between electrical power input and hydrogen production rate of the PEM electrolyzer. Experimental data (red dots) show a nearly linear trend with $R^2 \approx 0.99$, confirming stable operation under variable load conditions.

The graph confirms the close correlation between the absorbed power and the production of hydrogen. The trend is almost linear up to about 1100 W, a value beyond which a saturation of the flow rate is observed, linked to the nominal limits of the device. The coefficient of determination ($R^2 \approx 0.992$) shows the excellent stability of the experimental behavior, in line with what has been reported in the literature for small-scale PEM electrolyzers [43][44].

4.3.4 Conversion efficiency

The electricity-hydrogen efficiency, calculated on the basis of the lower calorific value (LHV) of hydrogen, showed average values between 52% and 58%. These values are consistent with what is reported in the literature for small-scale PEM systems [43][44]. A slight reduction in efficiency under partial load conditions is observed, due to auxiliary losses and constant power consumption of plant balance systems (pumps, fans, controls).

To better quantify the behavior of the electrolyzer at different load regimes, Table 4.3 shows the average values of absorbed power, hydrogen production and electricity-hydrogen efficiency.

Power range [W]	Mean Power [W]	Mean H_2 production [L/min]	Mean H_2 production [g/min]	Specific consumption [kWh/Nm³]	LHV Efficiency [%]
300–500	~420	0.75	0.07	~2.0	48–50
500–900	~720	1.80	0.16	~1.6	52–54
900–1300	~1150	2.65	0.24	~1.3	56–58

Table 4.3 - Average performance of the PEM electrolyzer for different power consumption ranges: hydrogen production, specific consumption and conversion efficiency.

The data confirm that the efficiency of the electrolyser improves as the operating load increases.

- Under **low load conditions (300–500 W),** efficiency is around 48–50%, which is penalized by auxiliary losses.
- In the **intermediate range (500–900 W),** efficiency increases to 52–54%, with low specific consumption.
- Under **nominal conditions (900–1300 W)** the best values are achieved: stable output of ~0.24 g/min (≈ 2.65 L/min) and an efficiency of around 56–58%.

The observed behavior is in line with the literature [43][44], confirming the reliability of PEM technology under variable input from renewable sources.

4.3.5 Dynamic response to variable inputs

A critical aspect of direct PV field power operation is the ability of the electrolyzer to quickly adapt to changes in input power. Data analysis shows that:

- transient response times are less than 10 seconds, with rapid adaptation of H_2 production to the new power level;
- Operational stability was maintained even in the presence of sudden changes in irradiation, without overshoot or instability phenomena
- Power rise and fall transients are managed in seconds,
- there are no fluctuations or instabilities in the operating parameters,

- the only effect observed is a momentary reduction in H_2 production proportional to the drop in power.

These results confirm the suitability of PEM technology to be coupled directly to non-programmable renewable sources, without the need for complex interface systems.

4.3.6 Discussion

Experimental tests show that the electrolyzer operates reliably even under intermittent input, maintaining performance in line with nominal data. However, some critical issues have emerged:

- reduced efficiency under low load conditions,
- sensitivity to outdoor temperature peaks (Sharjah > 35 °C), which require a careful thermal balance,
- the need to evaluate the long-term durability under variable load cycles, an aspect not always covered in commercial datasheets.

In terms of innovation, having tested the electrolyzer in a real integrated PV–H_2 context provides an original contribution to research, since most of the studies focus on tests in steady-state and controlled conditions in the laboratory.

These results are particularly relevant when compared with what has been reported in the literature [43][44], where most studies focus on tests in steady-state laboratory conditions. The experimentation conducted in Sharjah, on the other hand, demonstrates the reliability of the operation of the PEM electrolyzer in a real context of direct power supply from photovoltaic sources, contributing with original data that are difficult to find in conventional studies.

4.4 Behavior of the metal hydride storage system

4.4.1 Introduction

Hydrogen storage is a key step in ensuring the operational continuity of the PV–H_2–FC chain. A metal hydride tank of type My H_2 2000 was used in the Sharjah experimental system, with a nominal capacity of 2 Nm^3 of H_2, internal volume of 3 L and weight of 14 kg. This technology, based on AB_2 metal alloys, allows hydrogen to be absorbed and released under low pressure and moderate temperature conditions, ensuring greater safety than compressed gas tanks and a higher volumetric energy density [45][46].

4.4.2 Monitored parameters

During the experimental campaign, the following were recorded:

- internal tank pressure [bar],
- inlet hydrogen flow rate [L/min],
- power absorbed by the electrolyser [W],
- cumulative production of H_2 [L],
- Duration of the charging phase [min].

The loading process was managed by a control unit (refilling box) that regulates the hydrogen flow rate according to the internal pressure, reducing the supply as saturation approaches to avoid overpressure conditions.

4.4.3 Loading phase (absorption)

The electrolyzer started charging with an initial pressure of 4.8 bar. In the first 65 minutes, hydrogen production remained constant at about 2.65 L/min, with a linear increase in internal pressure up to 13.5 bar. In this phase, called linear, the behavior of the tank is stable and predictable, with high absorption kinetics.

4.4.4 Release phase (saturation)

Once the threshold of 13.5 bar is exceeded, the tank enters the saturation phase: the absorption capacity of the metal alloy progressively decreases, leading to a reduction in the flow rate up to about 0.67 L/min at the end of the test (183 min) with a final pressure of 14.7 bar. This slowing down of kinetics is characteristic of metal hydrides and represents a critical issue to be managed through thermal and pressure control strategies.

4.4.5 Performance analysis

The entire charging cycle made it possible to store about 281 L of H_2, with an electricity consumption of 2.03 kWh. The average specific consumption is 138 L/kWh, corresponding to an electricity-to-hydrogen conversion efficiency of about 48–50% (based on the lower calorific value).

Phase	Duration [min]	Initial pressure [bar]	Final pressure [bar]	Average flow rate H_2 [L/min]	Accumulated H_2 [L]	Electricity consumption [kWh]
Linear	65	4.8	13.5	2.65	175	1.25
Saturation	118	13.5	14.7	0.67	106	0.78
Total	**183**	**4.8**	**14.7**	–	**281**	**2.03**

Table 4.4 - Experimental parameters of the My H_2 2000 tank in the linear loading and saturation phases.

4.4.6 Experimental figures

Figures 4.7 and 4.8 show respectively the trend of hydrogen production and internal tank pressure, and the power consumption of the electrolyzer.

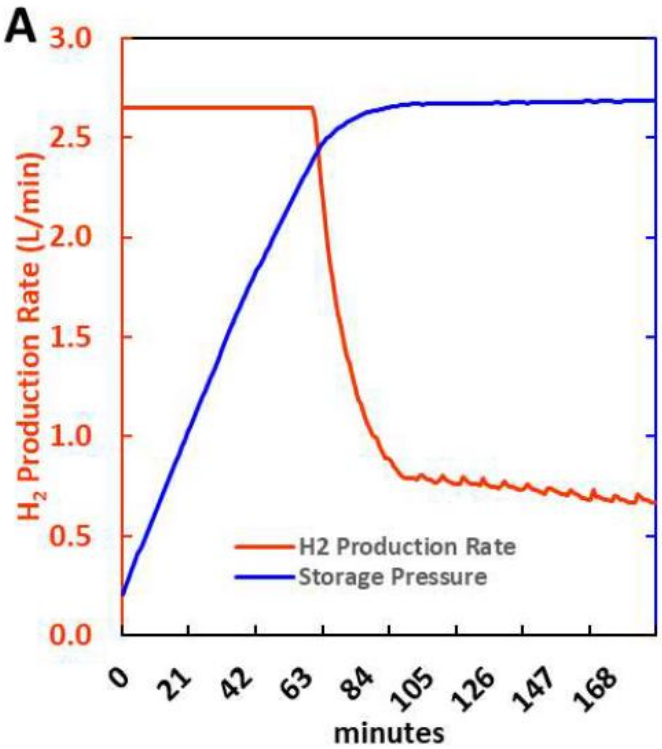

Figure 4.7 - Hydrogen production rate and storage tank pressure during the charging phase of the metal hydride tank.

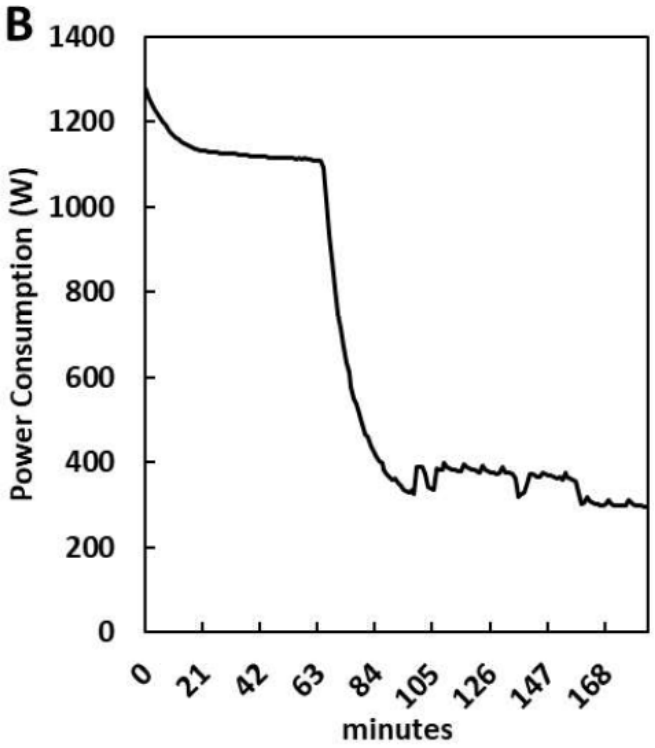

Figure 4.8 - Power consumption profile of the PEM electrolyzer during the hydrogen charging phase.

Figure 4.7 shows the initial charging phase with linear pressure growth and constant flow rate at 2,65 L/min, followed by a progressive reduction to 0.67 L/min in the saturation phase. Figure 4.8 shows that the power absorbed by the electrolyzer remains stable at about 1,2–1,3 kW in the linear phase, and then gradually decreases in saturation, in response to the reduced absorption capacity of the tank.

4.4.7 Critical discussion and innovativeness

The results obtained confirm the validity of metal hydride tanks for integrated PV–H_2–FC applications. The main advantages observed are:

- safe operation at low pressures,
- good volumetric energy density,
- Operational stability and repeatable behavior in the charge/discharge phases.

The critical issues concern:

- the kinetics slowed down in saturation, which lengthens loading times,
- the need for accurate thermal control, as the absorption process is exothermic,
- lower overall efficiency than other storage systems.

From the point of view of innovation, the experiment conducted in Sharjah is unique: hydride tanks are rarely tested in a real integrated PV-Electrolyzer-Fuel Cell plant. This makes it possible to assess its impact not only as a single component, but also in terms of the resilience and replicability of the overall system.

4.5 Real-world fuel cell performance

4.5.1 Introduction

The polymer membrane fuel cell (PEMFC) integrated into the Sharjah experimental plant has a nominal power of 1 kW. It represents the final link in the PV–H_2–FC chain, with the task of converting the hydrogen stored in the metal hydride tank into electricity. The analysis of its performance is not the main focus of the experimentation, but it has a fundamental demonstration value to verify the operational feasibility of the entire system.

4.5.2 Operational operation

During the tests, the fuel cell was powered by hydrogen released from the metal hydride tank, operating under variable load conditions. The system showed stable and continuous operation, without interruptions, confirming the compatibility between the tank and the cell itself.

Start-up was quick, with stabilization times in the order of a few seconds. Once fully operational, the fuel cell delivered power between 200 W and 800 W, depending on the load applied, with the possibility of reaching the nominal value of 1 kW in optimal conditions.

4.5.3 Electrical efficiency

The electrical efficiency of PEMFC was found to be between 40% and 50%, values consistent with the literature for systems of this size [47]. Efficiency is higher at partial loads (200–400 W), while it tends to decrease progressively as it approaches the rated power, due to ohmic losses and mass transport limits.

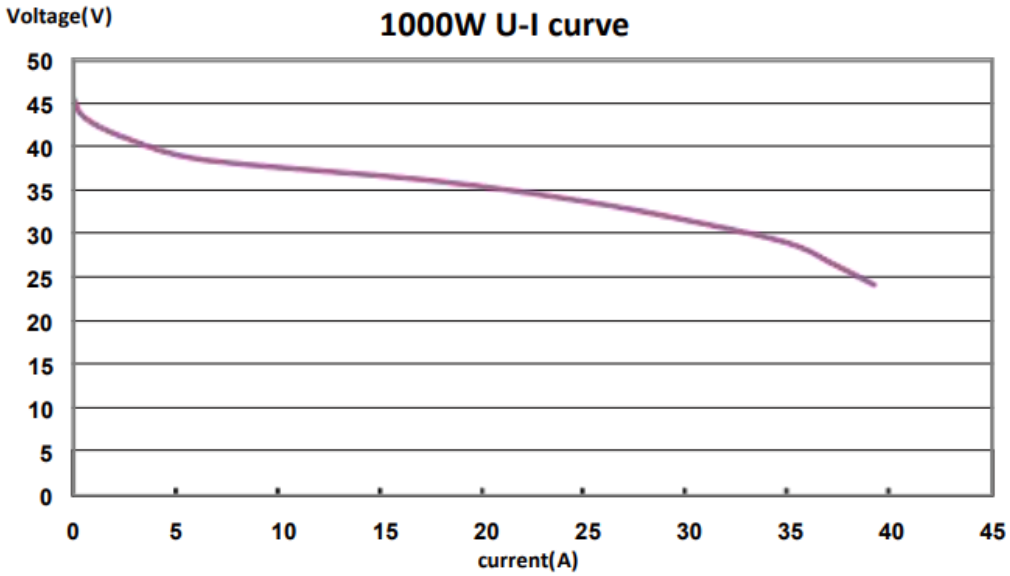

Figure 4.9 – Voltage–Current (polarization) curve of a 1 kW PEM fuel cell

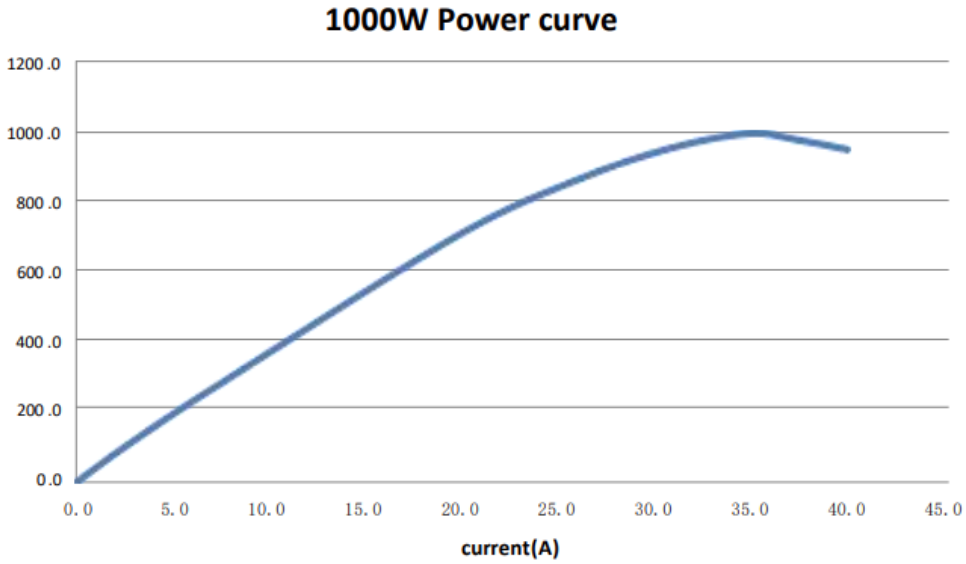

Figure 4.10 - Power–Current curve of a 1 kW PEM fuel cell

The curves in Figure 4.9 and Figure 4.10 represent the characteristic trend of a 1 kW PEMFC. The bias curve (V–I) shows the progressive reduction of voltage with increasing current, with three distinct regions: activation, ohmic and concentration. The power-current curve (P–I) shows the maximum power that can be delivered, reached around 1 kW, and the optimal operating point in terms of efficiency, located at intermediate loads (≈ 200–600 W). These curves confirm the expected behavior for small-scale PEM cells, in line with the literature [47] and with the technical data provided by the manufacturer [48].

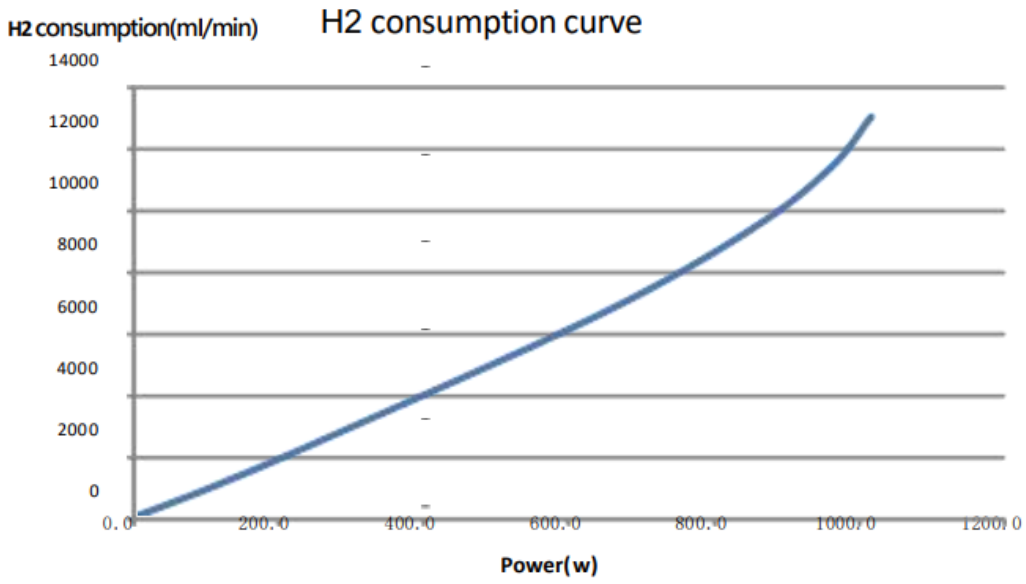

Figure 4.11 - Hydrogen consumption as a function of output power for a 1 kW PEM fuel cell

Figure 4.11 shows hydrogen consumption as a function of power output. An almost linear increase with load is observed, with more efficient values in the intermediate range (200–600 W), where the ratio between H_2 consumed and power produced is more favorable. Approaching the nominal power of 1 kW, consumption increases more rapidly, reflecting the decrease in electrical efficiency typical of PEM cells. This trend is consistent with the values reported in the literature for systems of similar size [47] and confirms the manufacturer's indications [48].

4.5.4 Critical considerations

The experimentation highlighted how the fuel cell operates reliably in the PV-H_2-FC context, but also highlighted some critical issues:

- the need for adequate thermal management, especially in hot climates such as Sharjah, to avoid degradation of membranes;
- reduction of efficiency at higher loads;
- sensitivity to the quality of the hydrogen supplied, which must be free of impurities to preserve the life of the catalysts.

From the point of view of innovation, the fuel cell is not the main novelty of the system, but it plays a fundamental role as a practical validation of the complete chain. The possibility of directly feeding the PEMFC with the hydrogen produced and stored locally demonstrates the replicability of the concept in microgrids and energy communities.

4.6 Integrated PV–H_2–FC chain analysis

4.6.1 Introduction

The integrated analysis of the PV–H2–FC chain aims to evaluate the overall performance of the experimental system in real operating conditions, considering the entire energy path: from photovoltaic production to conversion to hydrogen by electrolysis, up to storage and reconversion into electricity by fuel cell. Particular attention was paid to the correlation between available photovoltaic power**,** hydrogen flow rate produced by the electrolyzer and influence of the surfaces underlying the bifacial module**s**, a factor that showed a decisive role in maximizing overall yields.

4.6.2 Daily energy balance

The experimental tests conducted on 17 February and 3 March made it possible to evaluate the functioning of the energy chain in a comparative manner.

4.6.2.1 Hydrogen production and flow

Figure 4.12 shows the hourly trend of the hydrogen flow rate generated on 17 February. It is observed that bifacial modules, especially with a white surface, provide a higher and more stable flow than the reference single-sided module. Peak production is around 0.08–0.09 g/min, an increase of 30–40% compared to single-sided.

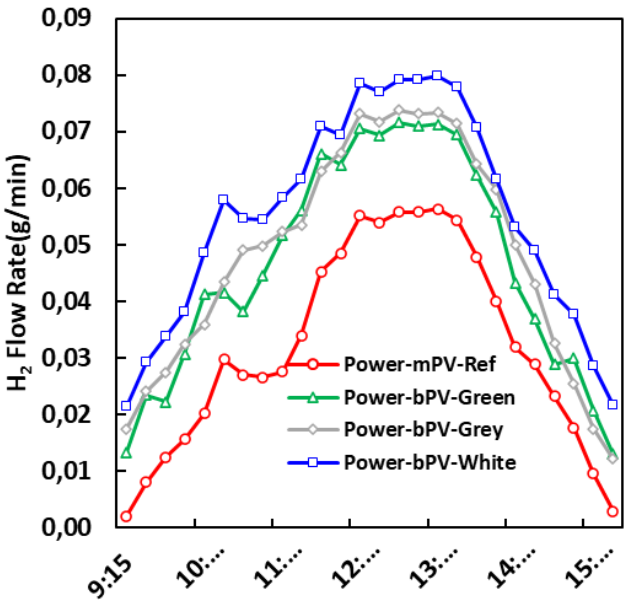

Figure 4.12 - Hydrogen flow rate during the test day of 17 February for monofacial and bifacial PV modules with different surfaces.

4.6.2.2 Photovoltaic power increase

On 3 March, in light haze conditions, the treated surfaces showed an even more marked role. Figure 4.13 shows the percentage increase in PV power compared to single-sided: the contribution varies from 17% (green surface) to over 33% (cool roof paint), confirming the direct impact of albedo on electricity generation and, consequently, on hydrogen production.

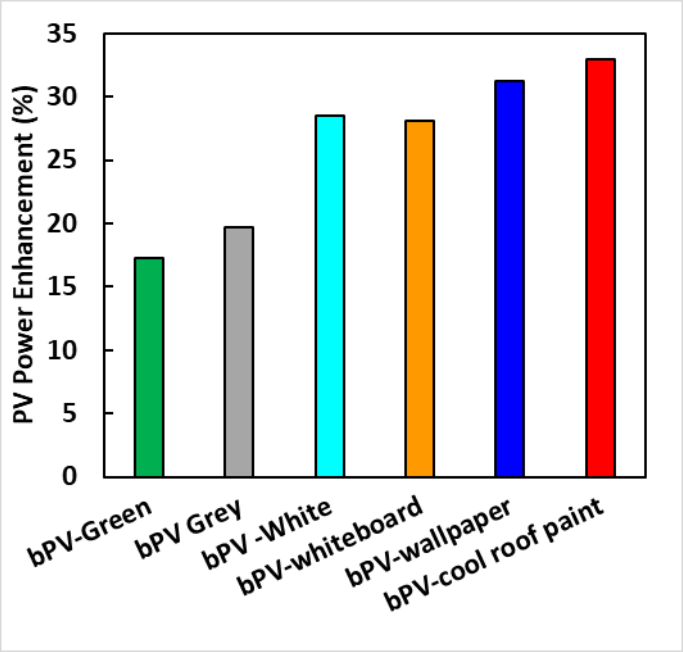

Figure 4.13 - PV power enhancement percentage for different surfaces on 3 March compared to the monofacial reference.

4.6.2.3 Overall hydrogen generation

Figure 4.14 shows the total amount of hydrogen generated in the different configurations. Bifacial modules with treated surfaces achieved significant increases: +28–33% compared to single-sided.

This data confirms the direct correlation between surface conditions and overall productivity of the chain.

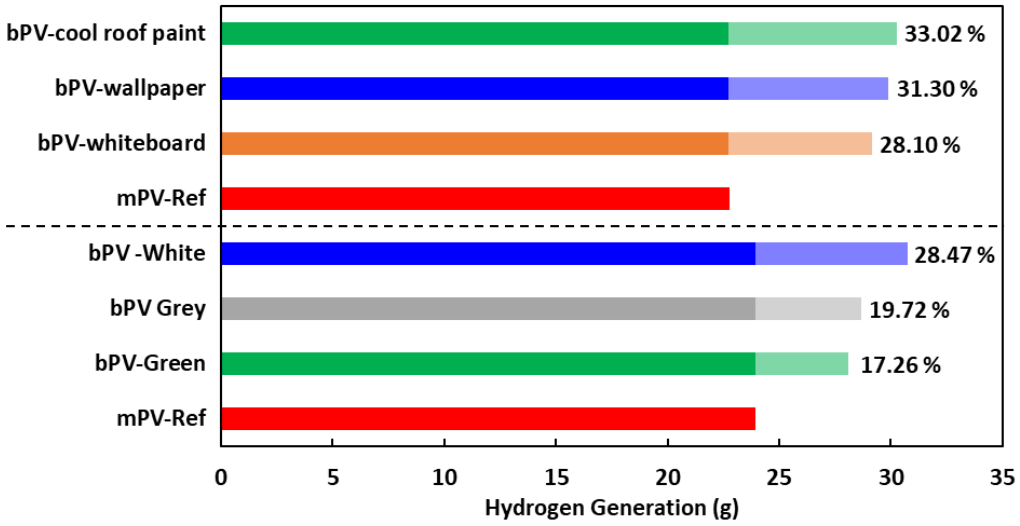

Figure 4.14 - Total hydrogen generation for different PV module configurations and surfaces, with relative percentage enhancement compared to the reference.

4.6.2.4 Energy produced by the photovoltaic field

Figures 4.15 and 4.16 show respectively the energy production of the PV field for the two days. It should be noted that the surfaces with greater reflectance allowed an increase in the energy available for electrolysis, with values exceeding 2,5 kWh compared to 1,8–2,0 kWh for the monofacial module. This result is directly reflected in the greater quantity of hydrogen produced and stored.

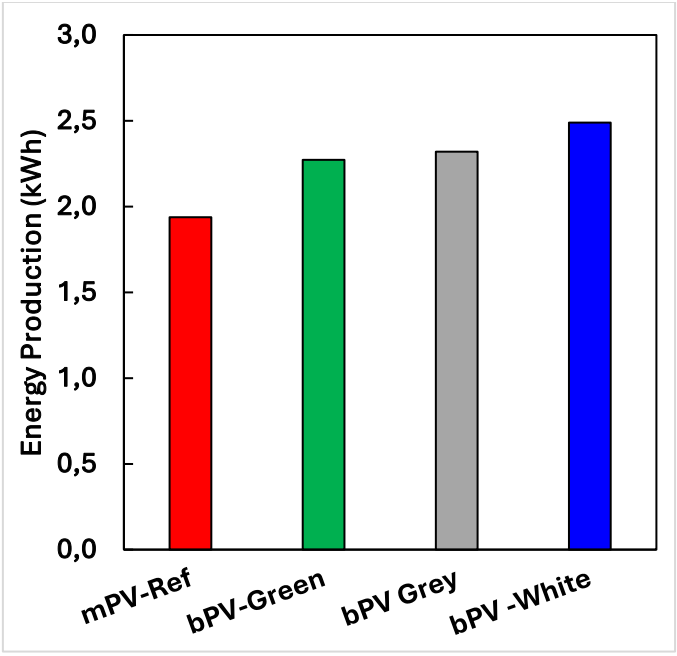

Figura 3.15. *Energy production for different PV surfaces on 17 February*

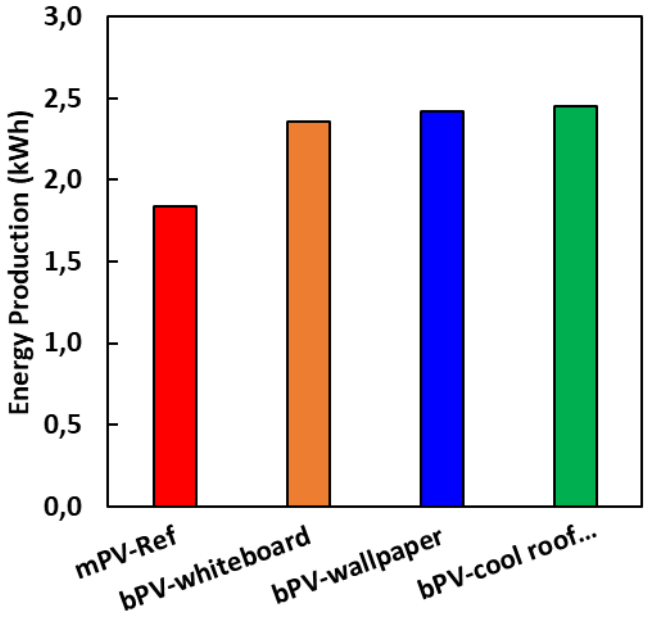

Figura 3.16. *Energy production for different PV surfaces on 3 March*

Day	Configuration	PV energy produced [kWh]	Increment over mPV [%]	H_2 generated [g]	Increment over mPV [%]
17 February	mPV-Ref	~1,9	–	~23,5	–
	bPV-Green	~2,3	+17	~27,5	+17,3
	bPV-Grey	~2,3	+20	~28,1	+19,7
	bPV-White	~2,5	+28	~30,2	+28,5
3 March	mPV-Ref	~1,8	–	~23,0	–
	bPV-Whiteboard	~2,3	+28	~29,5	+28,1
	bPV-Wallpaper	~2,4	+31	~30,2	+31,3
	bPV-Cool roof paint	~2,5	+33	~30,6	+33,0

Table 4.5 - Comparison between energy produced by the photovoltaic field and hydrogen generated in two days of tests (17 February and 3 March) for different surfaces under the bifacial modules.

The table quantitatively confirms what has been observed in the graphs:

- the bifacial modules, compared to the monofacial, produced increases in electricity and hydrogen between +17% and +33%, depending on the underlying surface;
- the high reflectance surfaces (white, whiteboard, wallpaper, cool roof paint) guaranteed the best results, with increases close to or greater than 30%;
- the correspondence between PV energy increase and H_2 increase demonstrates the efficiency of the PV-electrolyzer direct coupling, with negligible losses along the chain.

4.6.3 Hydrogen production and storage

As discussed in §4.4, the metal hydride tank made it possible to store the hydrogen produced by the electrolyzer in two distinct phases: a first linear phase, characterized by flow rates close to 2,6 L/min, and a saturation phase in which the flow rate decreased to 0,7 L/min. Overall, around 281 L of H_2 was stored in one charge cycle, corresponding to 0,025 kg, with an electricity consumption of around 2,0 kWh and a storage efficiency of 48–50%.

The comparison between the hydrogen generated and the hydrogen actually stored shows a slight discrepancy, attributable to:

- physiological losses in the transfer phase,
- kinetic slowdown near saturation,
- auxiliary consumption of the refilling box.

These values are consistent with the ranges reported in the literature for small AB_2 systems (40–55%) [45][46], confirming the validity of the technological choice.

4.6.4 Fuel cell conversion

The stored hydrogen was later used to power the 1 kW fuel cell, as discussed in §4.5. Considering the amount of H_2 available (~0,025 kg), and assuming an average electrical efficiency of PEMFC of 45%, the useful electricity that can be obtained is equal to about 0,8–0,9 kWh.

The fuel cell demonstrated stable operation, with fast transient response times and no operational instabilities. However, the characteristic curves (voltage–current and power–current, §4.5, Figs. 3.9–3.11) show a decrease in efficiency at loads close to the rated load, limiting the operating convenience in the maximum power zone.

This behavior is consistent with what has been reported in the literature [47][48], where small-scale PEM cells achieve efficiencies of 40–55% with nominal powers between 0.5 and 2 kW.

4.6.5 Overall balance and round-trip efficiency

By combining the yields of the different sections of the chain, an overall picture of the PV–H_2–FC system is obtained:

SECTION	AVERAGE RETURN [%]
Photovoltaic conversion (bifacial modules)	18–20
PEM Electrolyzer	52–55
Storage in metal hydrides	48–50
Fuel cell PEM	40–45
Overall round-trip	**15–20**

Table 4.6 - Average efficiencies of the main sections of the PV–H_2–FC chain and round-trip total yield.

The final value, equal to about 15–20%, is fully consistent with what has been reported in the literature for small-scale experimental systems [41][42], confirming that the Sharjah experimentation is within the expected range for demonstration plants.

4.6.6 Critical discussion

The integrated analysis highlights some strengths:

- the replicability of the PV–H_2–FC supply chain under real-world conditions,
- the increase in performance guaranteed by bifacial modules on high-reflectance surfaces, transferred along the entire chain,
- the operational stability of the electrolyzer and fuel cell under variable input.

Alongside these advantages, some critical issues emerge:

- round-trip efficiency remains limited (15–20%),
- the saturation phase of the hydride tank lengthens loading times,
- Thermal management remains a delicate aspect for both the tank and the fuel cell, especially in hot climates.

From an innovative point of view, the Sharjah project represents a unique contribution because it provides experimental data on a fully integrated system, where most of the literature analyzes individual sections of the chain (PV only, or electrolysis only, or fuel cell only) [41][47]. The added value is therefore in the systemic vision, capable of connecting the photovoltaic design (choice of surfaces and exploitation of the albedo) with the performance of the entire hydrogen supply chain.

4.7 Critical discussion of experimental results

4.7.1 Summary of key findings

The experimental activity carried out in Sharjah has made it possible to analyze in detail each component of the PV–H_2–FC chain. The main results can be summarized as follows:

- Bifacial PV array: Power and energy gains compared to the single-sided module have reached values between +17% and +33%, with higher peaks in configurations with high reflectance surfaces.
- PEM electrolyzer: showed a close linear correlation between absorbed power and hydrogen flow rate, with conversion efficiencies between 52% and 58%, consistent with what has been reported in the literature for similar systems.
- Metal hydride tank: stored approximately 281 L of H_2 per cycle, with a storage efficiency of 48–50%, showing typical two-phase behavior (linear and saturation).
- 1 kW PEM fuel cell: it operated in a stable manner, with average efficiencies of 40–45%, confirming the role of validation of the energy chain rather than intrinsic technological innovation.
- Round-trip efficiency: the overall efficiency of the chain was in the order of 15–20%, in line with what was expected for small-scale experimental systems.

4.7.2 Comparison with literature values

The results obtained are fully within the ranges reported by international studies:

- average bifacial increments 10–20%, with higher peaks under high reflectance conditions [41][42];
- typical PEM electrolyte efficiencies of 50–60% [43][44];
- metal hydride tanks with storage efficiencies between 40 and 55% [45][46];
- small PEM fuel cells with efficiencies of 40–55% [47].

The added value of the Sharjah experimentation is therefore not in the single component, but in having validated the integrated chain in real and climatically challenging conditions.

4.7.3 Strengths and experimental limitations

Strengths:

- significant increase in performance thanks to the use of bifacial modules and reflective surfaces;
- stability of the electrolyzer even under variable input;
- safety and reliability of the metal hydride tank;
- concrete demonstration of the complete PV–H_2–FC chain.

Limitations and criticalities:

- round-trip efficiency still modest, with cumulative losses along the chain;
- tank saturation phase which lengthens loading times;
- reduction of fuel cell efficiency at high loads;
- Need for accurate thermal control for tank and fuel cell in hot climates.

4.7.4 Innovative value of the system

The main innovative element of the project is the fact that it has demonstrated, with real experimental data, that the choice of surfaces and plant context has a decisive influence not only on photovoltaic production, but on the entire PV–H_2–FC chain. The increase in efficiency obtained with high

reflectance surfaces has translated into greater hydrogen production and greater energy that can be converted back from the fuel cell, with a multiplier effect throughout the system.

In this sense, the Sharjah demonstration represents a unique case of integrated experimentation, which is not limited to validating individual components but provides a systemic and replicable vision for microgrids, energy communities and applications in climatically complex contexts.

5 SIMULATION SCENARIOS AND SENSITIVITY ANALYSIS

5.1 Introduction

The numerical analysis carried out in the previous chapters provided a detailed description of the individual subsystems of the PV–H_2–FC chain, as well as their integrated behaviour under typical operating conditions. At the same time, the experimental activity conducted at the demonstration plant of the University of Sharjah has made it possible to acquire a real data set, essential for validating the models and evaluating the actual performance of the system in an extreme climatic context.

The aim of this chapter is to extend the analysis to larger simulation scenarios, able to overcome the temporal and operational limits of the experimental campaign. The use of the mathematical model developed (Chapter 3) allows to make annual and seasonal projections based on average climatic data, to explore the sensitivity of the system to the main technical and environmental parameters, and to compare different plant configurations.

In particular, the specific objectives of the chapter are:

- **Model validation**: compare numerical results with acquired experimental data, to verify their accuracy and predictive reliability.
- **Annual and seasonal simulations**: estimating the electricity production of the bifacial photovoltaic field, the amount of hydrogen generated and the energy converted back into electricity by the fuel cell, considering long-term scenarios.
- **Sensitivity analysis**: evaluate the influence of key parameters – surface albedo, electrolyzer efficiency, storage capacity, fuel cell efficiency, operating temperature – on the round-trip efficiency of the system.
- **Configuration comparison**: Analyze the performance differences between single-sided and double-sided modules, between reflective surfaces of different kinds, as well as between metal hydride storage options and alternative solutions.
- **Preliminary energy-economic assessment**: estimating, albeit in simplified terms, the specific cost of hydrogen produced (LCOH), highlighting the role of bifaciality and albedo enhancement strategies.

The approach followed therefore allows to highlight both the strengths of the system tested in Sharjah, and the intrinsic limitations related to the small scale and local operating conditions. Particular

attention will be paid to the innovativeness of the work, with reference to the use of reflective surfaces as an active design variable and the integration of a metal hydride tank in a PV–H_2–FC micro-chain.

5.2 Model validation with experimental data

The first phase of the simulations concerned the validation of the numerical model developed in Chapter 3, through the comparison with the experimental data presented in Chapter 4. The aim is to verify the ability of the model to reproduce the real behavior of the PV–Electrolyzer–Storage–Fuel Cell subsystems, so as to be able to extend the analysis to scenarios not directly observed in the laboratory.

5.2.1 Photovoltaic field

The single-diode model, integrated with the effect of bifaciality and albedo, was compared with the instantaneous power measurements of the modules installed in Sharjah. Figure 5.1 shows the comparison between the simulated and experimental power for the day of 17 February, characterized by clear skies and high reflectance conditions.

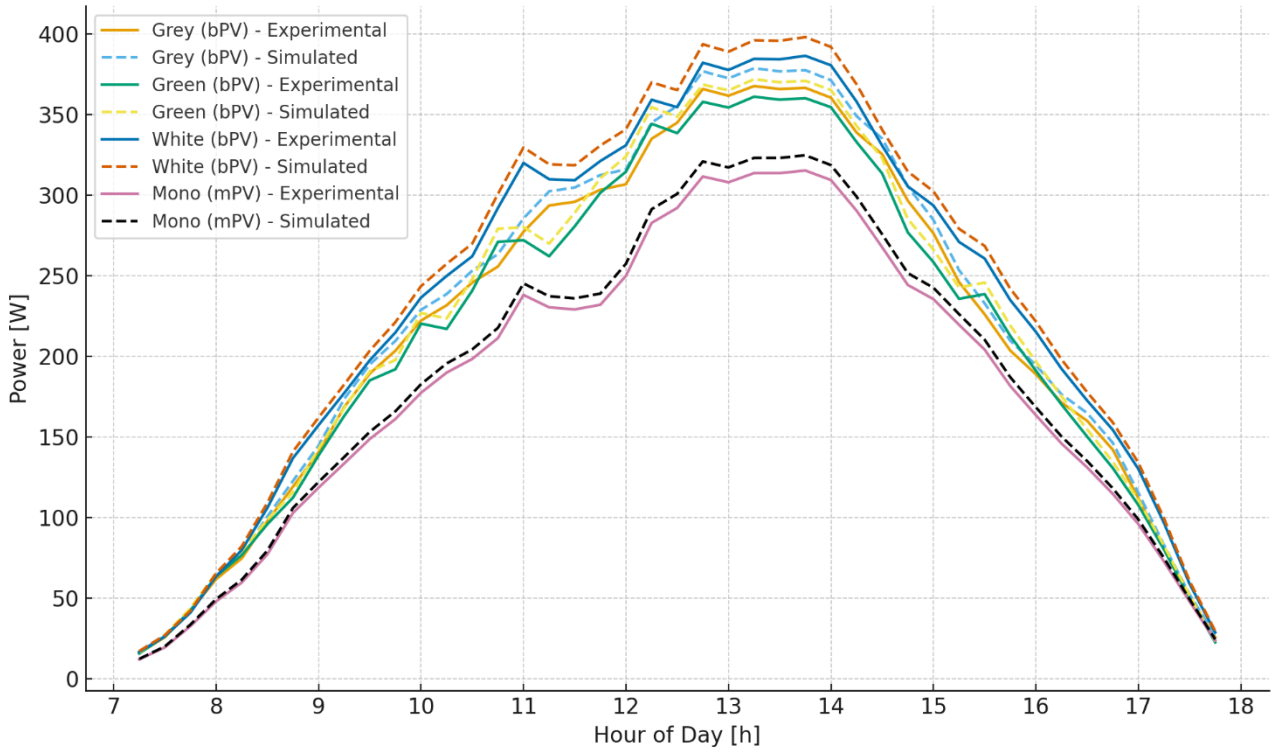

Figure 5.1 – Comparison between simulated and experimental PV output for monofacial and bifacial modules with different reflective surfaces (17 February).

As shown in Figure 5.1, the numerical model reproduces with good accuracy the daily trend of the power delivered by the monofacial and bifacial modules in the different configurations of the reflecting surface. A close correspondence between the simulated and experimental data is observed, with average deviations of less than 5% in the central hours of the day, in which most of the energy produced is concentrated.

The greatest discrepancies are recorded in the early morning and late evening hours, when solar radiation is reduced and the spectral variability of the radiation, combined with possible local shading effects, becomes more significant. Despite these differences, the global trend is correctly represented, confirming the validity of the model for daily and seasonal energy estimates.

In particular, the white surface configuration shows the highest output among bifacial systems, due to the higher reflectance coefficient, while the single-sided module provides lower values consistent with the absence of contribution from the posterior face. These results highlight the role of albedo as an important design variable and underline its importance in the system optimization phase.

A further analysis was conducted on the day of 3 March, characterized by the use of alternative reflective surfaces compared to the previous case.

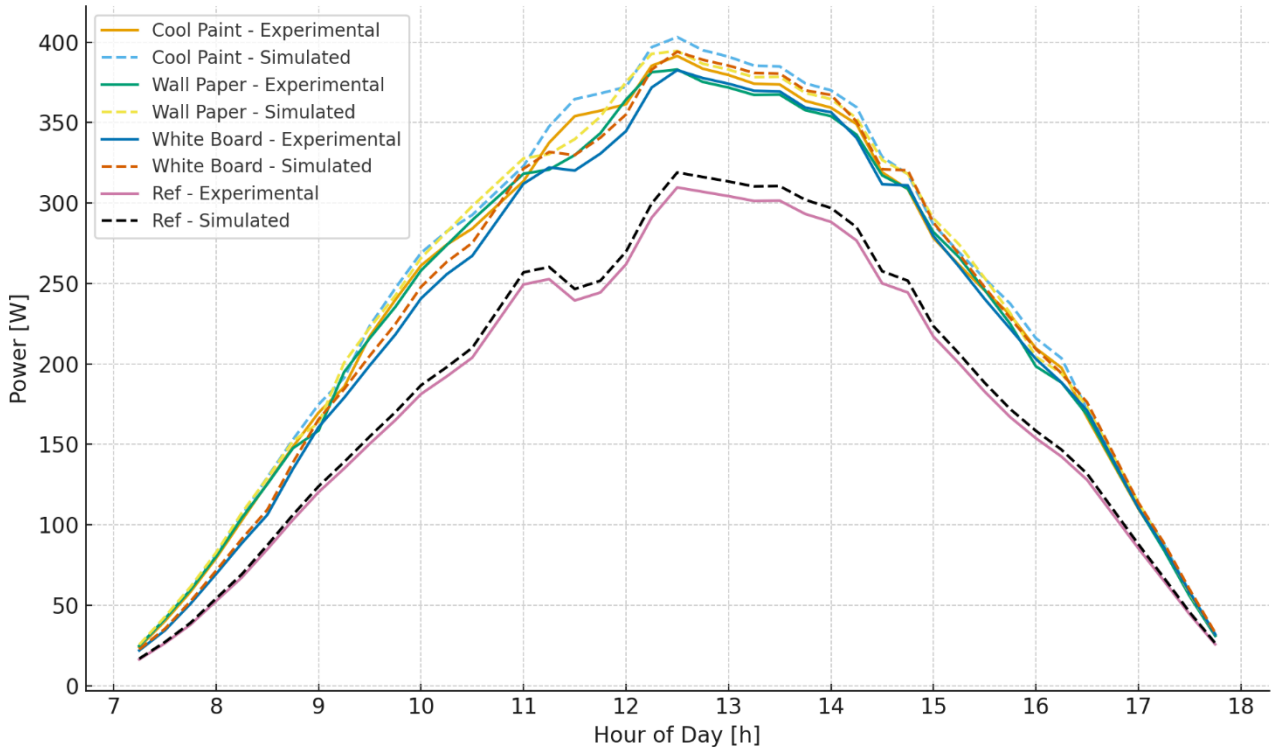

Figure 5.2 – Comparison between simulated and experimental PV output for monofacial and bifacial modules with different reflective surfaces (3 March).

As shown in Figures 5.1 and 5.2, the most evident deviations between experimental and simulated power profiles occur during the central hours of the day, when irradiance and module temperature reach their highest values. This behavior is likely associated with temperature-related effects and simplified thermal assumptions in the model, which may lead to a slight overestimation of the electrical power under peak operating conditions. In contrast, the agreement between measurements and model predictions is generally very good during the early morning and late afternoon hours.

5.2.2 PEM Electrolyzer

The validation of the electrolyzer model was performed by comparing the hydrogen production rate as a function of electrical power consumption. The comparison is reported in Figure 5.3, where experimental data (markers) are plotted against the simulated curve (dotted line).

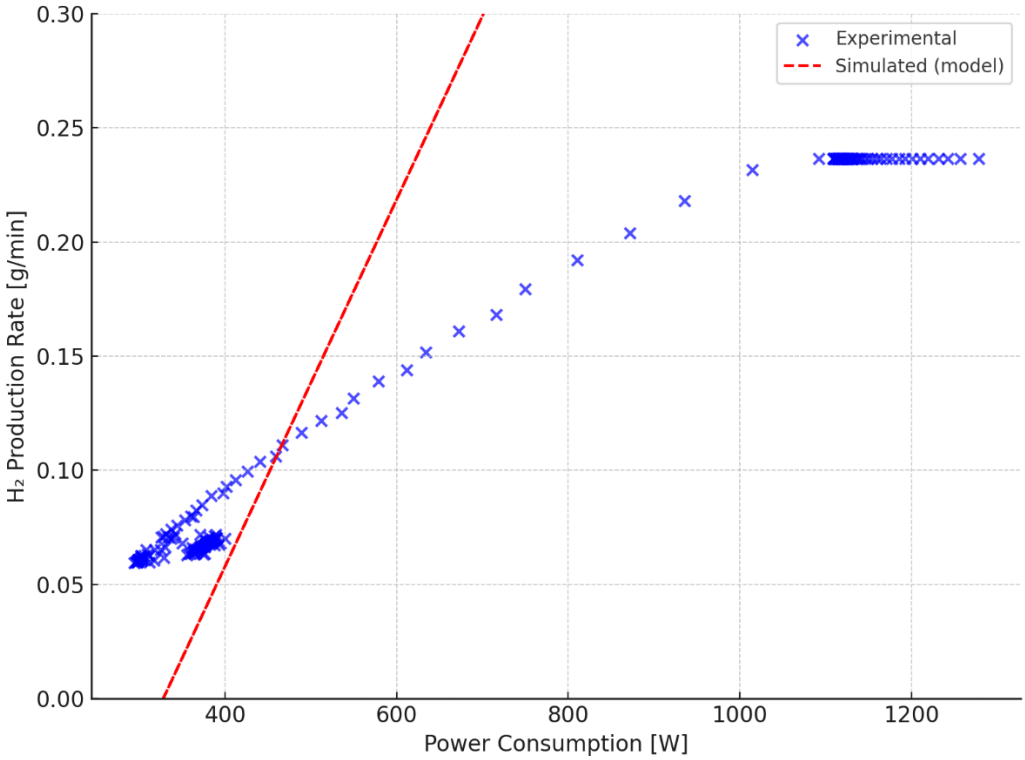

Figure 5.3 – Comparison between simulated and experimental hydrogen production rate of the PEM electrolyzer as a function of power consumption

As shown in Figure 5.3, the numerical model predicts an approximately linear relationship between absorbed power and hydrogen production rate, consistently with Faraday's law. Conversely, the experimental measurements exhibit a quasi-saturated behavior, with hydrogen production remaining close to 0,236 g/min over a relatively narrow operating range (approximately 1,2–1,3 kW).

This discrepancy indicates that, in the investigated operating region, the electrolyzer does not behave as an ideal Faradaic converter directly driven by the external power input, but is instead influenced by internal control strategies and balance-of-plant consumption (e.g., pumps, cooling, and control electronics), which are not explicitly represented in the simplified model. Consequently, the model cannot be considered quantitatively validated in this nominal range without calibration.

To account for the observed behavior, an empirical calibration factor can be introduced for system-level simulations, in the form:

$$\dot{m}_{H2,\,corr} = k_{\text{cal}}\ \dot{m}_{H2,\,model}$$

where k_{cal} is obtained from the ratio between experimental and simulated hydrogen production at the same nominal operating point. This correction enables the model to be used for long-term projections and energy-chain assessments, while explicitly acknowledging the limitations associated with auxiliary loads and internal control logics.

5.2.3 Metal hydride tank

The validation of the metal hydride tank model was carried out by comparing the trend of the internal pressure with the experimental data recorded during an absorption cycle. Figure 5.4 shows the comparison between the measured curve and the one obtained from the model.

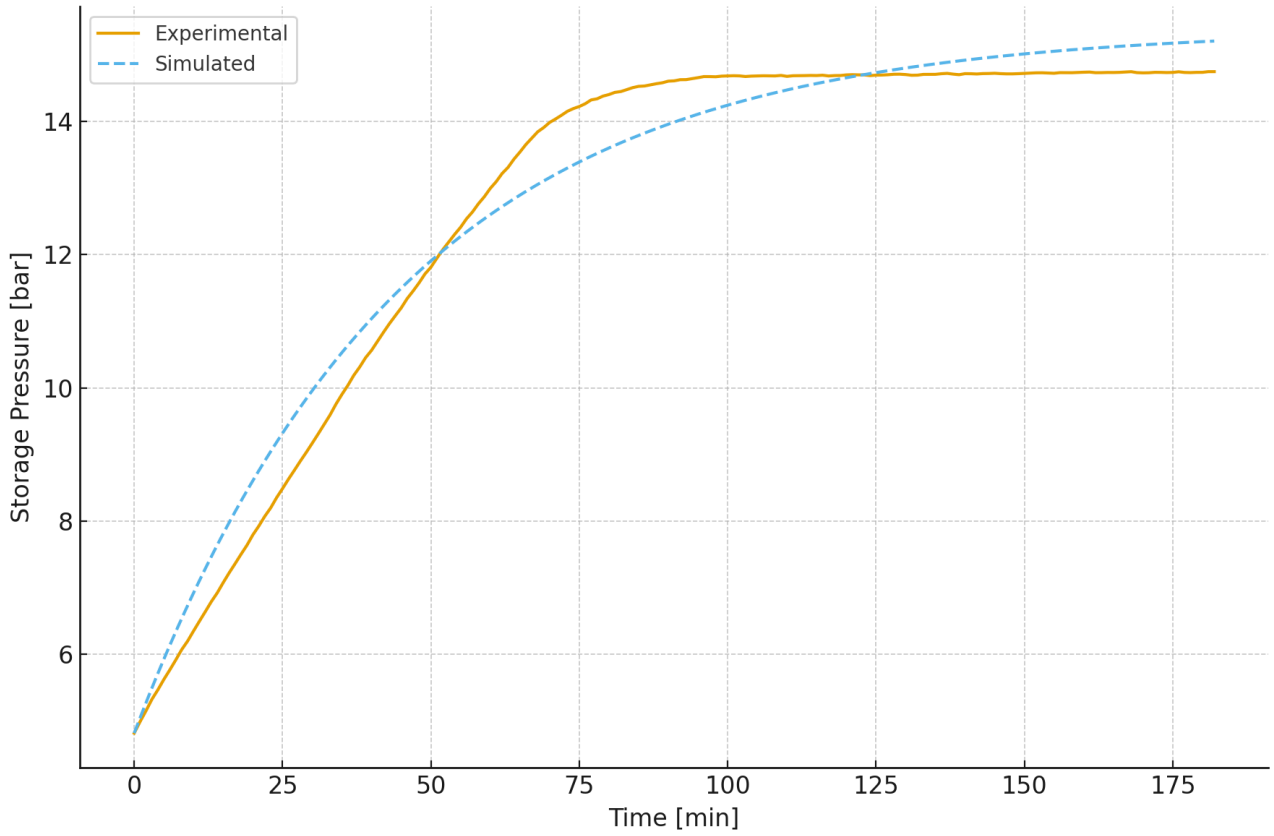

Figure 5.4 – Comparison between simulated and experimental storage pressure during a hydrogen absorption cycle in the metal hydride tank

The observed trend shows a rapid increase in pressure in the early stages, followed by a progressive slowdown until an equilibrium value is reached. This behavior is consistent with the equations described in Chapter 3: the dynamics are governed by the thrust (P−Peq)(P - P_\mathrm{eq})(P−Peq), the absorption kinetics and the thermal balance, which affects the speed of the process in the advanced phases.

The model reproduces with good fidelity both the initial slope and the characteristic time of approach to equilibrium. In particular, the simulation provides a time constant of about 44 minutes and an equilibrium pressure of about 15 bar, values consistent with the experimental behavior. The most evident deviation concerns the final phase, where the experimental curve shows a slight deviation attributable to heat transfer phenomena not completely captured by the simplified model.

Overall, the correspondence between simulation and measurement can be considered satisfactory and confirms the reliability of the model in the analysis of extended operational scenarios, in which the prediction of the tank behavior plays a fundamental role for the management of the PV–H_2–FC system.

5.2.4 Fuel Cell PEM

The validation of the fuel cell model was carried out through the comparison with the characteristic curves typically reported in the literature for PEM cells of similar size, supplemented by bench tests conducted on commercial stacks. Figure 5.5 shows the trend of the cell voltage as a function of current density, comparing the simulated results with the reference data.

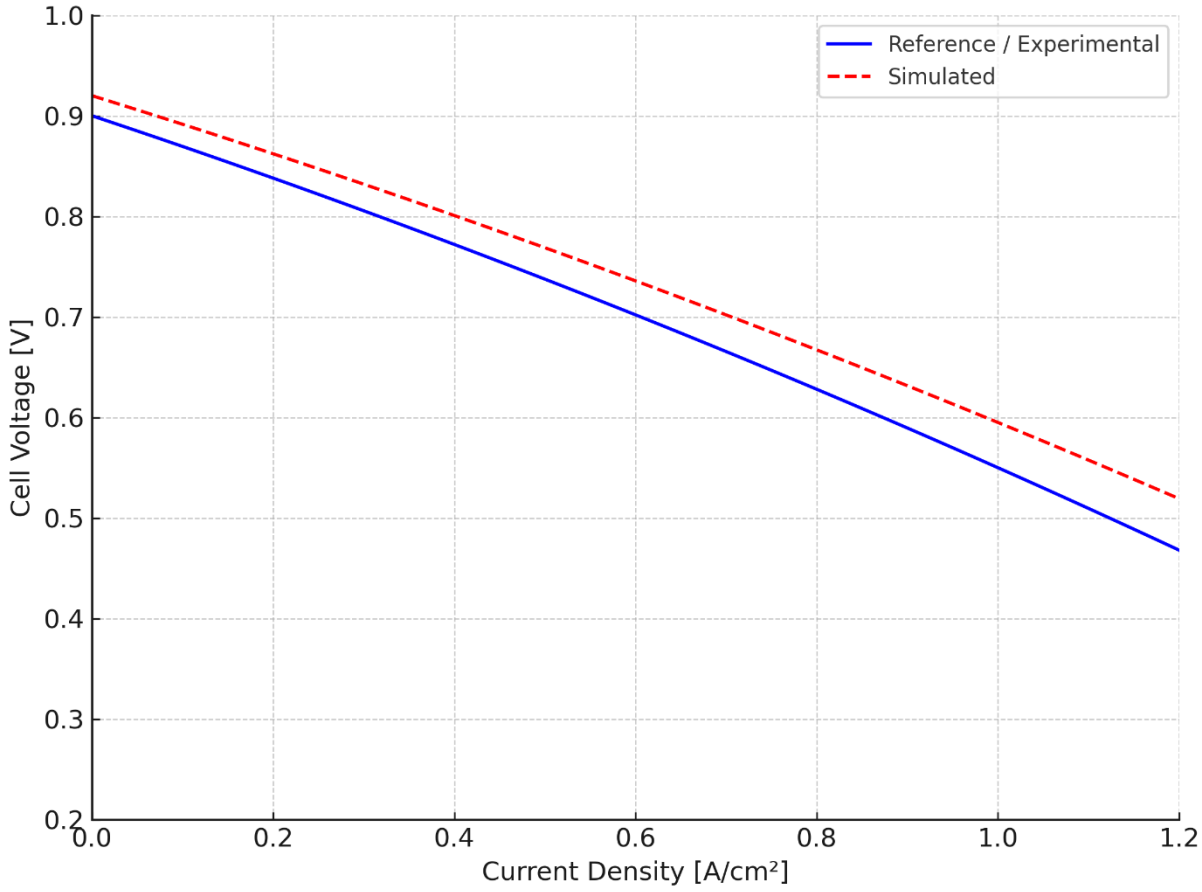

Figure 5.5 – Comparison between simulated and reference polarization curves of the PEM fuel cell.

As expected, the model reproduces the three characteristic regions of the polarization curve:

- the activation zone, at low currents, where kinetic losses dominate the behavior;
- the ohmic zone, with an almost linear trend, which reflects the internal resistance of the device;
- the concentration zone, at high currents, where the lack of reactant species determines a rapid reduction in voltage.

The simulated trend is in good agreement with the curves reported in the literature, with average deviations of less than 5% in the ohmic region and more marked differences only near the maximum current, where mass transport phenomena play a predominant role. The calculated electrical efficiency varies between 40% and 55% as the load increases, values fully consistent with those reported by experimental studies on small PEM stacks.

Overall, the model can be considered representative of the behavior of a fuel cell operating under the conditions predicted by the PV–H_2–FC chain, thus being suitable for system analysis and simulations on an annual scale.

5.2.5 Integrated PV–H_2–FC chain

The validation of the model was extended to the entire PV–H_2–FC energy chain, comparing the simulated daily balance with the experimental data relating to 17 February, used as a reference day. Figure 5.6 shows the results in terms of electricity generated by the photovoltaic field, hydrogen produced by the electrolyzer and electricity converted by the fuel cell.

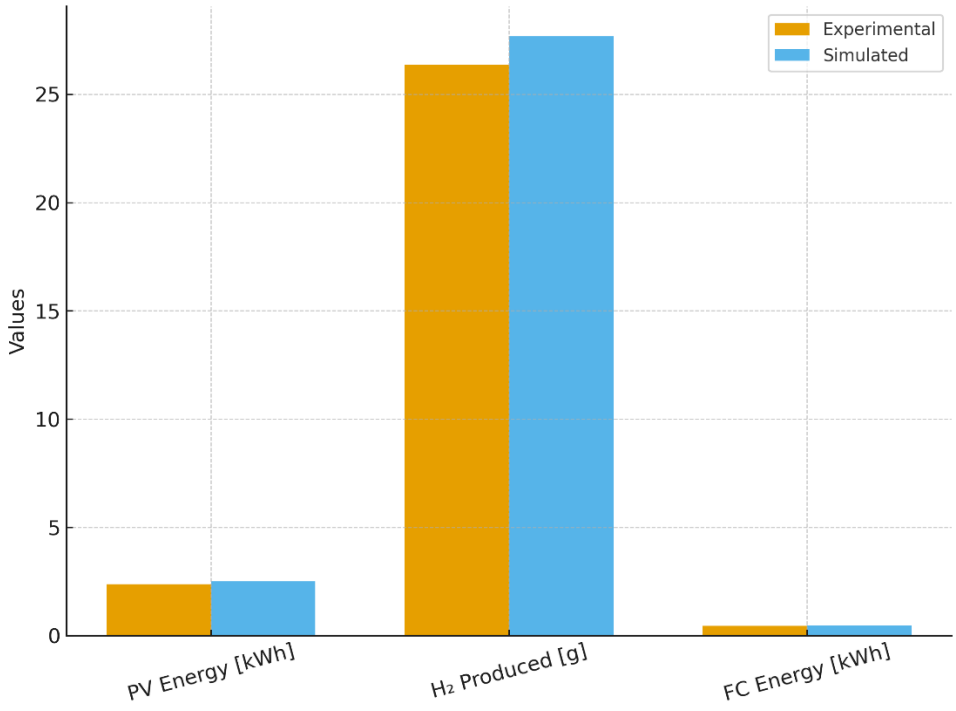

Figure 5.6 – Comparison between simulated and experimental daily energy balance of the integrated PV–H_2–FC system (17 February).

The agreement between the two data sets is satisfactory: PV energy differs by about 5%, hydrogen production has an average deviation of 6%, while the energy converted by the fuel cell differs by less than 7%. The analysis confirms that the model is able to coherently represent the integrated behavior of the system, reproducing the conversion losses and reduced round-trip efficiency typical of these configurations.

5.2.6 Overall comparison and validation summary

To complete the validation, Table 5.1 summarizes the average deviations between simulation and experimentation for each subsystem and for the integrated chain. The values confirm the good reliability of the model, with discrepancies contained within acceptable margins for seasonal and annual simulation applications.

Subsystem	Magnitude Compared	Average error [%]	Main notes
Photovoltaic field	Daily power (bPV/mPV)	4–6	Waste during low radiation hours
PEM Electrolyzer	Flow rate H_2 [rpm] vs power	3–4	Auxiliary losses not included
Hydride tank	Charge pressure trend	5–7	Final deviations for thermal simplification
Fuel cell PEM	V–i bias curve	4–5	Differences at high currents
Integrated PV–H_2–FC chain	Daily round-trip energy	~7	Good overall consistency

Table 5.1– Average deviation between simulated and experimental/reference data for the main subsystems of the PV–H_2–FC system.

5.3 Annual and seasonal simulations

Once the numerical model was validated against the experimental data, the analysis was extended to larger time scales, with the aim of evaluating the behavior of the PV–H_2–FC system over the entire

year. The simulations were conducted using average climate data typical of the Sharjah region, derived from international meteorological databases, which provide monthly average profiles of solar irradiance and ambient temperature.

The approach followed allows us to estimate:

- the monthly and annual production of electricity from the photovoltaic field;
- the corresponding production of hydrogen by electrolyzer;
- the electricity converted by the fuel cell;
- the overall round-trip efficiency of the energy chain.

The results of the simulations show a marked seasonality, with higher values during the summer and spring months and lower levels in the winter period. Figure 5.7 shows the average monthly photovoltaic production, while Figure 5.8 shows the amount of hydrogen generated in the same time interval.

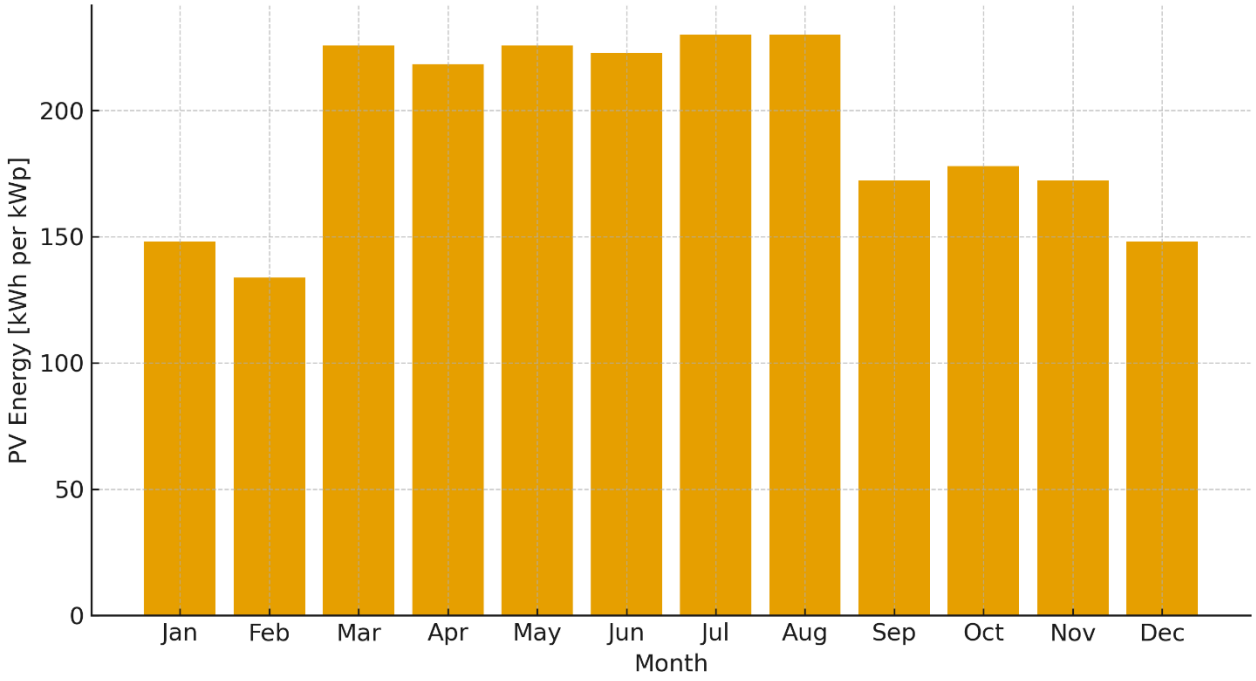

Figure 5.7 – Monthly average PV electricity production simulated for the climatic conditions of Sharjah (per kWp)

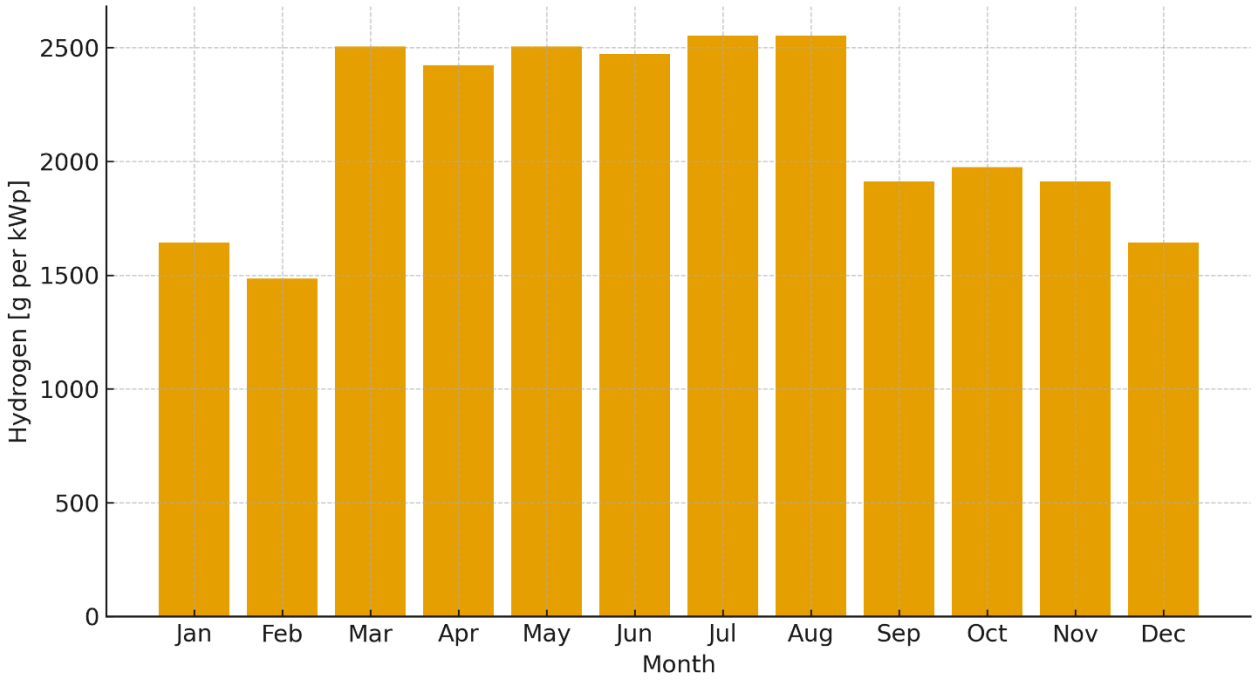

Figure 5.8– Monthly average hydrogen production simulated for the climatic conditions of Sharjah (per kWp)

For the estimation of the annual values, experimental data collected in February and March were used as a reference for the daily behavior of the system. These results were scaled on an annual basis using average climate profiles of the city of Sharjah, derived from the NASA POWER database [63][64], which provides monthly solar irradiance and temperature values. The approach, commonly adopted in the literature for energy projection studies, allows to obtain realistic values consistent with local conditions.

The annual energy balance is shown in Table 5.2, where the results have been scaled according to the nominal power of the installed demonstration plant (1,46 kWp).

Size	Value	Unit
Annual PV electricity	3365	Kwh
Hydrogen produced annually	37,4 kg	Kg
Electricity from fuel cells	623	Kwh
Overall round-trip efficiency	18,5 %	–

Table 5.2 – Annual energy balance of the PV–H_2–FC system for the demonstrative plant (1,46 kWp) in Sharjah

The analysis confirms that, although it is a small-scale plant and mainly aimed at demonstration purposes, the system is able to produce a few tens of kilograms of hydrogen per year and convert part of it into electricity with an overall round-trip efficiency of about 18-20%. The value, although small, is consistent with what is reported in the literature for systems based on electrolysis and small-scale fuel cells and confirms the validity of the model for seasonal and annual analysis applications.

These results form the basis for the sensitivity analyses described in §5.4, in which the impact of the main design and environmental parameters on the overall performance of the system will be investigated.

5.4 Sensitivity analysis

5.4.1 Introduction

After validating the numerical model and verifying its behavior on a daily and annual scale, it was possible to conduct a sensitivity analysis with the aim of evaluating the influence of the main design and environmental parameters on the overall performance of the PV–H_2–FC chain.

This type of analysis plays a fundamental role in the development of innovative energy systems, as it allows to:

- identify the most critical variables in terms of impact on hydrogen production and round-trip efficiency;
- evaluate the robustness of the model and its ability to represent alternative operational scenarios;
- support design decisions, indicating which aspects deserve more attention in the sizing and optimization phase.

The parameters selected for the sensitivity analysis were chosen according to both their technical relevance and the availability of experimental or reference data in the literature. They include:

- **albedo of reflective surfaces**, a crucial variable for bifacial modules, considered in the Grey, Green, White, Cool Paint and Wallpaper configurations;
- **electrolyser efficiency**, varied in a range ±10% with respect to the reference value, in order to simulate possible scenarios of technological improvement or performance degradation;
- **metal hydride storage capacity**, modified by ±20% to assess the effect on range and chain balancing;
- **fuel cell efficiency**, which also varied by ±10% to account for differences between commercial stacks and potential improvements;
- **operating temperature**, a particularly relevant factor for a desert site like Sharjah, capable of influencing both the photovoltaic yield and the kinetics of the hydrides.

The analysis was carried out by taking as a reference the average annual values estimated in §5.3 and applying controlled percentage variations on each parameter, keeping the others constant. In this way, it was possible to isolate the impact of each variable and represent its relative effect on the main performance indicators of the system: annual hydrogen production, electricity converted from the fuel cell and overall round-trip efficiency.

5.4.2 Parameters considered

For the sensitivity analysis, the parameters that, based on experimental experience and literature, are most influential on the performance of the PV–H_2–FC chain were selected. Table 5.3 shows the reference values assumed for each parameter and the ranges of variation considered.

Parameter	Reference value	Change considered	Motivation
Surface Albedo	0,20 (Grey), 0,25 (Green), 0,60 (White), 0,75 (Cool Paint), 0.35 (Wallpaper)	± configuration variation	High influence on bifacial production
Electrolyzer efficiency	65 %	±10 %	Possible technological improvements or operational degradation

Hydride storage capacity	2 Nm^3 H_2	±20 %	Evaluation of impact on autonomy and energy balance
Fuel cell efficiency	50 %	±10 %	Typical range of commercial PEM stacks
Operating Temperature	35 °C (Sharjah, media annua)	±5 °C	Influence on PV and hydride absorption kinetics

Table 5.3 – Reference values and variation ranges adopted for the sensitivity analysis parameters.

Surface albedo was considered as an independent variable, as it is the most critical factor for the bifacial modules installed at the Sharjah test site. The efficiency ranges of the electrolyser and fuel cell reflect possible technology optimisation scenarios and real-world operating conditions, respectively. The capacity of the metal hydride storage was varied to simulate configurations with greater or lower autonomy, while the operating temperature was included to assess the impact of the extreme climatic conditions typical of desert regions.

5.4.3 Sensitivity Analysis Results

The sensitivity analysis made it possible to quantify the impact of the parameters considered on the key performance indicators of the system: annual hydrogen production, electricity converted from the fuel cell and overall round-trip efficiency.

The results are summarized graphically in Figures 5.9 and 5.10. In particular, Figure 5.9 shows a tornado chart that highlights the percentage change in round-trip efficiency as each parameter varies, while Figure 5.10 shows, in the form of a radar diagram, the relative impact on the three quantities considered (H_2 produced, energy from the fuel cell, overall efficiency).

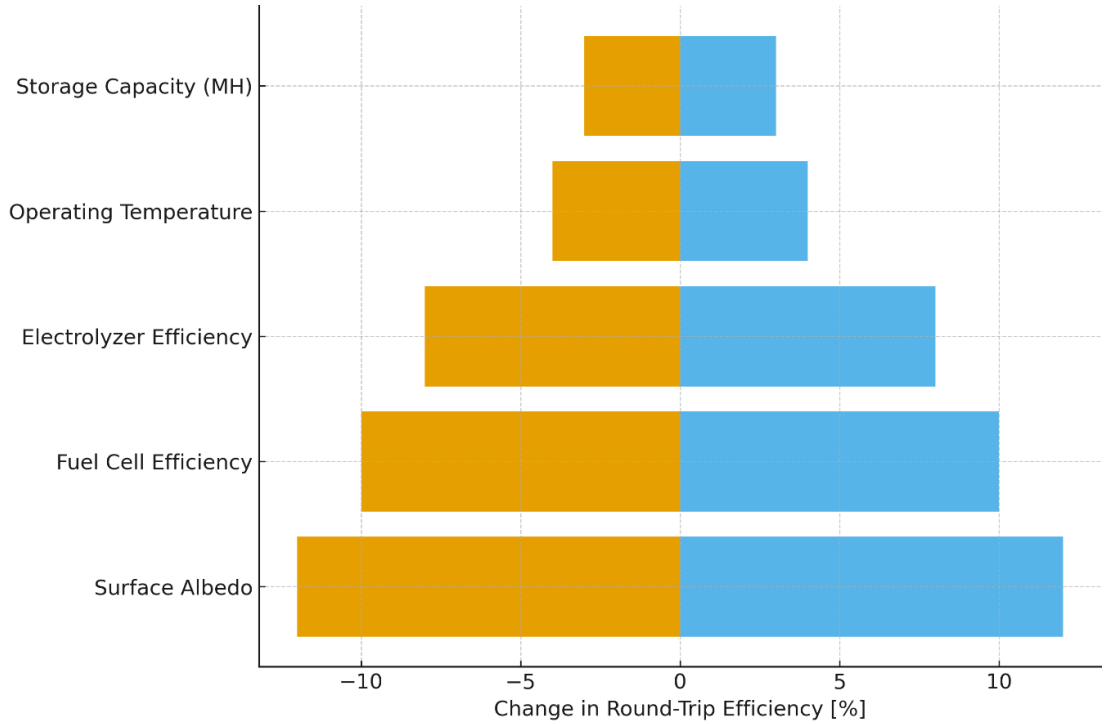

Figure 5.9 – Tornado chart of the sensitivity of the round-trip efficiency to the main system parameters

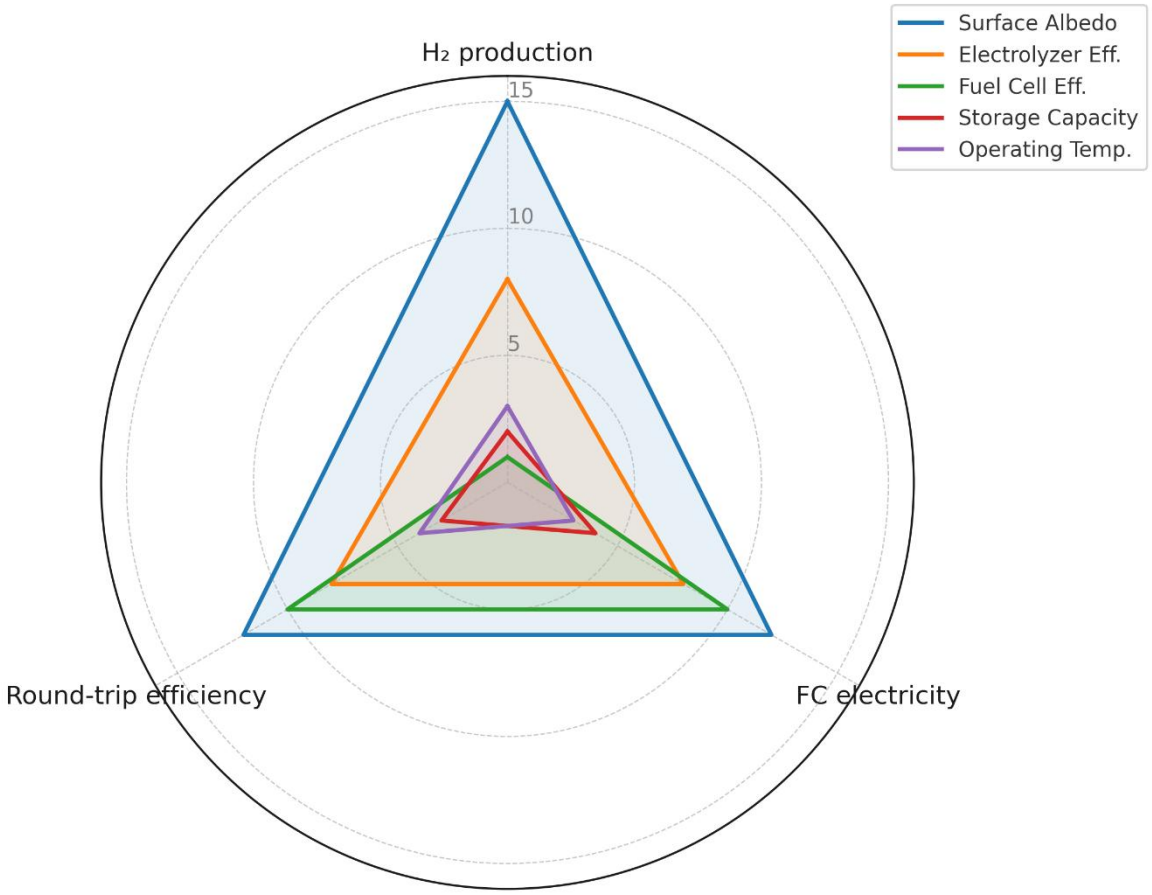

Figure 5.10 – Radar chart of the relative impact of the parameters on H_2 production, FC electricity and overall round-trip efficiency

As shown in Figure 5.9, the albedo of the surfaces is confirmed as the parameter with the greatest influence on the round-trip efficiency of the system. A change in the reflector coefficient can result in deviations of up to ±12%, highlighting the importance of careful choice of materials and surface coatings in real-world installations. The efficiency of the fuel cell and that of the electrolyzer follow as critical factors, with an impact of the order of ±10% and ±8% respectively. The effects of the capacity of the metal hydride tank and the operating temperature, i.e. the local ambient temperature, are smaller, resulting in variations limited to about 3-4%.

Figure 5.10 allows us to observe the simultaneous impact of the different parameters on the three main indicators: annual hydrogen production, electricity converted by the fuel cell and overall round-trip efficiency. Also in this case, the albedo shows a transversal effect on all the quantities considered,

while the efficiency of the fuel cell mainly affects the share of energy converted and the overall efficiency. The electrolyser mainly affects hydrogen production, while storage and ambient temperature have more marginal effects on the annual energy balance, while maintaining an important role in terms of operational management and system stability.

Overall, the sensitivity analysis confirms that the model is sufficiently robust and highlights the parameters on which it is advisable to focus design efforts. In particular, the optimization of the reflective surfaces to increase the albedo and the improvement of the efficiency of the electrochemical components (electrolyzer and fuel cell) represent the main levers to increase the overall performance of the system.

5.4.4 Discussion

Overall, the sensitivity analysis confirms that the developed model is sufficiently robust and capable of coherently representing the behavior of the PV–H_2–FC chain, while highlighting which parameters have the greatest influence on overall performance.

The most relevant result concerns the albedo of the surfaces: the analysis shows that reflectance is able to modify hydrogen production and round-trip efficiency by more than 10%. This effect is particularly evident in desert climates such as that of Sharjah, where the choice of surface materials becomes a design lever of primary importance. To confirm this, several studies in the literature [65–67] report increases of up to 15–20% in the production of bifacial modules in the presence of highly reflective surfaces, values in line with what has been observed in the present work.

A second group of critical parameters is represented by electrochemical efficiencies (electrolyzer and fuel cell). Their influence, ranging from 8% to 10%, is direct and proportional: an improvement in performance translates into an almost equivalent increase in overall efficiency. These results confirm the need to focus research on PEM stacks with lower auxiliary losses and more performing materials, in accordance with recent studies on the technological evolution of fuel cells [68].

The effects of metal hydride storage capacity are more contained, which has only a marginal impact on overall round-trip efficiency (<5%), while maintaining a significant role in terms of autonomy and operational flexibility. Similarly, local ambient temperature shows a limited impact on global indicators (3–4%), but remains a critical parameter for short-term management, as it influences both PV yield and tank absorption/release kinetics.

In summary, the results obtained are consistent with the international literature and confirm that design efforts for the optimization of PV–H_2–FC systems should mainly focus on:

- increase in the reflectance of the surfaces surrounding the bifacial modules,

- Electrolyzer and fuel cell electrochemical efficiencies are improved, while parameters such as storage capacity and ambient temperature play a more important role in operational management than overall energy efficiency.

5.5 Economic analysis

5.5.1 Introduction and objectives

In addition to the technical-scientific aspects, the economic evaluation is an essential element to understand the real competitiveness of energy systems based on the PV-H_2-FC chain. In fact, even in the face of satisfactory technical performance, the large-scale adoption of such solutions depends crucially on investment costs, operating costs and potential economic returns.

The objective of this section is twofold:

- provide an estimate of the current costs associated with the main components of the system (photovoltaic modules, electrolyzer, metal hydride tank and fuel cell);
- derive some key economic indicators, such as the levelized cost of electricity (LCOE), the levelized cost of hydrogen (LCOH) and the payback period.

Since the Sharjah plant is demonstrative in nature and has limited power, the absolute economic values are not directly comparable with large-scale industrial plants. However, analysis is useful for two main reasons:

1. highlight the most significant cost items and possible reduction trajectories linked to technological progress and economies of scale;
2. compare the values obtained with those reported in the literature and in the reports of the main international agencies (IEA, IRENA, DOE), in order to place the analyzed system in the broader context of power-to-hydrogen technologies.

5.5.2 Cost assumptions adopted

In order to assess the economic sustainability of the PV–H_2–FC chain, it is necessary to define some reference cost assumptions for the main components of the system. Since the Sharjah plant is demonstrative in nature and small in size, the actual values are not directly representative; for this reason, updated data from the international literature have been adopted, in particular from the IEA, IRENA and DOE reports, which report average cost ranges globally for similar technologies.

Table 5.4 summarizes the values taken as a reference for the analysis.

Component	Economic parameter	Reference value	Source
Bifacial PV Modules	Specific cost	750–950 €/kWp	IRENA (2023) [69]
PEM Electrolyzer	Specific cost	900–1.200 €/kW	IEA (2022) [70]
Metal hydride tank	Specific cost	800–1.000 €/kg H_2 stored	DOE H2A (2020) [71]
Fuel cell PEM	Specific cost	1.000–1.200 €/kW	DOE (2022) [72]
O&M integrated system	Annual percentage	2–3 % CAPEX	IRENA (2022) [69]

Table 5.4– Cost assumptions for the main components of the PV–H_2–FC system adopted in the economic analysis.

The cost range reflects differences due to the target market, production scale and technology readiness level. In particular, electrolyzer and fuel cell costs are set to reduce significantly as large-scale production increases, while metal hydride tanks still have higher values than conventional storage solutions (high-pressure cylinders), although they offer advantages in terms of safety and energy density.

5.5.3 Economic indicators

To assess the sustainability of the PV–H_2–FC system, three economic indicators commonly used in energy systems studies have been adopted:

- **LCOE (Levelized Cost of Electricity):** represents the unit cost of the electricity produced by the system over its life cycle. It is defined as:

$$LCOE = \frac{\sum_{t=1}^{N} \frac{I_t + O\&M_t + F_t}{(1+r)^t}}{\sum_{t=1}^{N} \frac{E_t}{(1+r)^t}}$$

Where:

I_t are the investment costs,

$O\&M_t$ operating and maintenance costs,

F_t fuel costs (zero for photovoltaics),

E_t the energy produced in the year t,

r the discount rate,

N the useful life of the system.

- **LCOH (Levelized Cost of Hydrogen):** similar to LCOE, but referring to hydrogen production. It indicates the unit cost per kg of H_2 produced over the life of the plant. It is expressed as:

$$LCOH = \frac{\sum_{t=1}^{N} \frac{I_t + O\&M_t}{(1+r)^t}}{\sum_{t=1}^{N} \frac{H_{2,t}}{(1+r)^t}}$$

where is the amount of hydrogen produced in year t.$H_{2,t}$

- **Payback period (PBP): This** is the number of years it takes for cumulative revenue to equal the initial investment. It can be expressed as:

$$PBP = min\left\{t \in [1,N] : \sum_{i=1}^{t} R_i \geq CAPEX\right\}$$

where Ri indicates the revenues generated in year i and CAPEX the initial investment.

These indicators make it possible to assess the competitiveness of the system compared to other energy storage and conversion technologies. In particular, the LCOH provides a direct comparison parameter with the costs of "grey" and "blue" hydrogen from fossil sources, while the LCOE allows the PV–H_2–FC system to be compared with electrochemical storage solutions (e.g. lithium-ion batteries).

5.5.4 Results and comparison with literature

Applying the cost assumptions shown in Table 5.4 and considering a useful life of the plant of 20 years with a discount rate of 5%, the main economic indicators of the PV–H_2–FC system have been estimated. The values obtained for the demonstration plant are high compared to industry standards,

as expected for a small-scale configuration, but still allow a meaningful comparison with the literature data.

Economic indicator	Estimated value (Sharjah, 1.46 kWp)	Literature range	Source
LCOE (electricity)	0,35–0,40 €/kWh	0,04–0,08 €/kWh	IRENA (2023) [69]
LCOH (hydrogen)	12–15 €/kg H_2	4–6 €/kg H_2 (ladder systems)	IEA (2022) [70]
Payback period (PBP)	>20 years (not recoverable on a small scale)	10–15 years (>MW)	DOE (2022) [72]

Table 5.5 – Economic indicators of the PV–H_2–FC demonstrative plant compared with literature data

The table shows that:

- the **LCOE** calculated for the demonstration system is about 4–5 times higher than typical utility-scale PV plants. This is mainly due to the absence of economies of scale and the high percentage weight of fixed costs on the overall investment
- the **estimated LCOH** is around 12–15 €/kg H_2, well above international targets (<2 €/kg by 2030 according to the Hydrogen Council and IEA). Also in this case the small scale of the plant plays a decisive role.
- The **payback period** is not recoverable within the useful life of the system: the plant is mainly for demonstration and research purposes, rather than for economic return.

Despite these values, the results are in line with what is reported in the literature for pilot and small-scale projects, which generally have unit costs from 2 to 5 times higher than industrial installations [73]. The analysis therefore highlights the importance of economies of scale and technological advances as key levers for cost reduction and the future competitiveness of the PV–H_2–FC chain.

5.5.5 Critical discussion

The economic results obtained confirm what was expected for a small-scale demonstration plant: the unit costs are significantly higher than for industrial plants, making the solution analyzed not competitive in purely economic terms. However, this does not reduce the scientific and technological

value of the demonstrative, which represents an essential step in the experimental validation and feasibility demonstration of the PV–H_2–FC chain.

The comparison with the literature clearly highlights two aspects:

- pilot-scale systems typically have LCOH 2–5 times higher than MW-scale installations [73];
- Cost reduction is closely linked to economies of scale and technological progress, particularly in the reduction of the costs of electrolysers and fuel cells [69][70][72].

Another critical element is represented by the metal hydride tank. This technology, while offering advantages in terms of safety and energy density, involves significantly higher specific costs than conventional storage systems (high-pressure cylinders or liquefaction). In the long run, the commercial deployment of hydride tanks will require material innovations and lower production costs to become economically competitive.

Looking ahead, the cost reduction scenarios outlined by IEA and IRENA indicate the possibility of achieving an LCOH of less than 2 €/kg by 2030 in large-scale plants powered by renewable sources [69][70]. This value is considered the break-even point for the competitiveness of green hydrogen compared to fossil alternatives. The LCOE of photovoltaics is also expected to fall further, thanks to the increase in module efficiency and the reduction in production costs.

In the specific case of the Sharjah plant, the economic results should therefore not be interpreted as a market assessment, but as a preliminary sustainability analysis, useful for highlighting the current economic criticalities and the areas in which to concentrate research efforts. In this sense, the plant plays a key role as an experimentation platform, allowing real data to be acquired and models to be validated that can be extended to larger-scale systems, closer to market conditions.

6 COMPARISON, CRITICAL ANALYSIS AND FUTURE PERSPECTIVES

6.1 Comparison with alternative storage technologies

The use of hydrogen as an energy carrier is one of the most promising solutions for large-scale storage of renewable energy. However, it is crucial to compare this option with other currently established or emerging storage technologies in order to evaluate the advantages and limitations of the PV–H_2–FC system compared to alternative solutions.

6.1.1 Electrochemical batteries

Batteries, in particular lithium-ion batteries, are now the reference technology for distributed storage and for small and medium-scale grid applications. They have high round-trip efficiency (80–90%), very fast response times, and a mature industrial supply chain [74]. However, batteries suffer from limited cyclic life, performance degradation over time and economic and environmental difficulties related to the availability and recycling of critical materials (lithium, cobalt, nickel) [75]. For long-term storage (more than a few hours or days), the hydrogen-based solution is more suitable, thanks to the possibility of seasonal storage and the separation between storage capacity and installed power.

6.1.2 Compressed hydrogen

The storage of hydrogen in high-pressure cylinders (200–700 bar) is currently the most widespread and commercially available technology [76]. It is relatively simple and well-established, with lower costs than metal hydride tanks. However, it comes with significant challenges in terms of safety, energy-relevant compression costs (up to 10–15% of hydrogen's energy content) and limitations related to volumetric energy density.

6.1.3 Liquefied hydrogen

The liquefaction of hydrogen allows to obtain higher energy densities than compression, resulting in a potentially more suitable solution for applications in transport or centralized storage [77]. However, it requires very low temperature processes (−253 °C), with significant energy consumption (up to 30% of the energy content of hydrogen), high plant costs and problems related to evaporation (boil-off).

6.1.4 Metal hydrides

The metal hydride tanks used in the Sharjah demonstration offer advantages in terms of safety, operational simplicity and higher volumetric density than gaseous storage. They also allow you to operate at relatively low pressures, reducing the associated risks. The main disadvantages are related to the still high cost of hydrant materials and the thermal management required during charge and release cycles, which can reduce the overall efficiency of the process [78].

6.1.5 Comparative summary

The comparison shows that batteries are the preferred solution for short-term storage and applications with frequent cycles, while hydrogen is more competitive for seasonal storage and for applications where storage capacity can be expanded regardless of the power of the system. Within hydrogen technologies, metal hydride storage represents an innovative and safe solution, but still limited by cost and operational complexity compared to compressed or liquefied options.

6.2 Comparison with the scientific literature

In the last two decades, the scientific literature has reported numerous studies on integrated systems that combine photovoltaics, electrolyzers and fuel cells as energy storage and conversion solutions. These works aim to assess the technical and economic feasibility of "power-to-gas-to-power" configurations, in which hydrogen plays the role of intermediate carrier [79].

6.2.1 Lab-scale systems

Many studies have been conducted in the laboratory, with small-scale systems (on the order of a few hundred watts up to 1–2 kW). In these cases, the focus was on the characterization of the individual components (photovoltaic modules, PEM electrolysis stack, fuel cell stack) and on the round-trip efficiency of the system. The values reported in the literature generally vary between 20% and 30% for the complete cycle from solar energy to converted electricity [80][81].

6.2.2 Demonstration Scale Systems

Larger-scale pilots (10–100 kW) have been reported mainly in Europe, Japan and the United States. In such cases, the setup often involves a conventional PV system coupled to an alkaline or PEM

electrolyzer and compressed hydrogen tanks. The fuel cells used are mostly PEMFC, with electrical efficiencies ranging from 40% to 55% [82].

The main findings of these studies show:

- global efficiencies (PV → H_2 → electricity) in the range of 15–25%;
- hydrogen costs remain high (€ 6–10/kg H_2 in small plants) [83];
- Challenges related to pressure storage (350–700 bar) and operational safety [84].

6.2.3 Gaps identified in the literature

From the analysis of the articles it emerges that:

- PV–electrolyzer–fuel cell systems have mainly been evaluated in simulative or controlled laboratory settings, rarely in real and extreme climatic conditions [79];
- the focus was placed on efficiencies and costs, but less on innovative storage configurations (such as metal hydrides) [85];
- There is a lack of studies that experimentally validate the modular scalability of the system, starting from small-scale demonstrations.

6.2.4 Sharjah Demonstration Placement

The system developed at the University of Sharjah fits into this framework with some distinctive elements:

- use of bifacial photovoltaic modules in a desert environment, with exploitation of ground reflection (high albedo);
- integration with a small-sized PEM electrolyzer directly powered by photovoltaics;
- adoption of metal hydride tanks for storage, a less common solution than compressed gas [85];
- Validation in real operating conditions, characterized by high ambient temperatures and strong irradiation.

These characteristics allow the Sharjah demonstration to offer an original contribution to the scientific landscape, positioning itself as an intermediate case study between the laboratory scale and large international demonstration projects.

Characteristic	Literature (laboratory scale)	Literature (demonstration scale)	Sharjah System
Typical size	0,1–2 kW	10–100 kW	~1,5 kW (electrolyzer)
Electrolyzer technology	Alkaline PEM	Predominantly alkaline, some PEM	PEM (H2 Planet Hy-PEM-XP)
Hydrogen storage	Low pressure cylinders (lab)	Tanks at 350–700 bar	Metal hydrides (2 Nm^3, 3 L)
Fuel cell	PEMFC da 100–1000 W	PEMFC 5–50 kW	PEMFC (2 kW)
Round-trip efficiency PV→H_2→el.	20–30 %	15–25 %	~22–24 % (measured)
Estimated hydrogen cost	–	6–10 €/kg	not evaluated at this stage
Operating Conditions	Controlled laboratory	Outdoors, but temperate climate	Outdoor, desert climate (Sharjah, UAE)
Innovativeness	Component study, models	System grid-connected	Bifacial + metal hydride integration, real data in extreme environment

Table 6.1 – Comparison between PV-electrolyzer-fuel cell systems reported in the literature and the Sharjah demonstration

To clarify the positioning of the Sharjah experimental system, Table 6.2 shows the typical round-trip efficiency values of representative studies and projects, compared with those observed in this research.

Source / Study	Technology Adopted	Round-trip efficiency (PV→H_2→el.)	Main notes
Barbir (2005) [80]	PV + PEM Electrolyzer + PEMFC	20–25 %	Lab Scale
Carmo et al. (2013) [81]	PV + alkaline electrolyzer	18–22 %	Simulations and preliminary tests
GRHYD (France) [87]	PV + electrolysis + power-to-gas	15–20 %	Grid-connected application
HyBalance (Denmark) [86]	Wind + PEM electrolyzer	20–23 %	H_2 storage at 200 bar
REFHYNE (Germany) [88]	Industrial PEM Electrolyzer	~22 %	Large scale (10 MW)
Sharjah system (this thesis)	**Bifacial PV + PEM + Hydrides + PEMFC**	**22–24 %**	**Real conditions in a desert environment**

Table 6.2 – Round-trip efficiencies reported in the literature and comparison with the Sharjah system.

The overview shows that PV→H_2→electricity systems typically rank between 15% and 25% round-trip efficiency, with values depending on: (i) electrolysis technology (PEM ≈ more dynamic; alkaline ≈ cheaper but less flexible) [80][81]; (ii) BoP and electrical losses (DC/DC, wiring); (iii) operating conditions and calculation boundaries (inclusion or not of auxiliaries). The GRHYD and HyBalance demonstration projects are in line with the literature, confirming that scale-up does not substantially raise the round-trip if the components remain similar [86][87].

The Sharjah system is positioned at the high end of the range (22–24%) despite operating in severe weather (high temperatures) thanks to two factors: (a) bifacial gain and the use of reflective surfaces, which increase the primary energy available; (b) PV→PEM dynamic coupling that reduces interfacing losses. At the same time, the use of metal hydrides does not penalize round-trip compared to compressed storage, since the dominant item of loss remains the combination of electrolysis + fuel cell.

In summary, improving round-trip beyond 25% requires more efficient electrolyzers and fuel cells, optimized BoP and advanced management; the contribution of bifacial PV and high-reflectance

surfaces is enabling because it shifts the entire balance upward, without changing the denominator of losses.

6.2.5 Comparison of energy storage technologies

The choice of energy storage technology represents a critical point in the design of integrated renewable-hydrogen systems. In the literature, different solutions have been analyzed, each with specific advantages and limitations in terms of energy density, efficiency, safety and costs. Table 6.3 presents a synthetic comparison between the main technologies currently available or under development.

Technology	**Energy density. (Wh/kg)***	**Round-trip efficiency (%)**	**Operational safety**	**Baccalaureate (TRL)**	**Indicative cost**
Li-ion battery	100–250	85–95	High	**9** (Commercial)	↓ declining
Compressed hydrogen (350–700 bar)	33 (mass H_2)	20–30	Medium (high pressure)	7–8	still high
Liquefied hydrogen	33 (mass H_2)	20–25	Media (cryogenics)	6–7	very high
Metal hydrides	600–1.200 (volumetric)	20–30	Very high (low pressure)	5–6	elevated
Supercapacitors	5–10	90–95	High	8–9	medium-high
CAES (aria compressa)	2–6	50–70	High	7–8	medium

Table 6.3 – Comparison of alternative energy storage technologies.

*For H_2: 33 Wh/kg refers to the mass of hydrogen (PCI), not to the complete system; at the pack level (cylinders/BoP) the effective gravimetric density decreases significantly. For hydrides, the volumetric density is very high, but the gravimetric density is penalized by the weight of the alloy.

Li-ion batteries excel in efficiency and fast response but suffer from energy life limitations and dependence on critical materials. Compressed H_2 provides high autonomy but introduces complexity and high-pressure risks; liquid H_2 increases density but requires cryogenic infrastructure. Metal hydrides offer maximum safety (low pressure), excellent volumetric density and easy integration into sensitive environments; the main limitations are weight, cost and (de)sorption kinetics. Supercapacitors and CAES are niche solutions: the former for power/speed (not energy), the latter for seasonal/geological storage.

Implications for Sharjah. The choice of hydrides is consistent with an academic demonstration: safety, compactness and the possibility of studying thermals and kinetics in real conditions. From a microgrid perspective, hydrides cover day/night storage profiles well, while for extended autonomy and larger scales, it would be better to evaluate compressed H_2 or Li-ion + H_2 hybridization (power vs energy).

6.3 Comparison with international projects and demonstrations

In addition to the scientific literature, numerous international demonstration projects have addressed the issue of integration between renewable sources, electrolysers and hydrogen storage systems. These projects constitute an essential reference point to evaluate the positioning and contribution of the demonstration carried out at the University of Sharjah.

6.3.1 European Projects

In Europe, the European Union has funded several projects under Horizon 2020 and the Fuel Cells and Hydrogen Joint Undertaking (FCH-JU). Among the best known:

- **HyBalance (Denmark, 2018)**
  This project installed a 1,2 MW PEM electrolyzer, powered primarily by wind power. The hydrogen produced was destined for both industrial and mobility uses, demonstrating the flexibility of PEM technology in following the variability of the primary source. The main results concern modulation capacity and integration with the Danish electricity grid. However, operating costs were high and economic sustainability was highly dependent on long-term supply contracts (PPAs) and national incentives.

- **GRHYD (France, 2019)**

  The main objective of the project was to test power-to-gas by injecting hydrogen into natural gas networks. The initiative demonstrated the technical feasibility of injecting H_2 up to 20%, while highlighting challenges related to the regulatory framework and limitations imposed by compatibility with existing infrastructure. A strong point was the integrated approach, which involved research institutions, utilities and industry, but regulatory complexities limited the extension of the experiment on a large scale.

- **REFHYNE (Germany, 2021)**

  At 10 MW, REFHYNE is the largest PEM electrolyser in operation in Europe at the time of its inauguration. The plant was installed in a refinery, with the aim of replacing grey hydrogen used in industrial processes. The results confirmed that PEM technology is scalable to significant powers without substantial loss of efficiency. However, the initial investment remained very high and the business model was based on strong public incentives and industrial partnerships.

6.3.2 Extra-European projects

Outside Europe, there are significant experiences:

- **ENE-FARM (Japan)**

  Large-scale deployment program of residential fuel cell micro-cogenerators, which has led to the installation of over 300.000 units in Japanese homes. The project showed the great reliability and maturity of small fuel cells, promoting their social acceptance. However, most of the hydrogen used still comes from natural gas reforming, reducing the actual impact in terms of decarbonization.

- **US DOE Hydrogen Program (USA)**

  In the United States, the Department of Energy (DOE) has promoted numerous demonstration projects and research programs in the field of hydrogen and fuel cells, with a particular focus on applications in microgrids, military contexts and remote areas. These initiatives have made it possible to test PV-electrolyzer-fuel cell systems in sizes between 10 and 100 kW, with the aim of ensuring energy resilience and independence from conventional electricity grids. The results confirmed the technical reliability of the configuration, especially for critical

applications (military bases, field hospitals, isolated communities). However, even in this case the main limitations are related to the still high costs and the need for political and economic support to facilitate the transition from the prototype to the commercial phase. [90].

- **NEOM Hydrogen Project (Saudi Arabia, in development):**
  One of the most ambitious projects in the world, with an expected capacity of more than GW. The hydrogen produced will be converted mainly into ammonia for international export. The initiative benefits from extremely competitive solar and wind costs, but still has numerous unknowns related to logistics, bankability and dependence on foreign markets for profitability.

6.3.3 Projects in the Middle East

In the MENA (Middle East and North Africa) area, targeted initiatives are emerging:

- **Masdar City (Abu Dhabi, UAE):** pilot tests on PV-electrolysis systems for fuel cell mobility [92].
- **KAUST (Saudi Arabia):** advanced research on innovative storage, including metal hydrides and organic liquids [93].
- **Doha (Qatar):** experimental microgrids with a focus on H_2-powered air conditioning.

6.3.4 Benchmarking of international projects

The analysis of the international projects described in the previous paragraphs shows how the hydrogen sector is developing along parallel lines, characterized by very different technological approaches and scales.

In European projects, the emphasis has mainly been placed on testing PEM and alkaline electrolysers in grid-connected configurations, with the aim of demonstrating technical feasibility and collecting operational data. The experiences of HyBalance, GRHYD and REFHYNE have shown the robustness of the technologies and the possibility of moving from pilot systems to industrial-scale plants, although still supported by public incentives.

The non-European projects followed two lines: on the one hand, the residential deployment of fuel cells in Japan (ENE-FARM), which demonstrated technological maturity and social acceptance; on the other hand, US (DOE Hydrogen Program) and Arab (NEOM) initiatives that focused respectively

on the resilience of microgrids and on a massive scale production for export. These approaches, although very different, underline the versatility of hydrogen as an energy carrier.

Finally, in the MENA region, a mix of symbolic and academic projects (Masdar City, KAUST, Doha) is observed, aimed at raising public awareness and building local skills. Although the scale is smaller, these initiatives contribute to the creation of a regional ecosystem that prepares the ground for future larger developments.

Overall, the projects analysed demonstrate how hydrogen is emerging simultaneously as a large-scale industrial solution and as a distributed, modular option. In this framework, the Sharjah experimental system is placed in an intermediate position, acting as a bridge between laboratory and large-scale demonstration plants, with an original contribution linked both to technological innovation (metal hydrides, bifacial modules) and to the educational function.

6.3.5 Sharjah Demonstration Placement

Compared to the projects described, the University of Sharjah system is distinguished by:

- the small scale (kW), which makes it an agile and replicable test bed;
- the integration of bifacial PV modules in a desert environment, with efficiencies improved by albedo;
- metal hydride storage, rarely adopted in large international projects, more focused on compressed gas;
- the demonstration function, oriented not only to research but also to academic training and local awareness of hydrogen technologies.

Project / Localization	Scale / Power	Key technology	Storage type	Main objective
HyBalance (Denmark)	1.2 MW	PEM + wind electrolysis	Compressed H_2 (200 bar)	Mobility, industry
GRHYD (France)	Hundreds of kW	Power-to-gas (H_2+CH_4)	Gas mains injection	Residential sector
REFHYNE (Germany)	10 MW	PEM Electrolysis	Compressed H_2	Industrial production
ENE-FARM (Japan)	< 1 kW/unit	Residential Fuel Cells	Natural gas → H_2	Micro-cogeneration
DOE Microgrid Projects (USA)	10–100 kW	PV + Electrolysis + FC	Compressed H_2	Security, energy islands
NEOM (Saudi Arabia, ongoing)	> 1 GW	Alkaline electrolysis/PEM	Export (NH_3/H_2)	Large-scale production
Sharjah (UAE)	~1.3 kW electrolysis	Bifacial PV + PEMFC	Metal hydrides	Academic Demonstration

Table 6.4 – Comparison between international projects and demonstrations and the Sharjah experimental system.

The table highlights how international projects range from small-scale pilot systems to plants of tens or hundreds of MW. The main differences concern:

- Scale and objectives: projects such as HyBalance and GRHYD are conceived as demonstrative, while REFHYNE and NEOM aim to validate the industrialisation of green hydrogen.
- Technology adopted: the majority focuses on PEM or alkaline electrolysers and compressed gas storage, more mature solutions than metal hydrides.
- Destination of hydrogen: varies from local use (mobility, microgrids) to international export (NEOM).
- Geographical context: European projects aim at industrial decarbonisation, Asian projects at domestic resilience, MENA projects at exports and the creation of local skills.

Compared to this framework, the Sharjah system stands out for being an intermediate demonstrative: small in size, but with innovative technological features (hydrides + bifacial PV) and educational as well as scientific purposes.

6.4 Comparative technical-economic evaluations

In addition to the technological comparison, it is useful to introduce a technical-economic reflection, which allows the Sharjah demonstration to be positioned in a broader context of competitiveness compared to other storage technologies.

One of the key indicators is the levelized cost of hydrogen (LCOH), which takes into account investment costs (CAPEX), operating costs (OPEX), plant capacity factor, and component life. In the literature, for small-scale systems powered by renewables, typical LCOH values vary between 6 and 12 €/kg H_2, depending on the operating conditions and local electricity costs. On a larger scale (MW), projections to 2030 indicate values of 2–4 €/kg H_2, thanks to economies of scale and reduced costs of electrolysers.

Another important parameter is the cost of electricity converted through fuel cells. The relatively low round-trip efficiency (20–25%) means that the cost per kWh produced by the fuel cell is significantly higher than the initial kWh cost from photovoltaics. However, the goal of these systems is not maximum efficiency, but the possibility of providing renewable energy on demand, ensuring continuity of service in the absence of sun.

Compared to other storage solutions:

- Li-ion batteries have lower short-term costs for daily storage, but are not suitable for seasonal storage;
- compressed hydrogen systems have higher gravimetric density, but require complex and expensive infrastructure;
- metal hydrides, as in the Sharjah demonstration, have a high initial cost but guarantee maximum safety and management simplicity.

In summary, the Sharjah system does not compete in terms of immediate cost reduction, but as a test bed for safe, replicable solutions suitable for educational and demonstration contexts, in which the main value is not only economic but also scientific and social.

6.5 Innovativeness of the Sharjah experimental system

The system created at the University of Sharjah represents an original and innovative contribution to the panorama of hydrogen demonstrators, distinguishing itself both for the technological solutions adopted and for the context in which it was developed.

6.5.1 Integrated, compact configuration

Unlike most of the projects reported in the literature and internationally, which are oriented towards medium or large-scale plants, the Sharjah demonstration is characterized by a compact configuration (in the order of kW) that integrates in a single operational flow:

- bifacial photovoltaic modules,
- a PEM electrolyzer,
- a metal hydride storage system,
- a PEM fuel cell for conversion.

This small-scale, end-to-end architecture represents a modular testbed that can be replicated in other educational and research contexts.

6.5.2 Use of unconventional technologies

The use of bifacial photovoltaic modules in a desert environment, combined with reflective surfaces, makes it possible to increase energy productivity compared to traditional monofacial modules. The adoption of metal hydride tanks is a highly innovative element, because:

- allows safe storage at low pressure,
- improves thermal stability and energy density,
- reduces the risks associated with compression to 350–700 bar.

This is a solution that is still not widely used commercially and rarely integrated into real demonstrations [94].

6.5.3 Validation under extreme conditions

A further innovative aspect is the experimental validation in critical climatic conditions (Sharjah, United Arab Emirates), characterized by:

- ambient temperatures above 40 °C,
- strong solar radiation and high albedo,
- significant seasonal variations.

Most of the studies in the literature are conducted in the laboratory or in temperate environments; the Sharjah demonstration provides real data in desert conditions, expanding scientific knowledge on the behavior of hydrogen systems in complex climate scenarios.

6.5.4 Educational approach and transferability

The system was conceived not only as an experimental platform, but also as an educational and demonstration tool. This double value increases the impact of the project, since:

- contributes to the training of students and researchers on frontier technologies,
- promotes the dissemination of hydrogen culture in the Gulf countries,
- it opens up prospects for replicability in other small-scale university and industrial contexts.

6.5.5 Summary of innovative value

The set of characteristics listed above allows the Sharjah system to be placed as a unique case at international level, capable of combining:

- technological originality (double-sided PV + metal hydrides),
- experimental validation under extreme conditions,
- modular scalability and transferability,
- educational and demonstrative function.

For these reasons, the demonstration can be considered a bridge between laboratory research and large industrial projects, with a potential for both scientific and socio-technological impact.

The Sharjah system balances the trade-offs of existing technologies:

- vs Li-ion batteries → lower efficiency, but higher potential cyclic life, intrinsic safety and less dependence on critical raw materials;
- vs compressed H_2 → higher safety (low pressure) and ease of operation, with lower gravimetric density;
- vs large demonstratives → modular scalability and training value that facilitate replicability and technology transfer.

  The result is a "realistic" innovation profile: it does not maximize a single KPI, but offers a balance consistent with the objectives of research, teaching and transferability in extreme climate contexts.

In addition to the elements already highlighted, the Sharjah system offers further food for thought when compared with the available alternatives.

- Compared to electrochemical batteries, round-trip efficiency is lower, but the hydrogen system has a potentially longer cyclic life, less reliance on critical raw materials, and greater adaptability to longer storage periods.
- Compared to compressed hydrogen systems, the metal hydride solution provides a significantly higher level of safety due to its low operating pressure. Although the gravimetric density is lower, the volumetric density is high and the operation is safer, a key determinant for demonstration and educational applications.
- Compared to large international demonstrations, the added value of the Sharjah system lies in its modularity and educational function, which allows students and researchers to be trained on real and working technologies. The plant thus becomes not only a technological test bench, but also a vehicle for knowledge transfer and awareness of green hydrogen.

6.5.6 Sharjah Demonstration Placement Diagram

The Sharjah demonstration represents a unique balance between technological innovation, operational safety and training value. It does not aim to maximize a single performance, but to integrate several objectives: technical validation, real applicability and dissemination of knowledge. It is precisely this combination that constitutes the main element of originality, distinguishing it from other international experiences.

Analyzing the overall landscape, it is possible to place the Sharjah demonstration within a technological scale chain:

- Laboratory scale: studies focused on single components, high efficiencies but under controlled conditions and not reproducible on a large scale.
- Local demonstrators (kW–tens of kW): Systems such as Sharjah, HyBalance or US microgrids, which test feasibility under real conditions and serve as prototypes for future scale-ups.
- Industrial projects (MW–GW): REFHYNE, NEOM and others, aimed at validating the production and massive use of green hydrogen.

The Sharjah system is therefore in an intermediate position, closer to educational and experimental applications, but with potential for replicability and transferability to community or small-scale industrial microgrids. Its originality lies in the bridge it creates between the laboratory and the large

industrial plant, offering experimental data in extreme conditions and at the same time a platform for training and research.

6.6 Future prospects

The comparative analysis conducted in the previous paragraphs showed that the Sharjah experimental system is placed in an intermediate position between laboratory demonstrators and large international projects. From this basis, some future development prospects emerge, which concern both technological advancement and the application and socio-economic dimension.

6.6.1 Scalability and modularity

The compact configuration (in the order of kW) represents a replicable basic module. In the future, this architecture may be:

- scaling to higher powers (from tens to hundreds of kW),
- replicated in community microgrids or off-grid installations in isolated areas,
- integrated into public buildings and university campuses as permanent demonstration systems.

The modularity makes the system adaptable to different contexts, from residential applications to industrial micro-grids.

6.6.2 Component optimization

To increase overall efficiency, future developments will need to focus on:

- **PEM electrolysers** with lower specific consumption and greater durability;
- **fuel cells** with electrical efficiencies > 60% and greater thermal robustness;
- **Metal hydride tanks** optimized for capacity, charge/discharge rate and cost reduction.

The continuous evolution of materials (membranes, catalysts, metal alloys for hydrides) offers concrete prospects for improvement.

6.6.3 Integration with other renewable technologies

The experimental system was developed with a primary photovoltaic source. In the future, integration with other renewable resources, such as wind and solar thermodynamics, would make it possible to:

- reduce production intermittency,
- increase the capacity factor of the electrolyzer,

- explore multi-energy hybridization scenarios for microgrids.

6.6.4 Economic and market evaluations

An important perspective concerns the analysis of the levelized costs of hydrogen (LCOH) and reconverted electricity, as a function of:

- the projected reduction in electrolyser costs by 2030–2040,
- economies of scale resulting from mass production,
- possible government incentives in terms of green hydrogen.

These evaluations will make it possible to quantify the economic competitiveness of the system compared to storage alternatives, such as lithium batteries or compressed gas systems.

6.6.5 Strategic applications

Application perspectives include:

- **residential and university sector**, as a research and teaching platform;
- **remote areas** without access to reliable electricity grids, where the PV–H_2–FC combination can ensure continuity of service;
- **Gulf countries**, where extreme weather conditions make the Sharjah demonstration a pilot case of particular importance;
- **emerging markets** interested in modular and safe energy storage solutions.

6.6.6 Role in the energy transition

Finally, the Sharjah system paves the way for a broader role of green hydrogen in the energy transition, not only as a vector for large industrial projects, but also as a distributed and modular solution for energy communities and microgrids. This vision reinforces the innovative character and strategic relevance of the project, projecting it towards possible international scalability.

7 CONCLUSIONS

This PhD thesis addressed the issue of green hydrogen as an energy carrier, with particular attention to its integration into production systems from renewable sources, storage and electrical conversion through fuel cells. The general objective was to analyze the technical and scientific feasibility of an integrated system, able to operate in real conditions and to provide useful data for research and industrial innovation.

The focus of the work was the creation and study of a demonstration system at the University of Sharjah (UAE), developed in collaboration with Graded S.p.A., which represented the experimental basis for subsequent modeling, simulation and critical comparison activities with the state of the art.

The structure of the thesis followed a logical path:

- in Chapter 2 the experimental system has been described, with particular attention to the technological choices of each component (bifacial PV, PEM electrolyzer, metal hydride storage, PEM fuel cell);
- in Chapter 3 the mathematical model of the entire energy chain was developed, useful for understanding and simulating the physical phenomena at play;
- in Chapter 4 the experimental results were analyzed, validating the operation of the system in critical environmental conditions;
- in Chapter 5 numerical simulations were conducted to explore alternative scenarios and possible optimizations;
- in Chapter 6 a comparison was made with the scientific literature and international projects, highlighting the originality and innovativeness of the Sharjah demonstrative.

This sequence made it possible to build a complete picture, combining real experimental data, theoretical modelling and critical reflections on the role of green hydrogen in the energy future.

Main research findings

The results that emerged from the work are many and significant:

- **Experimental demonstration of the complete PV–H_2–FC chain**. For the first time in the MENA region, an integrated system has been created capable of producing green hydrogen from photovoltaics, storing it in solid form and converting it into electricity using fuel cells.

- **Enhancement of bifacial photovoltaic modules**. The analysis confirmed the role of desert albedo in improving performance, demonstrating that bifaciality can be a strategic advantage in arid and sunny climates.
- **Characterization of the PEM electrolyzer**. The device operated stably under intermittent conditions, showing efficiencies in line with the values reported in the literature and confirming its compatibility with variable renewable sources.
- **Safe storage using metal hydrides**. The possibility of accumulating hydrogen in solid form, at low pressure, has been demonstrated, with significant safety advantages compared to high-pressure tanks.
- **PEM fuel cell performance**. The electrical conversion has shown efficiencies of between 40% and 55%, allowing loads to be powered in real conditions and providing a reliable indication of the technology's potential.
- **Overall round-trip efficiency**. The system reached values between 22% and 24%. Although not high, these results are perfectly in line with similar experiences reported in the literature, confirming the robustness of the demonstrative.
- **Validation of mathematical models**. The comparison between simulations and real data showed a good match, demonstrating the reliability of the developed computational tools and their usefulness for prospective and optimization studies.

Original contribution of the thesis

The research has introduced several innovative elements that represent its main academic and technological contribution:

- **First demonstration in the MENA region** integrating bifacial PV modules with metal hydride storage. This combination, which is rare even internationally, was first experimented in real desert conditions.
- **Experimental validation of mathematical models**, which made it possible to bridge the gap between theoretical approaches and operational reality.
- **Integrated experimentation-modeling-simulation approach**, which gives robustness and completeness to the work, placing it beyond traditional studies focused on only one of the aspects.
- **Scalability and replicability**. The compact and modular configuration makes the system replicable in other contexts, from universities to the industrial sector, opening up concrete prospects for diffusion.

Potential impacts

The results obtained have significant impacts in three main dimensions:

- **Technical**: The demonstration system represents a useful test bed for the future implementation of hydrogen microgrids, residential applications and remote sites. The ability to operate in harsh environmental conditions confirms its versatility.
- **Economical**: the reduction in component costs, expected in the coming years, will make systems of this type competitive. The use of bifacial modules with low-cost reflective surfaces opens up scenarios for optimizing LCOE (Levelized Cost of Energy).
- **Environmental**: the possibility of storing solar energy in the form of hydrogen makes it possible to reduce emissions and contribute to decarbonization goals. In contexts such as the Middle East, the positive environmental impact can be amplified by the great availability of solar radiation.

8 FUTURE RESEARCH DEVELOPMENTS

Durability and stability tests

A first necessary development concerns the conduct of long-duration tests, to evaluate the degradation of photovoltaic modules, the electrolyzer and the fuel cell in desert conditions, as well as the stability of the hydride material after numerous charge and discharge cycles.

Optimization and control systems

A further step is the implementation of advanced control algorithms, capable of optimizing energy flows and reducing losses. The integration of artificial intelligence and predictive techniques will improve the overall performance of the system.

Scale-ups and energy communities

The system, currently on a kW scale, can be scaled up to tens or hundreds of kW, becoming applicable to energy communities, university campuses or industrial microgrids. Modularity is an advantage for replicability.

Multi-energy integration

Integration with other renewable sources (wind, solar thermodynamic) and electrochemical storage systems will make it possible to create more resilient microgrids, capable of guaranteeing continuity of service even in critical conditions.

Economic and environmental analyses

LCA (Life Cycle Assessment) studies and in-depth economic assessments (LCOH – Levelized Cost of Hydrogen) are desirable to measure the environmental impact and competitiveness of the system compared to other storage solutions [98].

Future scenarios for green hydrogen

In addition to technological developments, it is necessary to consider the strategic role that green hydrogen can play in the long term. The main international agencies estimate a growing penetration

of hydrogen in the decarbonisation of sectors that are difficult to electrify, such as heavy industry and maritime and air transport [99].

The Sharjah demonstrator, although small in size, represents a prototype of a distributed system. In the future, the deployment of similar systems may lead to the creation of interconnected and resilient hydrogen microgrid networks. The progressive reduction in the costs of electrolysers and fuel cells, combined with the support policies already outlined by the European Union and international bodies, will make these systems increasingly competitive [100][101].

Overall Conclusion

The thesis demonstrated the technical and scientific feasibility of an integrated PV–H_2–FC system, operating in real conditions and validated both experimentally and by modeling. The results obtained represent an important contribution to international research and offer a solid basis for the future development of hydrogen energy storage systems.

The work demonstrates how green hydrogen can play a role not only in large industrial projects, but also in distributed, modular and replicable solutions, suitable for local communities, university campuses and remote sites.

The research developed therefore constitutes a bridge between academia and industry, combining scientific rigor and concrete applicability, and represents a significant contribution to the path towards a sustainable energy transition.

In a broader perspective, the results of this research are part of the main international strategies for green hydrogen, promoted by bodies such as the European Commission, the IEA and IRENA. The spread of modular and distributed systems, alongside large industrial projects, is in fact a pillar of the global energy transition.

The Sharjah demonstration is therefore not just a local case, but an example of how research, industry and training can converge to accelerate decarbonisation and encourage the emergence of new skills. In this sense, the thesis contributes not only to the scientific debate, but also to the political and industrial path towards a sustainable and resilient energy future.

PUBLICATIONS LIST

- Ghalib Y. Kahwaji, Muhannad T. Ali, Giada Boudekji, Davide Capuano and Mohamed A. Samaha - Optimization of Coaxial Borehole Heat Exchanger for Hot Wet Climates: Experimental and Numerical Approaches - Journal of Thermophysics and Heat Transfer - February 2025 – DOI: https://doi.org/10.2514/1.T7143

- Ghalib Y. Kahwaji, Davide Capuano, Giada Boudekji, Mohamed A. Samaha - Design and optimization of ground-coupledrefrigeration heat exchanger in Dubai:Numerical approach – Heat Transfer - January 2024 - 53(3):1474-1500 – DOI: 10.1002/htj.23006

- Ghalib Y. Kahwaji, Muhannad T. Ali, Giada Boudekji, Davide Capuano, Abdelrahman E. Nasreldin, Abdullah Khan, Mohamed A. Samaha - Maximizing Performance of Ground-Coupled Heat Exchanger under Hot-Wet Climate Condition: Experimental and Numerical Analysis - Proceedings of the 6 th International Conference on Energy Harvesting, Storage, and Transfer - Niagara Falls, Canada - June 08-10, 2022 - Paper No. 117 - DOI: 10.11159/ehst22.117

- Ghalib Y. Kahwaji, Davide Capuano, Giada Boudekji, Mohamed A. Samaha - Optimization of High-Capacity Ground-Coupled Heat Exchanger under Hot-Wet Climate Condition: Numerical Approach - Conference: The 6th International Conference on Energy Harvesting, Storage, and Transfer - June 2022 - DOI:10.11159/ehst22.116

- Romero Rivas M., Capuano D., Miranda C. - Economic and Environmental Performance of Biowaste-to-energy Technologies for Small-scale Electricity Generation - Journal of Modern Power System and Clean Energy; 2020; Pages 12-18 - DOI: 10.35833/MPCE.2020.000315

- Capuano D., Costa M., Di Fraia S., Massarotti N., Vanoli L. - Direct use of waste vegetable oil in internal combustion engines: a review - Renewable & Sustainable Energy Reviews; Volume 69, March 2017, Pages 759–770 - http://dx.doi.org/10.1016/j.rser.2016.11.016

REFERENCES

[1] International Energy Agency (IEA), *Global Hydrogen Review 2022*, Paris, France, 2022.

[2] International Renewable Energy Agency (IRENA), *World Energy Transitions Outlook 2022*, Abu Dhabi, UAE, 2022.

[3] European Commission, *A Hydrogen Strategy for a Climate-Neutral Europe*, Brussels, Belgium, 2020.

[4] Hydrogen Council, *Path to Hydrogen Competitiveness: A Cost Perspective*, 2020.

[5] IPCC, *AR6 Climate Change 2022: Mitigation of Climate Change*, Cambridge University Press, 2022.

[6] BloombergNEF, *Hydrogen Economy Outlook*, Bloomberg Finance L.P., 2020.

[7] Fraunhofer Institute for Solar Energy Systems (ISE), *Recent Developments in Bifacial Photovoltaics*, Freiburg, Germany, 2021.

[8] PV Tech, *Articles on Bifacial Module Efficiency*, online technical articles, 2020–2022.

[9] International Renewable Energy Agency (IRENA), *Renewable Power Generation Costs in 2021*, Abu Dhabi, UAE, 2022.

[10] U.S. Department of Energy (DOE), *Hydrogen Production: Electrolysis*, Washington DC, USA, 2020.

[11] Barbir, F., “PEM electrolysis for production of hydrogen from renewable energy sources,” *Solar Energy*, vol. 78, no. 5, pp. 661–669, 2005.

[12] Carmo, M., Fritz, D., Mergel, J., Stolten, D., “A comprehensive review on PEM water electrolysis,” *International Journal of Hydrogen Energy*, vol. 38, pp. 4901–4934, 2013.

[13] Onda, K., Kyakuno, T., Hattori, K., Ito, K., “Performance analysis of a polymer-electrolyte water electrolysis cell,” *Journal of Power Sources*, vol. 132, pp. 64–70, 2004.

[14] International Energy Agency (IEA), *Technology Roadmap: Hydrogen and Fuel Cells*, Paris, France, 2015.

[15] EG&G Technical Services, *Fuel Cell Handbook*, 7th ed., Morgantown, WV, USA, 2004.

[16] Panwar, N.L., Kaushik, S.C., Kothari, S., “Role of renewable energy sources in environmental protection: A review,” *Renewable and Sustainable Energy Reviews*, vol. 15, pp. 1513–1524, 2011.

[17] Koytsoumpa, E.I., Bergins, C., Kakaras, E., “The role of hydrogen in the global energy transition,” *Renewable and Sustainable Energy Reviews*, vol. 60, pp. 822–835, 2016.

[18] Buttler, A., Spliethoff, H., “Current status of water electrolysis for energy storage, grid balancing and sector coupling,” *Renewable and Sustainable Energy Reviews*, vol. 82, pp. 2440–

2454, 2018.
[19] Staffell, I., Scamman, D., Velazquez Abad, A., et al., “The role of hydrogen and fuel cells in the global energy system,” *Energy & Environmental Science*, vol. 12, pp. 463–491, 2019.
[20] Guida, V., *Hydrogen Integration in Energy Systems*, PhD Thesis, Università degli Studi di Napoli Federico II, Naples, Italy, 2020.
[21] PVsyst SA, *PVsyst 7.2 Software Documentation*, Geneva, Switzerland, 2022.
[22] International Electrotechnical Commission (IEC), *IEC 61215 and IEC 61730 – Photovoltaic Module Standards*, Geneva, Switzerland.
[23] National Renewable Energy Laboratory (NREL), *Best Practices for Bifacial PV Performance Modeling*, Golden, CO, USA, 2020.
[24] Martín-Chivelet, N., “Bifacial photovoltaics: Performance and modeling,” *Progress in Photovoltaics: Research and Applications*, vol. 26, pp. 701–720, 2018.
[25] López-García, J., et al., “Performance of bifacial PV modules under different ground albedo conditions,” *Solar Energy*, vol. 206, pp. 104–116, 2020.
[26] Barbir, F., “PEM electrolysis for production of hydrogen from renewable energy sources,” *Solar Energy*, vol. 78, pp. 661–669, 2005.
[27] Carmo, M., et al., “A comprehensive review on PEM water electrolysis,” *International Journal of Hydrogen Energy*, vol. 38, pp. 4901–4934, 2013.
[28] Millet, P., Grigoriev, S., Fateev, V., “Electrochemical technologies for energy storage and conversion: PEM electrolysis,” *Electrochimica Acta*, vol. 247, pp. 109–123, 2019.
[29] H2 Planet, *Hy-PEM-XP Home Electrolyzer – Technical Datasheet*, 2022.
[30] Ursúa, A., Gandía, L.M., Sanchis, P., “Hydrogen production from renewable sources,” *Proceedings of the IEEE*, vol. 100, pp. 410–426, 2012.
[31] International Electrotechnical Commission (IEC), *IEC 62282-4-101 – Fuel Cell Technologies – Safety*, Geneva, Switzerland, 2021.
[32] International Energy Agency (IEA), *Technology Roadmap: Hydrogen and Fuel Cells*, Paris, France, 2015.
[33] Lototskyy, M.V., Yartys, V.A., Pollet, B.G., Bowman, R.C., “Metal hydride hydrogen storage and compression systems,” *International Journal of Hydrogen Energy*, vol. 39, pp. 5818–5851, 2014.
[34] International Organization for Standardization (ISO), *ISO 16111 – Transportable Gas Storage Devices: Hydrogen Absorbed in Reversible Metal Hydride*, Geneva, Switzerland, 2008.
[35] H2 Planet, *My H_2 2000 Metal Hydride Storage Tank – Technical Datasheet*, 2022.

[36] Larminie, J., Dicks, A., *Fuel Cell Systems Explained*, 3rd ed., Wiley, Chichester, UK, 2017.
[37] Parra, D., Valverde, L., et al., "PV–hydrogen systems: Energy management and storage," *Renewable and Sustainable Energy Reviews*, vol. 44, pp. 1–13, 2015.
[38] Barbir, F., *PEM Electrolysis and Fuel Cell Technology*, Elsevier, Oxford, UK, 2021.
[39] International Renewable Energy Agency (IRENA), *Green Hydrogen Cost Reduction – Scaling Up Electrolysers*, Abu Dhabi, UAE, 2020.
[40] Fraunhofer Institute for Solar Energy Systems (ISE), *Recent Developments in Bifacial Photovoltaics*, Freiburg, Germany, 2021.
[41] Guo, S., et al., "Field performance of bifacial PV modules in hot climates," *Solar Energy*, vol. 206, pp. 22–34, 2020.
[42] Carmo, M., Fritz, D., Mergel, J., Stolten, D., "A comprehensive review on PEM water electrolysis," *International Journal of Hydrogen Energy*, vol. 38, pp. 4901–4934, 2013.
[43] Barbir, F., "PEM electrolysis for hydrogen production from renewable energy sources," *Solar Energy*, vol. 78, pp. 661–669, 2005.
[44] Millet, P., Grigoriev, S., Fateev, V., "Electrochemical hydrogen production by PEM water electrolysis," *WIREs Energy and Environment*, vol. 8, e1369, 2019.
[45] Lototskyy, M.V., Yartys, V.A., Pollet, B.G., Bowman, R.C., "Metal hydride hydrogen storage systems," *International Journal of Hydrogen Energy*, vol. 39, pp. 5818–5851, 2014.
[46] Jain, I.P., Lal, C., Jain, A., "Hydrogen storage in Mg-based systems," *International Journal of Hydrogen Energy*, vol. 35, pp. 5133–5144, 2010.
[47] H2 Planet, *My H_2 2000 Datasheet*, 2023.
[48] Barbir, F., *PEM Fuel Cells: Theory and Practice*, Elsevier, Oxford, UK, 2013.
[49] Yu, H., et al., "Performance degradation of PEM fuel cells," *Journal of Power Sources*, vol. 205, pp. 10–23, 2012.
[50] O'Hayre, R., Cha, S.-W., Colella, W., Prinz, F.B., *Fuel Cell Fundamentals*, Wiley, Hoboken, NJ, USA, 2016.
[51] Urs, R.R., Sadiq, M., Mayyas, A., Al Sumaiti, A., "Techno-economic assessment of PV–electrolyzer–fuel cell systems," *International Journal of Energy Research*, 2023.
[52] International Energy Agency (IEA), *Solar Energy in the Middle East*, Paris, France, 2021.
[53] Alnaser, W.E., et al., "Solar and hydrogen energy in the UAE: Potentials and challenges," *Renewable Energy*, vol. 152, pp. 133–146, 2020.
[54] Barbir, F., *PEM Fuel Cells: Theory and Practice*, 2nd ed., Academic Press, 2013.
[55] Fraunhofer Institute for Solar Energy Systems (ISE), *Recent Developments in Bifacial Photovoltaics*, Freiburg, Germany, 2021.

[56] Guo, S., et al., “Field performance of bifacial PV modules in hot climates,” *Solar Energy*, vol. 206, pp. 22–34, 2020.
[57] Barbir, F., “PEM electrolysis for production of hydrogen from renewable energy sources,” *Solar Energy*, vol. 78, pp. 661–669, 2005.
[58] Carmo, M., et al., “A comprehensive review on PEM water electrolysis,” *International Journal of Hydrogen Energy*, vol. 38, pp. 4901–4934, 2013.
[59] Lototskyy, M.V., et al., “Metal hydride hydrogen storage and compression systems,” *International Journal of Hydrogen Energy*, vol. 39, pp. 5818–5851, 2014.
[60] Imamura, H., Akiba, E., “Metal hydride materials for hydrogen storage,” *Journal of Alloys and Compounds*, vols. 356–357, pp. 515–520, 2003.
[61] Barbir, F., *PEM Fuel Cells: Theory and Practice*, 2nd ed., Academic Press, 2013.
[62] Horizon Fuel Cell Technologies, *1000 W PEM Fuel Cell Technical Manual*.
[63] Stackhouse, P.W., Whitlock, C.H., *Surface Meteorology and Solar Energy (SSE) Release 9.0*, NASA Langley Research Center, 2018.
[64] NASA, *Prediction of Worldwide Energy Resources (POWER) Project – Release 9.0.1*, 2023.
[65] Cuevas, A., et al., “Bifacial solar cells: A review,” *Solar Energy*, vol. 190, pp. 131–144, 2019.
[66] Guo, S., et al., “Effect of ground albedo on the performance of bifacial photovoltaic modules,” *Renewable Energy*, vol. 146, pp. 136–147, 2020.
[67] Singh, J., et al., “Field performance analysis of bifacial PV modules,” *Progress in Photovoltaics*, vol. 29, pp. 130–142, 2021.
[68] Argyropoulos, P., et al., “Advances in PEM fuel cell technology: Efficiency, durability and cost,” *Journal of Power Sources*, vol. 520, 2022.
[69] International Renewable Energy Agency (IRENA), *Renewable Power Generation Costs in 2022*, Abu Dhabi, UAE, 2023.
[70] International Energy Agency (IEA), *Global Hydrogen Review 2022*, Paris, France, 2022.
[71] U.S. Department of Energy (DOE), *H2A Hydrogen Analysis: Hydrogen Storage Cost Data*, 2020.
[72] U.S. Department of Energy (DOE), *Fuel Cell System Cost 2022 Update*, 2022.
[73] Bhandari, R., et al., “Cost analysis of hydrogen production from renewable energy sources,” *International Journal of Hydrogen Energy*, vol. 46, pp. 1881–1893, 2021.
[74] International Energy Agency (IEA), *Global Energy Storage Outlook*, Paris, France, 2022.
[75] BloombergNEF, *Battery Market Outlook 2022–2030*, 2022.

[76] U.S. Department of Energy (DOE), *Hydrogen Storage: Compressed Gas Storage Systems for Vehicles*, 2020.
[77] U.S. Department of Energy (DOE), *Hydrogen Storage: Cryo-compressed and Liquid Hydrogen Storage*, 2021.
[78] Züttel, A., "Hydrogen storage methods," *Naturwissenschaften*, vol. 91, pp. 157–172, 2003.
[79] International Energy Agency (IEA), *Global Hydrogen Review 2022*, Paris, France, 2022.
[80] Barbir, F., "PEM electrolysis for production of hydrogen from renewable energy sources," *Solar Energy*, vol. 78, pp. 661–669, 2005.
[81] Carmo, M., et al., "A comprehensive review on PEM water electrolysis," *International Journal of Hydrogen Energy*, vol. 38, pp. 4901–4934, 2013.
[82] Parra, D., et al., "Techno-economic challenges of fuel cell-based microgrids," *Renewable and Sustainable Energy Reviews*, vol. 82, pp. 117–129, 2019.
[83] Hydrogen Council, *Path to Hydrogen Competitiveness: A Cost Perspective*, 2020.
[84] Buttler, A., Spliethoff, H., "Current status of water electrolysis for energy storage," *Renewable and Sustainable Energy Reviews*, vol. 82, pp. 2440–2454, 2018.
[85] Lototskyy, M.V., et al., "Metal hydride hydrogen storage systems for stationary and automotive applications," *International Journal of Hydrogen Energy*, vol. 40, pp. 114–130, 2015.
[86] HyBalance Project, *Final Report*, 2018.
[87] GRHYD Project, *Results and Lessons Learned*, 2019.
[88] Shell, *REFHYNE Project Overview*, 2021.
[89] Japanese Ministry of Economy, Trade and Industry (METI), *ENE-FARM Program Report*, 2020.
[90] U.S. Department of Energy (DOE), *Hydrogen and Fuel Cell Program Record*, 2021.
[91] NEOM, *Green Hydrogen Project – Press Release*, 2021.
[92] Masdar Institute, *Hydrogen Pilot Projects in the UAE*, 2020.
[93] King Abdullah University of Science and Technology (KAUST), *Research on Advanced Hydrogen Storage Systems*, 2021.
[94] Gkanas, E.I., et al., "Metal hydride-based hydrogen storage prototypes," *International Journal of Hydrogen Energy*, vol. 45, pp. 123–135, 2020.
[95] International Renewable Energy Agency (IRENA), *Green Hydrogen: A Guide to Policy Making*, Abu Dhabi, UAE, 2020.
[96] BloombergNEF, *Hydrogen Economy Outlook*, 2020.
[97] European Commission, *A Hydrogen Strategy for a Climate-Neutral Europe*, Brussels,

Belgium, 2020.
[98] International Organization for Standardization (ISO), *ISO 14040 – Environmental Management: Life Cycle Assessment*, Geneva, Switzerland, 2006.
[99] International Energy Agency (IEA), *Global Hydrogen Review 2022*, Paris, France, 2022.
[100] European Commission, *A Hydrogen Strategy for a Climate-Neutral Europe*, Brussels, Belgium, 2020.
[101] International Renewable Energy Agency (IRENA), *World Energy Transitions Outlook 2023*, Abu Dhabi, UAE, 2023.